Landslide magnitude-frequency analysis to better define warning criteria for warning levels in Sogn og Fjordane, Norway

A study to improve landslide warning

Håvard Harnes Mongstad

Master thesis in Geoscience

Study program: Geohazards

60 study points

Institute of geoscience

Faculty of mathematics and natural sciences

UNIVERSITY OF OSLO

06.2018

2018

Magnitude-frequency analysis to better define warning criteria for warning levels in Sogn og Fjordane, Norway

Håvard Harnes Mongstad

http://www.duo.uio.no

Press: Reprosentralen, Universitetet i Oslo

Summary

The county of Sogn og Fjordane in Western Norway has a climate and topography which makes it vulnerable for debris avalanches, debris flows, shallow slides and slush flows. The recently established landslide forecasting and warning service at Norwegian Water Resources and Energy Directorate (NVE), at www.varsom.no, is able to predict their regional, spatial and temporal occurrence.

The landslide warning levels, which goes from 1 to 4, suggest an expected outcome pursuant to the upcoming hydro-meteorological event. These levels are defined based on the expected number of landslides that will occur in a warning area with an extension of 10.000-15.000 km^2. Expected magnitude of the landslides is also included within the definition of warning levels in a qualitative and very general way. For example, a level 3 warning will indicate that "Large landslides that disturb infrastructure and roads may occur". However, NVE has throughout the first 5 years of the operation observed that, depending on the region, not always only "large" landslides occur during a level 3 warning. It may happen that many small landslides occur that can create severe damages and serious disruptions to the society in that region.

The Norwegian landslide database is quite rich with a great number of events registered through many years. However, the events do not contain landslide magnitude information. In this study, the following questions are addressed: How large are the rainfall-induced landslides in this region, and which landslide magnitude is the most frequent? And how can landslide magnitude become incorporated within the definition of the regional landslide warning levels? This thesis aims to find the typical and frequent landslide magnitudes in Sogn og Fjordane by performing a magnitude-frequency analysis. It will also propose a way of incorporating the results into the landslide warning levels and investigate how it can be communicated to public and authorities.

A cumulative distribution was applied to investigate the relationship between magnitude and frequency. The results revealed landslides to have an extension of 147-123228 m^2 in the region, with the most frequent magnitude being 10000 m^2. An incorporation of magnitudes was accomplished by investigating magnitudes from specific events as well as considering their associated warning level. A "small" landslide is proposed to have a range from 0-10.000

m^2, a “medium” landslide as 10.000-50.000 m^2 and a “large” landslide to be greater than 50.000 m^2. My findings show that an event with level 4 warning should expect an unusual high number of initiated events at all scales as well as several large magnitude landslides. A warning level 3 should expect multiple landslides with medium magnitude, also with likelihood of dealing with a large landslide. At last, a level 2 event should consider a single event with medium magnitude.

This work is part of an ongoing project that aims to map more systematically the magnitude of recent landslide events at national level, because a better understanding of these processes, their spatial distribution, dimensions, mechanisms and frequency are needed to improve the performance of the landslide forecasting and warning service, especially at local scale.

Prologue

This thesis was formed during spring 2017. It was desirable with a research related to rainfall-induced landslides. A meeting with Graziella Devoli, senior Geologist at NVE and Associate Professor in the section of Physical geography and Hydrology at the University of Oslo, was therefore arranged. She quickly introduced me for the challenges related to the landslide EWS and that a magnitude-frequency analysis could be helpful for the service. The type of research had never been performed in Norway before, which is why I thought the topic was very interesting. I also wanted to involve Karianne Staalesen Lilleøren as my supervisor due to here expert knowledge in GIS and for her being an honest person that would give clear feedback during my work.

I therefore want to give a big hand to my supervisors Graziella Devoli and Karianne Staalesen Lilleøren that helped me to accomplish my research. Thank you for being constructive, giving me well formulated feedback and by helping me to organize my work. It must have been challenging to have a student doing his research in another city. Thank you for being supportive Karianne, regardless of the situation that turned up during my thesis. Thanks to you Graziella, I have learned a lot about landslide-processes and about the landslide early warning service, just like I wanted to. It has been very easiy to communicate with you despite being in another city and you have responded quickly to questions that showed up. It was also a great experience to visit the EGU-conference 2018. Thank you both for organizing that. I wish you all the best for the future.

I want to give a big hand to Søren Boje at NVE for giving me a quick-introduction on NVE`s threshold data and how I could use them to perform analysis. A big hand to Helga Harnes that helped me getting my grammar into place. Thank you Erlend Løvfall for allowing me to use his user account at UiB. And at last, thanks to Karoline Harnes Mongstad for being supportive through my work.

Table of contents

1 Introduction

1.1 Background

Norway is a country exposed to rainfall-induced landslides that causes economic loss as well as loss of human lives (Soleng et al., 2018). Landslide processes are usually classified depending on the type of material and their kinematics, but also based on their triggering conditions. With the term "rainfall-induced landslides" in this thesis I refer to landslide types like debris flows, debris avalanches and shallow slides that commonly are triggered by intense rainfall and/or in combination with intense melting of snow (Hungr et al., 2001). In addition, this general term includes slushflows. Historical events in Norway shows that these landslides may have devastating outcomes with an estimate of 100 people being killed in the last 100 years (Soleng et al., 2018). A recent analysis made by the Norwegian Water Resources and Energy Directorate (NVE) shows that seven fatalities were caused by slushflows (figure 1) in the period from 2009-2016 and five have been killed by debris avalanches and debris flows. These landslides are a considerable threat to the county of Sogn og Fjordane and they are causing considerable damage on roads and railways (figure 2). This enlightens the need of mitigation measures at local and regional scale to reduce economic loss and to assure that inhabitants maintain secure when landslide risk is considered as high.

Figure 1. A slushflow were unfortunate to kill two people in Tuftadalen in the municipality of Balestrand, 2011. Photo Fjellanger Widerøe / NRK

Figure 2. Example of a debris flow that caused great damages on road 242 in Skjerdal in the municipality of Aurland, 2013. Photo: Jan Helge Aalbu.

Debris slides are typically observed as shallow and small slides with a reduced potential of causing damage to society. They originate in weak layers or thin zones of high shear strain, but can enlarge downslope and develop into an extremely rapid and destructive debris avalanche (Hungr et al., 2001). Debris flows appears in established channels as saturated surges of debris, typically in fine-grained material, together with some vegetation and boulders (Iverson, 1997). It can reach extremely high velocities and becomes typically destructive at the point where the river outlet meets the cutting road (figure 2). Slushflows are, in addition, associated with melting of snow and hence temperature (Decaulne and Sæmundsson, 2006).

Climatic profiles propose an expected increase in number of rainfall-induced landslides in respond to an increased number of hydro-meteorological events associated with intensive rainfall and higher temperatures (Hisdal et al., 2017). More frequent and destructive landslides are therefore expected in the future and the understanding of these processes are crucial to perform mitigation measures in a feasible way.

Measures on rainfall-induced landslides are commonly introduced to protect inhabitants in a better way. One measure is to implement a correct land-use planning that will benefit from

susceptibility and hazard maps. Susceptibility maps are maps that point out areas susceptible to landslides by using material and terrain components like slope angle and soil type (McDonald et al., 1999). A hazard map can be produced as well by adding the relative likelihood of the landslide to occur (McDonald et al., 1999). The resulting maps becomes useful for land-use planning purposes by identifying secure and unsecure areas and to e.g. introduce building codes. Physical measurements can also be applied to prevent slope failure or by leading the mass in another direction from the exposed area (Popescu and Sasahara, 2009). An example could be construction of barriers, catching nets or by terrain modifications. Another measure is to forecast landslides through a landslide early warning service (EWS).

A landslide forecasting and warning service is an important measure that forecast upcoming hydro-meteorological events and communicates landslide risk both locally and regionally if risk is considered as high. The tool aims to reduce the vulnerability and exposure of a society by moving the elements at risk out of the way. It allows municipalities to perform their own mitigation measures considering the issued warning message (Intrieri et al., 2013). A general landslide EWS can roughly be divided into four components (Intrieri et al., 2013). First, it is a necessity to have knowledge of the natural hazard of which occurrence should be monitored and forecasted in advance. This can be achieved by preparing inventory maps where landslides are drawn to document and determine different parameters and statistics of the hazard (Guzzetti et al., 2012). Another component is the monitoring part which is either site-specific or by forecasting at a regional level like the recently established landslide EWS in Norway. It uses components as precipitation, soil moisture and melting of snow to evaluate the water input (Colleuille et al., 2017). A landslide EWS will typically issue one out of four warning levels that depends on the expected outcome of the event. A successful EWS will disseminate the warning to vulnerable societies in a timely and understandable way as well as proposing a stage of preparedness (UNISDR, 2009).

1.2 Motivation

The recently established landslide EWS at the Norwegian Water Resources and Energy Directorate (NVE) forecasts the spatial and temporal occurrence of landslides. The service has established thresholds for rainfall-induced landslides at both national and regional scale that are used to help issuing a correct warning level. The EWS propose an expected outcome

pursuant to the upcoming hydro-meteorological event (Colleuille et al., 2017). The tool has developed to become very useful mainly regionally, but also locally. At a regional scale, it helps authorities to increase the stage of preparedness so that prospective landslides events and their associated outcome will be solved in an efficient way. Locally, it can help authorities to decide whether roads should be closed or not, assuring that no one will put themselves in danger. The landslide EWS is constantly trying to improve themselves and to become more accurate by performing different types of analysis. However, some challenges are still present.

A landslide warning level informs about the expected numbers of landslides that will occur under the event over a warned region as well as in a general and qualitative way on their magnitudes. However, no previous studies have been performed to investigate the typical magnitudes for rainfall-induced landslides in Norway. A common approach from international studies (Guthrie and Evans, 2004, Hungr et al., 2008, Dahl et al., 2013) is to produce a magnitude-frequency curve that would help pointing out the typical magnitudes in the county and at the same time indicate their frequency. However, Norway is unfortunate to have lack of systematic mapping of landslide magnitude as well as lack of landslide inventory maps. Creating an inventory map of landslide events, together with an analysis of typical landslide magnitudes and other characteristic landslide parameters are thought as a clever way to improve the landslide EWS.

1.3 Objectives

This research is aiming to create a landslide inventory map by investigating an already existing landslide inventory (NLDB) so that characteristic rainfall-induced landslide magnitudes can be calculated. The results will be used for risk assessment by investigating if the landslide EWS can be improved by finding a magnitude-frequency relationship of landslides. Landslides can appear in a great variety of magnitudes. Large magnitudes will naturally have potential of performing more damage to society than a landslide of low magnitude. Magnitude is therefore a crucial element in risk assessment in addition to their frequency of occurrence (Dahl et al., 2013). Investigation of landslide magnitude and their frequency will help to understand the influence of the hazard in my study area and can help to improve risk assessment by developing the already established landslide EWS.

Other objectives for the research includes a regional characterization of the landslides, as well as a characterization of landslide parameters differentiated between rainfall-induced landslide typologies. An analyse of thresholds will be performed in addition to see how well observed threshold values fit to the established threshold limits from NVE. The research aims also to update and improve the quality of the national database through my investigations. Pros and cons of my pioneer approach for reaching my objectives will at last be discussed.

2 Theory

2.1 Rainfall-induced landslides and their prediction

2.1.1 Material properties and kinematics

A landslide can be recognized by the type of involved material. A soil is defined as a mixture of solid particles (Hungr et al., 2001). It is a combination of coarse and fine grained material, that varies typically between sand, silt, rock fragments, mud, peat or as any combination of these (Colleuille et al., 2017). The soil is classified as either a debris or an earth which depends on the distribution of grain size (Cruden and Varnes, 1996). An earth soil consists of more than 80 % fine grained material (particles less than 2 millimeters). A debris soil consist of 20-80% of the particles to be larger than 2 millimeters, with the remaining particles smaller than 2 millimeters (Cruden and Varnes, 1996). The typical composition of material for both debris (in volcanic and non-volcanic environments) and earth flows are presented in figure 3 (Hungr et al., 2001).

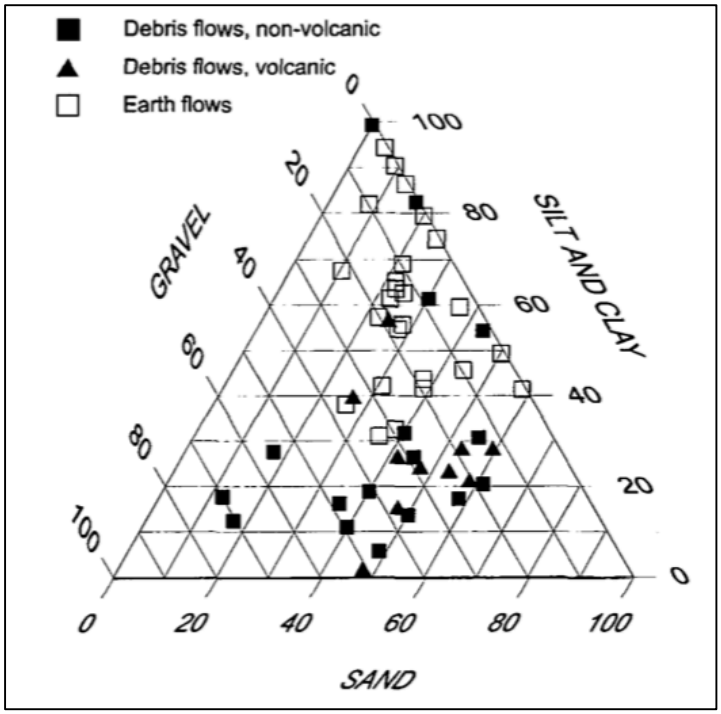

Figure 3. Triangle plot shows the differences in textural composition of debris flows (volcanic and non-volcanic) and earth flows. Grain size: gravel 2-18 mm, silt and clay <0.074 mm, sand 0.074 – 2 mm. From Hungr et al. (2001).

The soil is a result of accumulated material over a time of period, often located on top of the bedrock. The material can descend from different sources. Either as weathered material, transported colluvium material (from previous landslides), glacier deposits, or as unsorted waste-dump from humans (Hungr et al., 2001). They are common to appear in combination with organic material as well.

Kinematics is another way of distinguishing between landslide types and can help to understand the potential consequences it may have. Figure 4 presents the six main types of landslide behaviour: topple, slide, flow, fall, spread and slope deformation. Table 1 presents the landslide typologies and their associated kinematics. Slide and flow are most important regarding rainfall-induced landslides (Hungr et al., 2014). A landslide can act as a complex system by changing from one kinematic behaviour to another or by behaving as a combination of these while the mass moves downslope. Components like soil condition, water input, terrain features can e.g. cause a debris avalanche to develop into a debris flow (Cruden and Varnes, 1996, Highland and Bobrowsky, 2008).

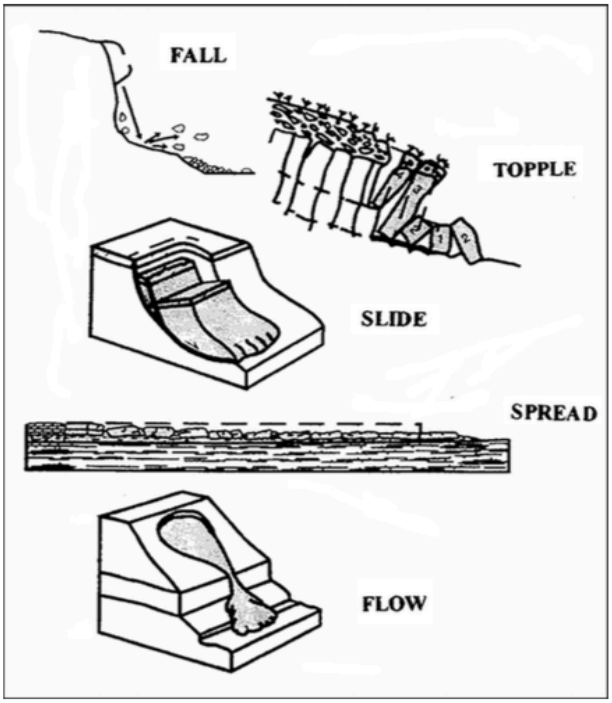

Figure 4. Classification of kinematic behaviour of landslides (Cruden and Varnes, 1996)

Table 1. The kinematics of the different rainfall-induced landslides as well as the Norwegian terms.

Type	Kinematic
Debris slide Utglidning	Slide
Debris avalanche Jordskred	Slide / Flow
Debris flow Flomskred	Flow
Slushflow Sørpeskred	Flow

Slide is the kinematic behaviour of debris slides. It usually originate along a surface of rupture, but weak layers of typically thin zones of high shear strain can be the cause of initiation (Cruden and Varnes, 1996). The movement is recognized by starting as a local

failure, before enlarging the area of displaced material. There are three main type of slides: rotational, translational and compound slides. A rotational slide is characterized by having a concave shape with a curved surface of rupture that the mass moves along. Minor internal movement are associated with this type of kinematic. A translational slide has a planar or undulating surface that the mass moves along (Cruden and Varnes, 1996). The last type are compound slides, which is a combination of rotational and translational slides. Slides may originate from different types of compositions (Hungr et al., 2014). It can appear in homogenous material like clay and silt slides (rotational, translational and compound slides) and on granular material (gravel, sand or/and debris). Granular slides are planar slides in weathered or colluvium materials, often found on top of a stronger medium (Hungr et al., 2014). Slides usually initiate at slopes from 30°-60° degrees, but are observed to initiate down to 20°. Thicknesses of granular slides vary typically from 0.5 – 2 meters (Hungr et al., 2014).

A flow is a continuous movement of rock or soil, characterized by having an internal distortion of mass while the mass moves downslope (Cruden and Varnes, 1996). It starts as a slide, but develops into a flow (Hungr et al., 2001). Particles will move relatively to each other inside the mass and surface shear are therefore usually short-lived. The material can be sorted or unsorted. Sorted material includes marine, fluvial, eolian or lacustrine sediments. Unsorted are typical for colluvium, glacial, residual and anthropogenic sediments (Hungr et al., 2001). Landslides may behave in between a slide and a flow. A gradual transition takes place, depending on water content, kinematics and mobility (Cruden and Varnes, 1996). The velocity will depend on the type of flow, ranging from slower (0.1m/s) to extremely rapid (> 10 m/s) velocities (Hungr et al., 2001). Flows can be dry, partially saturated or liquefied (Hungr et al., 2014). They can appear in channelized slopes and at open slopes. An example of an open slope flow are debris avalanches characterized by its large extent and rapid movement (Cruden and Varnes, 1996). A channelized flow develops most often into a debris flow (Cruden and Varnes, 1996).

2.1.2 Triggering causes

Landslides can be classified based on their triggering cause. Water content and corresponding water pressure are the most efficient triggering component for rainfall-induced landslides. Precipitation from short duration events with high intensity or by long lasting rainfall over several days have potential of initiating landslides (Johnson and Sitar, 1989, Cruden and Varnes, 1996, Hungr et al., 2001, Corominas et al., 2014). A sudden load of the soil can be a

triggering component as well by e.g. a rock fall. The cohesion of the soil is reduced as a response of the partially or fully saturated soil and are therefore vulnerable for a sudden liquefaction or an undrained loading process that can cause the soil to lose their bonds between the particles (Sassa, 1984, Hungr et al., 2014). Debris flows may, in addition to precipitation, be generated due to surface water runoff (Kean et al., 2013). Another way is by achieving a sudden flow of water resulting from a blockade in the channel. It can be caused by transported mass from a landslide, trees or any obstructing object in the channel. A sudden breakthrough of the water can lead to the initiation of a debris flow (Hungr et al., 2001).

2.1.3 Types of rainfall-induced landslides

Debris slides are shallow slides of mass that can change its kinematics into a flow if favorable conditions are present (Hungr et al., 2014). They consist of granular material and are usually found to have distinctly lower magnitudes than the other considered landslide types, as also confirmed by an analysis of landslide events in Trøndelag in 2012 (Væringstad and Devoli, 2012). An example of a debris slide from my research is presented in figure 5.

Figure 5. Example of a debris slide from Matbjøra in the municipality of Gaular, 09.11.2017. Photos: The Norwegian Public Road Administration (regobs.no).

A debris avalanche is a partially to fully saturated and extremely rapid landslide (Hungr et al., 2001). They start as a shallow debris slide, but develops quickly into a flow if mass continues to move downslope (Hungr et al., 2001). It initiates in steep, open hillsides with no

established channel. A debris avalanche occurring in the same area are therefore rather uncommon due to previous removal of mass (Hungr et al., 2001). The involving mass are normally a product of either (or combination of) colluvium, residual, glacial or organic deposits (Hungr et al., 2014). The destabilization at initiation, caused by undrained loading, spreads in width that triggers more mass to become involved (Hungr et al., 2014). They can therefore get a characteristic triangle shape, while others end up with a more irregular form (figure 6a). It may also enter already established channels on its way downslope and continue to follow these (Hungr et al., 2001). Debris avalanches may occur at all scales. Based on analysis of previous studies and observations NVE (2013) pointed out that a normal run-out length of a debris avalanche in Norway reaches up to 500 metres, with potential of reaching distances to a kilometre. However, these estimates are based on observations in the entire country and are not necessarily correct for this region. No information about typical velocities for debris avalanches are available in Norway. A typical release angle are proposed as steeper than 25° degrees (NVE, 2014a). An example of a debris avalanche from my research is presented in figure 6b.

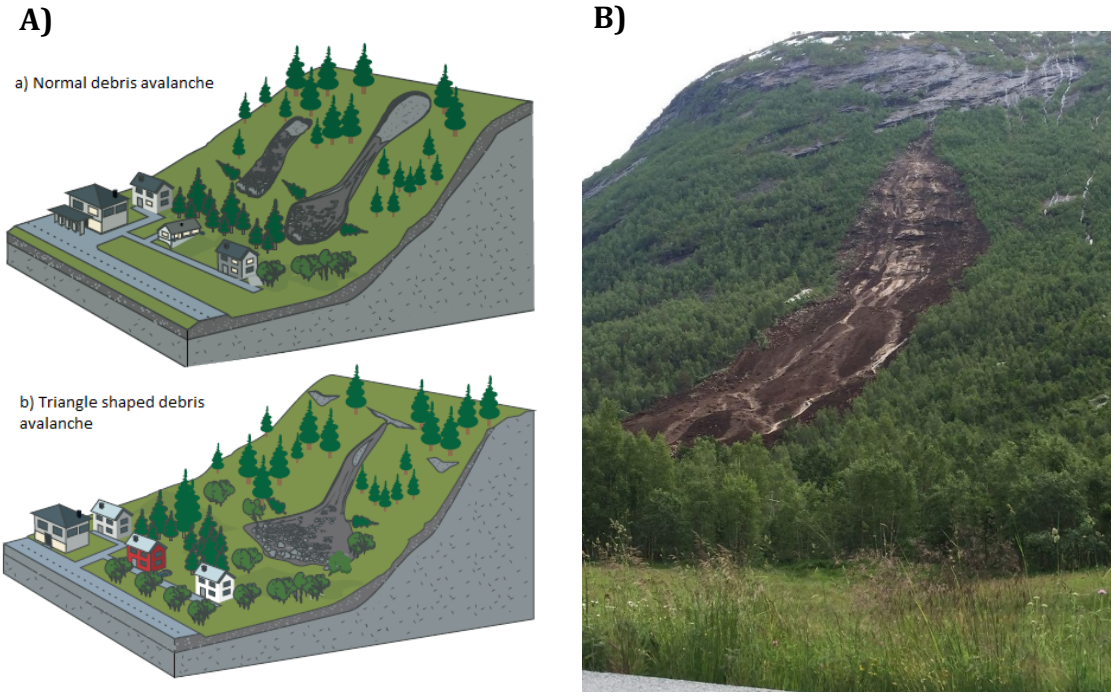

Figure 6. A: Different shapes of a debris avalanche (Colleuille et al., 2017) B: Example of a debris avalanche from Krundalen in the municipality of Luster, 2015. Photo: http://www.regobs.no/Registration/65514.

Debris flows are surges of saturated debris that appears in already established channels (figure 7) (Hungr et al., 2001). It has the potential of eroding and transporting considerable amounts of sediments. It can contain fine-grained sediments from clay to larger boulders but sand, gravel and larger grains constitute most of the moving mass (Iverson, 1997). Trees and

different types of organic material is often involved. Low-lying parts of the channel will provide more water as a respond to a continuous supply of water to the channel. Potential erosional force of the flow will therefore naturally become higher in the lower parts. The flow will then start eroding in- and along the banks and add even more material into the flow (Hungr et al., 2014). Their channelized occurrence them predictable by knowing where they show up and they can appear in the same channel which gives them a periodically occurrence. It can reach velocities from very rapid to extremely high with a range from 1 m/s to 20 m/s (Hungr et al., 2001). There is lack on information of typical velocities for debris flows in Norway because rarely measured or estimated. The typical runout distances varies from 500 meters to a kilometre (NVE, 2013), but again also these estimations are based on few events in the country and do not necessarily represent the runout for my region. A typical release angle is proposed to range from 25°-45° degrees (NVE, 2014a). An example of how a debris flow develops is shown in figure 7 while an event from my research at Hjelle in 2013 is presented in figure 8.

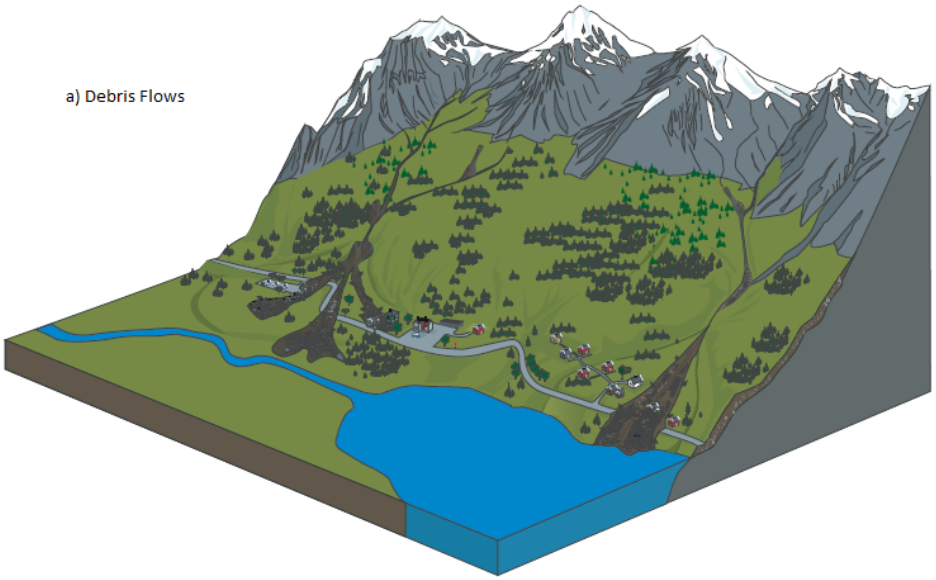

Figure 7. Examples of debris flows and their path from starting point towards depositional area (NVE, 2013).

A rough sorting of sediments is carried out as the flow-surge travels downslope (Costa, 1984). Number of surges can vary from one to hundreds (Hungr et al., 2014). The coarsest material are brought upwards within the flow due to a vertical velocity gradient, which leads to inverse grading and sorting of sediments (Hungr et al., 2001). Fine-grained material will therefore move along the bottom of the surge. Each surge creates a front that consists of coarse material (Hungr et al., 2014). The frontal part can create levees of coarse material or create deposits as abandoned fronts. The flow will continue in the channel until it reaches the channel mouth, where the debris are spread out over the alluvial fan as seen from figure 8. Slope angle is at

this point around 5° – 20° degrees (Hungr et al., 2014). The material is crudely sorted with the coarsest material in the front, while finer materials are spread out (Hungr et al., 2014). Some individual large particles are also common to be found around.

Figure 8. Example of a debris flow and the spread of material in the alluvial fan. Coarse and fine-grained material are indicated with respectively red and blue color. Event is from Hjelle in the municipality of Stryn, 2013. Photo: Jan Helge Aalbu.

Slushflows occur when a super-saturated snow pack start to flow downslope acting like a liquid (figure 9). It erodes and picks up debris, mud or other deposits on its way (Decaulne and Sæmundsson, 2006). It is similar as a debris flow in several ways, but initiates differently. However, it may develop into a debris flow on its way downslope. The initiating process requires a snow pack to become super-saturated by free water supply from rainfall and melting of snow (Onesti, 1987). A characteristic blue-grey colour can identify snow packs under such conditions (Hestnes, 1985). Initiation can occur if the input of free water exceeds the output drainage capacity of the snow pack. Frozen ground are therefore a component that is associated with slushflows as it eliminates the possibility of water to drain out of the system through the soil (Onesti, 1987). An impermeable ice layer or a rock surface may cause the same conditions (Hestnes, 1985). Slushflows may flow at gradual slopes, unlike debris flows

and debris avalanches. They are likely to initiate at slope angles below 15° degrees (Gude and Scherer, 1998). The slope gradient may vary along its track (Hestnes, 1985).

The occurrences of slushflows are associated with the period of when melting of snow occurs (Onesti, 1987). Spring is the most likely period to initiate slushflows within the study area. Temperatures may increase rapidly at this point of year at which accumulated snow from the winter starts to melt. However, slushflows can appear if the area experiences a sudden warm period after days of considerable amounts of snowfall (Onesti, 1987). These conditions are typically present in late autumn/early winter. Temperature decreases towards winter and large amounts of snowfall is likely to build up considerably layers of snow. However, the climatic conditions at this point of year are often unstable in the region. A cold meteorological period with precipitation may therefore be followed by a rapid increase in temperature. It can result in rapid melting that could create favourable conditions for slushflows, especially in combination with rainfall.

Figure 9. Example of a slushflow event from Flesje in the municipality of Balestrand, 2011. Event killed two people. Photo: Arve Uglum / NRK.

2.2 Landslide inventory map and magnitude-frequency curves

A landslide inventory map is defined by Guzzetti et al. (2012) as a record of historical landslides. The record contains valuable information of the event like location, date of occurrence (when known) and the type of mass movement that were present (Guzzetti et al.,

2012). An inventory map is a useful tool by allowing to investigate landslide distribution, typology and recurrence which can be used to perform different types of risk assessment. Extreme precipitation events have, as mentioned in chapter 2.1.2, through several studies been linked to the initiation of debris slides, debris avalanches, debris flows (Johnson and Sitar, 1989, Cruden and Varnes, 1996, Hungr et al., 2001, Corominas et al., 2014) as well as slushflows (Gude and Scherer, 1998, Decaulne and Sæmundsson, 2006). The objective is usually to determine the component of rainfall which can explain the instability and hence the triggering of landslide (Corominas et al., 2014). Historical events have shown that landslides can cause fatal damages to society, like the Vargas State disaster in Venezuela where debris avalanches and debris flows killed approximately 15000 people (Larsen and Wieczorek, 2006, Hungr et al., 2014).

Landslide frequency and magnitude are important components for the quantitative assessment of risk and hazard (Corominas and Moya, 2008). Finding the landslide frequency allows you to e.g. perform hazard zoning that can be valuable for land-use planning purposes. The probability, or frequency, have normally been studied from two different approaches (Corominas and Moya, 2008). Either determined by calculating the probability of slope failure (Gokceoglu et al., 2000, Silva et al., 2008) or by performing statistical analysis of historical landslide events (Larsen and Torres-Sánchez, 1998, Flentje et al., 2011, Guzzetti et al., 2012). The second option requires a near-complete landslide inventory with information regarding historical and recent landslide events. Landslide risk analysis requires also knowledge of the hazard probability of occurrence as well as the potential severity of harm it may cause. Magnitude is therefore a crucial component to the quantitative risk analysis as it can help to define the extent of the landslide and hence its consequences (Hungr et al., 2008). Both magnitude and frequency can be used to help authorities to point out the most vulnerable and exposed areas for the population (Flentje et al., 2011, Corominas et al., 2014). Guzzetti et al. (2012) point out the importance of having a proper landslide inventory that arrange for these types of analysis, as well as other types of landslide analysis to improve risk assessment. Important components like landslide distribution, patterns, susceptibility, hazard, vulnerability and risk have been analyzed closely from such inventories (Guzzetti et al., 2012).

Previous studies have been investigated typical landslide magnitudes and frequencies in different regions by performing a magnitude-frequency analysis (Guthrie and Evans, 2004, Hungr et al., 2008, Stoffel, 2010, Dahl et al., 2013). However, no similar magnitude-

frequency study has been performed in Norway so far. The probability and frequency of landslide magnitudes can be prepared from either cumulative statistics or non-cumulative statistics, with each of them having advantages and disadvantages (Guzzetti, 2005). Guzzetti (2005) point out that cumulative distributions have been a preferred approach because 1) it may be derived from a very small dataset of landslides and 2) cumulative distribution and required statistics are simply to obtain. However, Guzzetti (2005) conclude that a non-cumulative distribution is a more accurate approach to investigate the relation of magnitude and frequency and the point of roll-over is established with a higher accuracy from this distribution. Stark and Hovius (2001) explains that a cumulative distribution will hide the roll-over point due to integration smoothing. Furthermore, the data are one-sided with the residuals asymmetrical distributed when a regression fit commonly assumes normally distributed residuals (Stark and Hovius, 2001). An example of a non-cumulative distribution of probability density and landslide magnitude expressed as landslide area (m^2) is shown in figure 10.

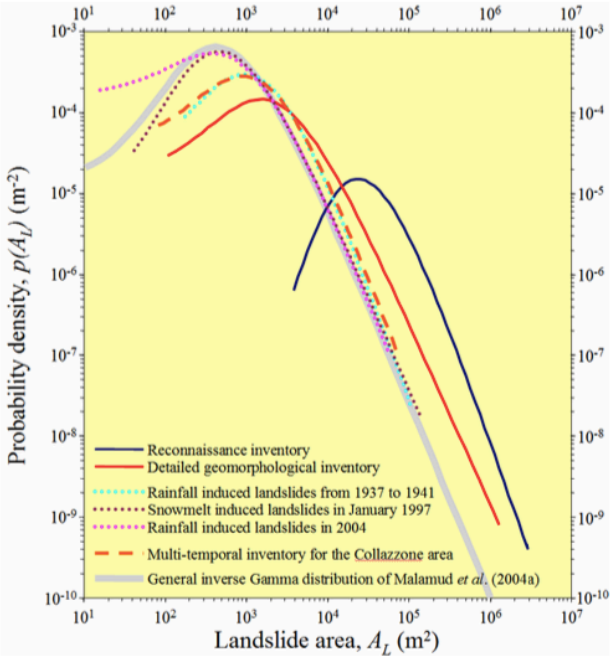

Figure 10. Example of a non-cumulative landslide distribution that shows the probability density in relation to landslide area (m²) for different landslide inventories (Guzzetti, 2005).

A magnitude-frequency analysis, performed with a cumulative distribution, was accomplished in British Columbia by Guthrie and Evans (2004) on a storm event that triggered 101 landslide events. The aim was to strengthen the theory of the roll-over - the point at which landslide magnitudes can be described by a mathematical power-law relationship. For this

approach, they prepared a landslide inventory through fieldwork and aerial photo interpretations (API). A total of 101 events were mapped from the storm event. Furthermore, all data was processed in the software GIS where statistical parameters were calculated. A power-law relationship for landslides was found in their magnitude-frequency plot for landslide magnitudes larger than 1000 m^2 (figure 11a). Regarding the roll-over effect, they argue it to not represent an error of API censoring. A similar research was performed by Dahl et al. (2013) that generated a debris slide inventory map from the Faroe Islands. Their goal was to provide data for hazard and risk assessment for landslides in soil. The landslides were mapped through API and later verified through fieldwork, local photographs, newspaper articles and anecdotal sources. Their magnitude-frequency relationship (cumulative distribution) showed the same trend as for Guthrie and Evans (2004), however, with their magnitude expressed as topographic scar area (m^2). A power-law relationship was derived, with its steepening trend discussed as a result from the limitations of the landscape in the Faroe Island (figure 11b). The observed events above the roll-over point was argued, distinct from Guthrie and Evans (2004), as an error of API censoring as well as shallow landslides being prevented by cohesion within the soil.

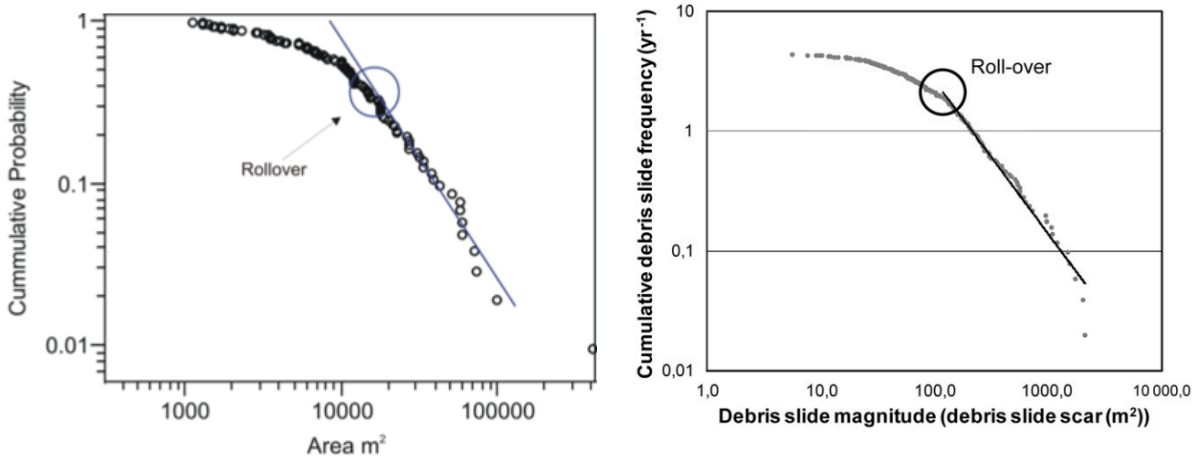

Figure 11. A) M-F curve from British Columbia by Guthrie and Evans (2004). Point of roll-over and the power-law are visualized. B) M-F curve from the Faroe Islands by Dahl et al. (2013). Point of roll-over and power-law are visualized.

2.3 Landslide Early Warning Service

2.3.1 General

Landslide EWS has been developed as a tool to predict the occurrence of both slow moving and rapid moving landslides aiming to improve the preparedness and to reduce economic and

human loss. Awareness or warning levels have been established and warning messages are issued if landslide risk is considered as high.

There are few countries in the world that operate landslide EWS at regional and local scale for rainfall-induced landslides (e.g. Italy, USA and Norway) (Devoli et al., 2018). The Norwegian one discussed herein, is among of them. The Italian EWS (Regional Agency for Environmental Protection), with the administrative region ARPA Piemonte deals, with landslide assessment and issues warning messages for a certain region (Devoli et al., 2018). Their objective is to improve the state of preparedness, increase safety and predictability as well as save lives by reducing landslide risk. They operate with three models that evaluates the risk differentiated between landslide typologies with all of them using empirical rainfall thresholds designed for different slope processes (Devoli et al., 2018). Segoni et al. (2018) have also investigated whether they can implement soil moisture conditions to play a more important role in the EWS. Another landslide EWS prototype is under development in Seattle, Washington area in USA. Their EWS uses real-time monitoring of precipitation, pore pressure, soil moisture, automatic tracking of rainfall relative to the thresholds and finally a decision tree to help to interpret the thresholds to determine warning level (Baum and Godt, 2010). Both the American and Italian landslide EWS operate with 4 warning levels.

The landslide EWS for Norway was established by NVE the 21`st of October 2013 after a testing period of two years (Boje et al., 2014). The service aims to warn regional and local authorities and increase their state of preparedness so that rainfall-induced landslides can be handled in a way to reduce any possible damage to infrastructure or population (Colleuille et al., 2017). The forecasting service do not consider the prediction of rock fall, rock avalanche, clay- and quick-clay avalanches. A warning message is issued for several counties or as a composition of vulnerable municipalities (Krøgli et al., 2018).

The warning has a total of four awareness levels. These are presented in table 2 where a general explanation for each awareness level is given, as well as the classification criteria that are used to evaluate the performance of the landslide EWS. Each level refers to a state of preparedness that should be performed by authorities to deal with the expected outcome of the event in a proper way. The prediction requires forecasting of variables that contributes to the water input in the area which consequently affects the landslide risk. That is why NVE uses a climatological GWB-model (Gridded Water Balance). The model divides Norway into grids of 1 km^2 where variables like soil saturation capacity, runoff, melting of snow, groundwater

level and presence of frozen ground can be simulated (Colleuille et al., 2017). Estimates of precipitation and temperature are given by the Meteorological Institute. These are all valuable to define if a region are at risk of landslides or not (Krøgli et al., 2018). Each grid interpolates temperature and precipitation as a function of distance to nearby weather stations, together with mean height for the grid cell (Lussana et al., 2018). There are also tools or applications that are used by experts, like xgeo.no, that are used for different purposes like monitoring, decide state of readiness and for flood- and landslide warning evaluations (Colleuille et al., 2017).

Table 2. The Norwegian Landslide EWS warning table is presented. There are four levels of landslide warning, each with an associated general description of the situation, together with the expected outcome. Classification criteria is used for validation of performance. Modified from NVE (2018) and Piciullo et al. (2017)

Level	General Explanation	Classification Criteria used to Evaluate the Performance of the Landslide EW
4	• Extreme situation that occurs very rarely and that requires immediate attention. • Many landslide events are expected, several with considerable consequences	• > 14 landslide events • Large and smaller landslides are expected in many numbers and within a large geographical area. • Several road blockings due to landslides or flooding.
3	• Severe situation that occurs rarely that requires preparedness. • Many landslide events are expected, some with considerable consequences.	• 6-10 landslides • Large and small landslides are expected in an area of about 10-15.000km^2. • Several road blockings due to landslides or flooding.
2	• Situation that requires vigilance. • Some landslide events are expected, certain large events may occur.	• 1-4 landslides • Expected in an area of about 10-15.000km^2. • Flooding/erosion in streams
1	• Generally safe conditions	• No landslides are expected • 1-2 landslide may be triggered from local rain showers. • Man-made landslides may occur

2.3.2 Thresholds

Different hydro-meteorological parameters are now predictable and enables the possibility to forecast landslide hazards (Krøgli et al., 2018). Rainfall-thresholds are therefore applied in operative landslide EWS, like in Italy and Norway, as an mitigation measure to predict landslide risk (Krøgli et al., 2018). The established thresholds in the Norwegian landslide EWS are based on the soil water saturation degree, given as percentage of the maximum soil saturation simulated in the reference period from 1981-2010, and the water supply relatively to mean annual water supply from 1981-2010 (Boje et al., 2014, Krøgli et al., 2018). The relative water supply is a product of rainfall if no snow pack is present, or as water input from both rainfall and water drainage from the snow pack (Krøgli et al., 2018). Figure 12 presents the established Hydmet-threshold plot (hydro-meteorological index) that has been obtained for the region, based on previous landslide events and their associated hydro-meteorological

conditions. The threshold limits are shown as colours and refers to the different awareness levels.

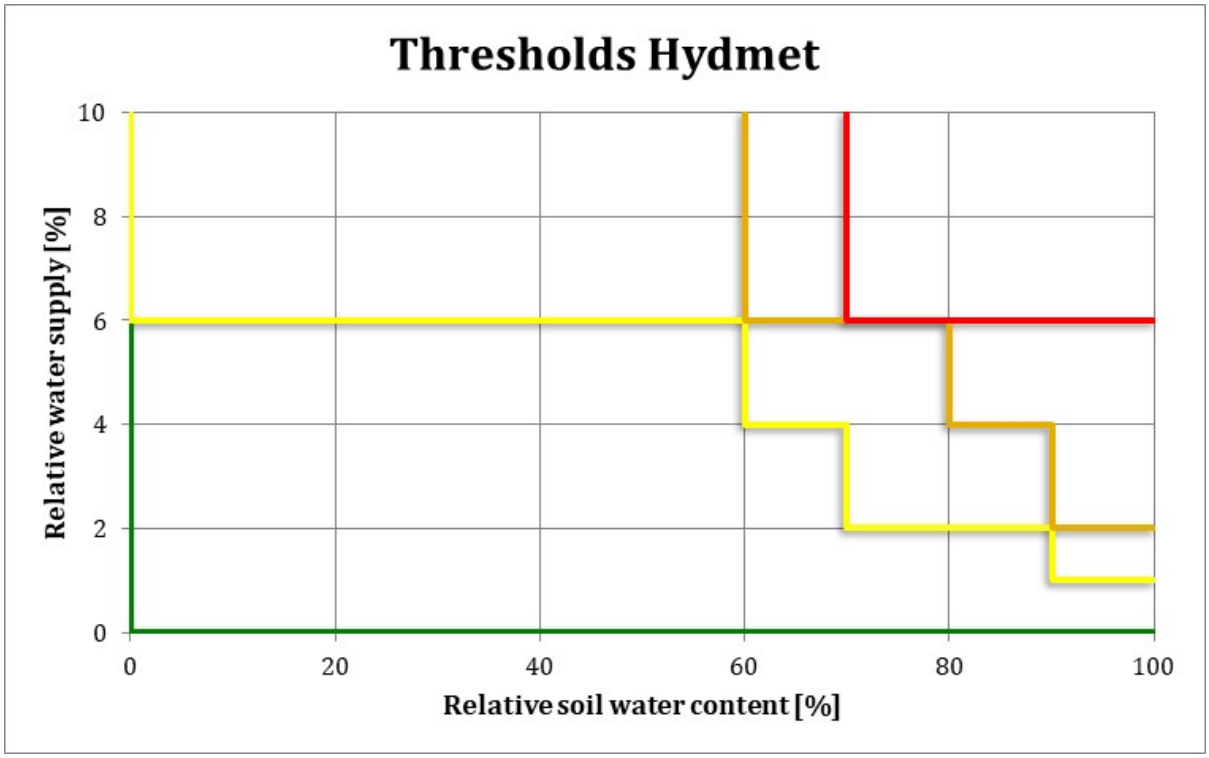

Figure 12. The threshold limits that are obtained for the region are presented. The water supply is relatively to mean annual water supply from 1981-2010. The soil water saturation degree is given as percentage of the maximum soil saturation simulated from 1981-2010 (Boje, 2017).

3 Study area

The county Sogn og Fjordane is located in Western Norway (figure 13). It borders to Hordaland county in the south, Møre og Romsdal in the North and Oppland and Buskerud in the east. It is 18622 square kilometers big that includes surfaces of water, and has a total of 106194 inhabitants, January 1. 2017; (Statistisk-Sentralbyrå, 2017a). The city of Førde is the most populated with 10255 inhabitants, January 1. 2016; (Statistisk-Sentralbyrå, 2017b).

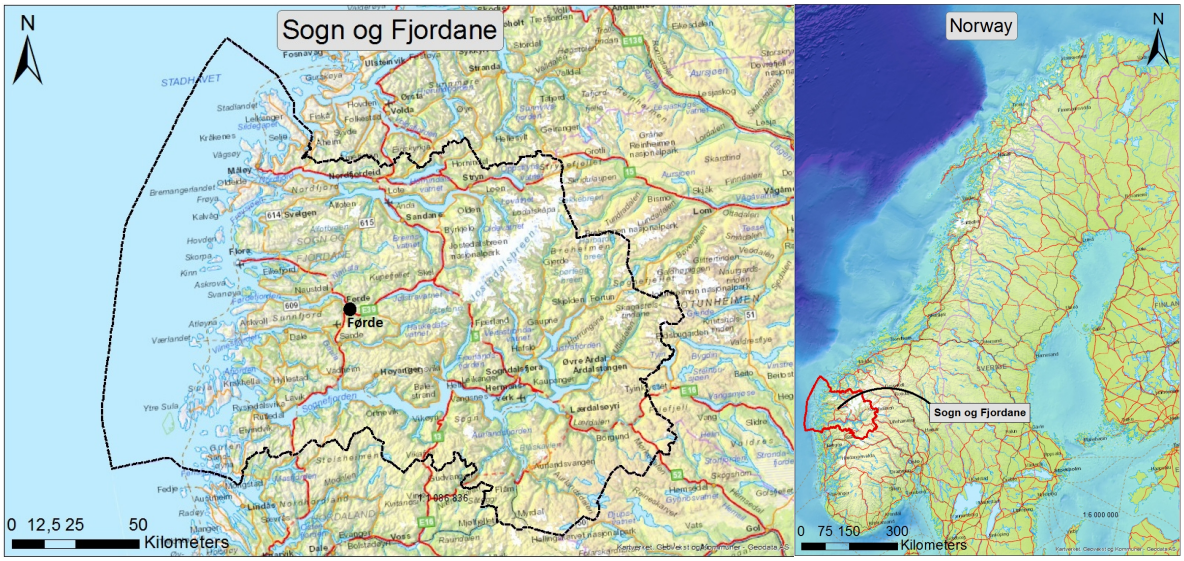

Figure 13. Sogn og Fjordane is in the western part of Norway with Førde being the most populated city.

3.1 Landforms and geology

Glaciers, fjords, alpine mountains and coastal strandflats are all characteristic landforms in the region (figure 14). An automatic regional classification of the Norwegian landforms and topography was proposed by Etzelmüller et al. (2007). Based on this classification it is found that the region consists mostly of either hills with accentuated relief with moderate slopes, plains and strandflat or as glacially scoured low mountains and valleys. The landform classified as alpine relief or glacial relief with steep slopes of heavily over-deepened glacial valleys are present further inland as well as high paleic mountains with glacial incisions consisting of mostly moderate slopes. Some areas of higher mountain plateaux are present. Figure 15 shows the great variety in elevation for the region. The highest elevated areas are in the eastern parts of the region and have a decreasing trend in elevation towards the coast. The municipality of Luster claim the highest mountain peak at 2405 meters with Store Skagastølstind (Kartverket, 2017).

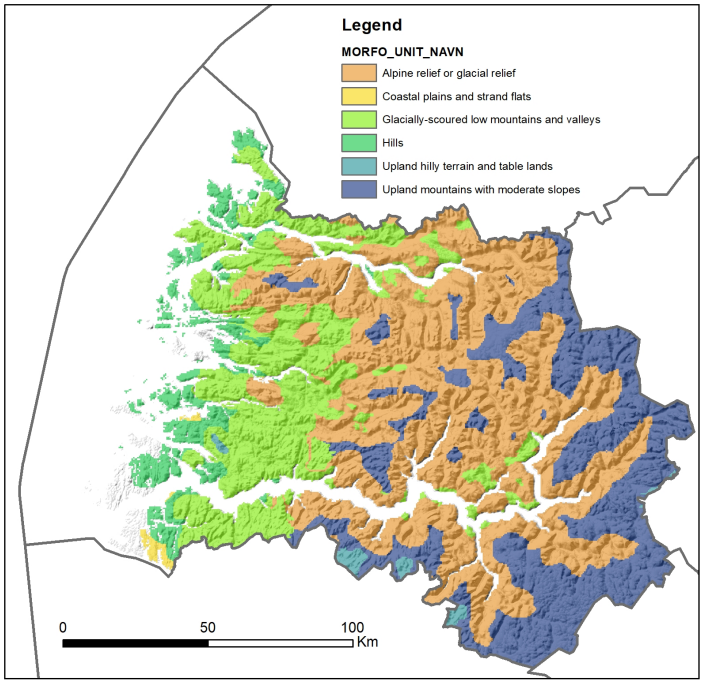

Figure 14. The distribution of landforms for our region is presented, based on a regional landform classification (Etzelmüller et al., 2007)

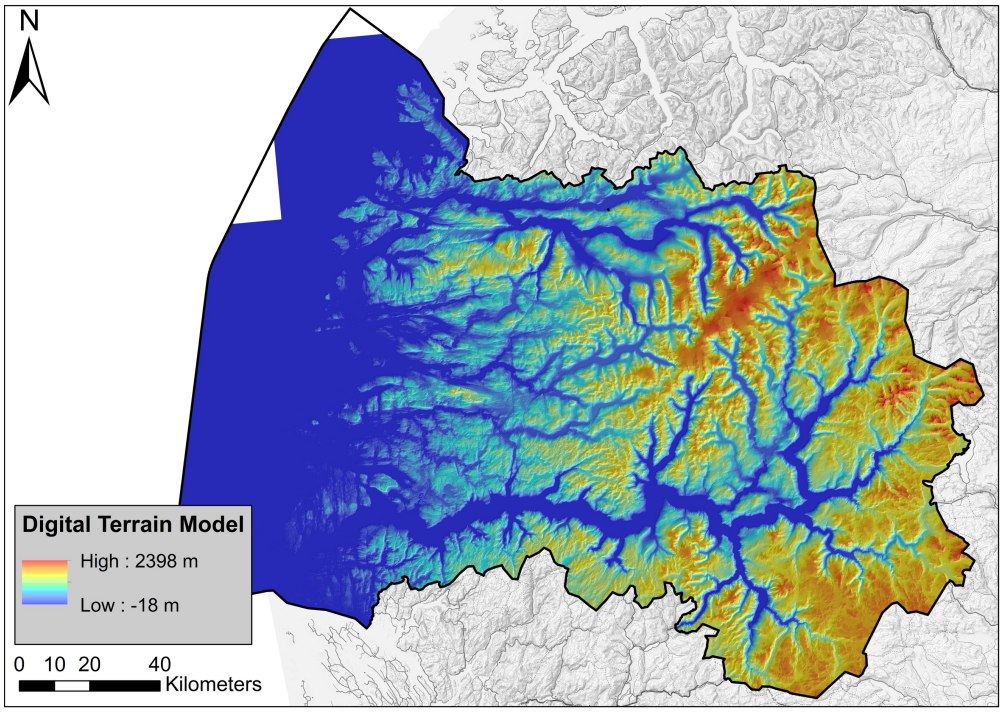

Figure 15. A digital terrain model presents the elevation for the region.

Jostedalsbreen is one of the glaciers located in the region (figure 16) and are in addition the largest glacier in Norway with an extinction of 474 km^2 (NVE, 2017a). Glaciers located close to the coast is found to have a high mass turnover, compared to glaciers located further inland (Andreassen et al., 2005). The glaciers within the region are classified as maritime as a response to their dependency of their winter balance.

The landscape is dominated by three major fjords in west-east direction, Sognefjorden (the southernmost fjord), Førdefjorden (fjord in the middle) and Nordfjord (the northernmost fjord). The fjords have been formed through several glaciations (Vorren and Mangerud, 2013). The process started when the land surface begun to rise in Paleogene 66 million years ago and in Neogene 23 million years ago (Vorren and Mangerud, 2013). River currents begun to erode in the ground and started slowly to form river shaped valleys. Glaciers moved along these already existing river valleys and eroded them even deeper and wider over time, while the mountainsides became steeper (Vorren and Mangerud, 2013). Some glaciers managed to dig beneath the ocean floor that created some of the fjords we see today (figure 16). Sognefjorden is the longest fjord in Norway with a total length of 205 km and with a maximum depth of 1308 metres. However, glaciers that didn't reach the ocean floor can be seen as U-shaped valleys in the landscape (Erikstad et al., 2009).

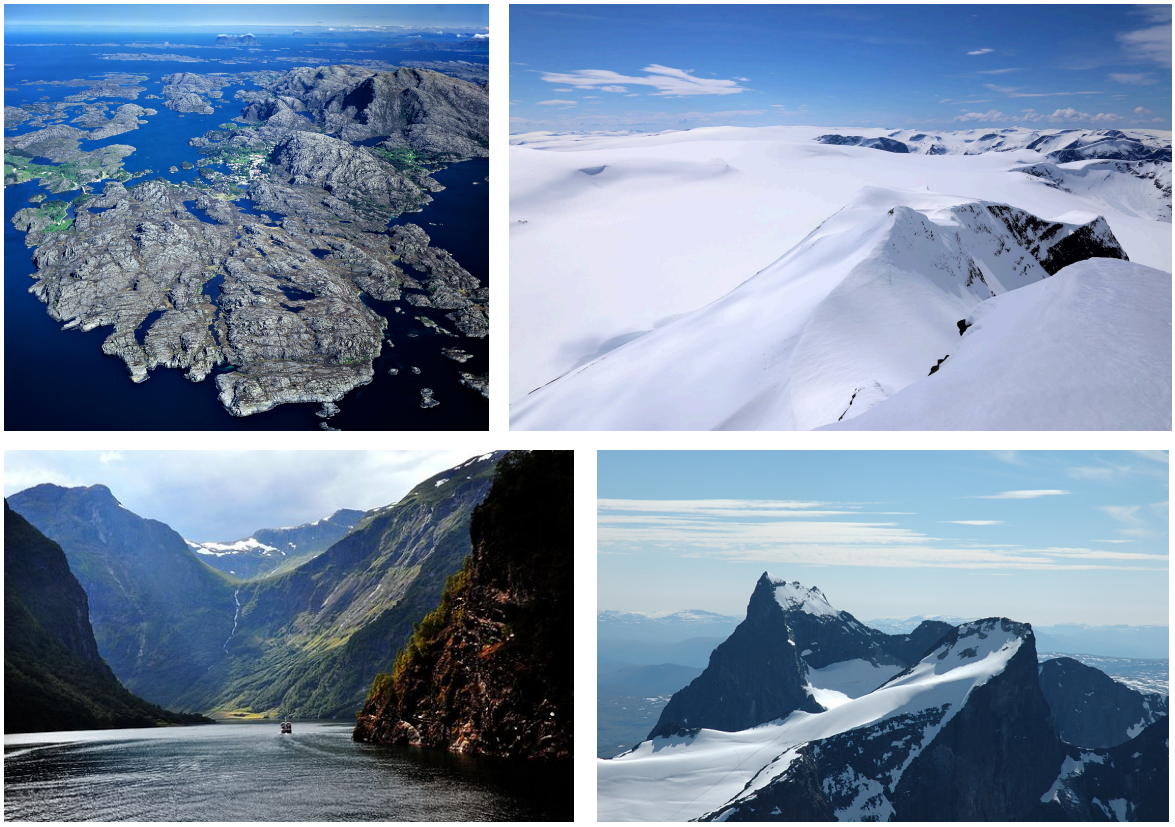

Figure 16. Illustrative pictures from the varied landscape of Sogn og Fjordane.

The rivers in the landscape are commonly seen as steep, with a short travel path from their starting point towards the fjord. They are typically seen along the fjords because of the presence of steep valleys in these areas. Rivers located at mountain plateaus are more common for having longer paths due to a reduction in slope gradient. The distribution of slope

gradients in the region is presented in figure 17. Surrounding valleys of fjords and lakes have typically the highest slope angles.

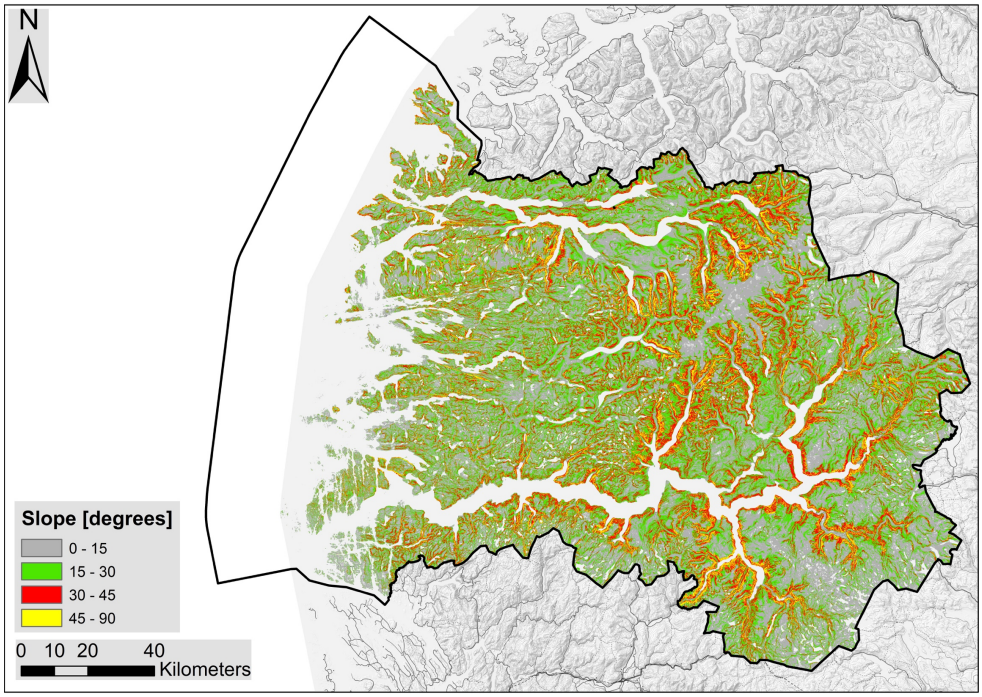

Figure 17. Slope angles for the region are presented.

Coastal areas have limited amount of vegetation and consist mostly of heather and swamps (Puschmann, 2005). The vegetation becomes more varied further inland as a respond to increasing precipitation and by increased distance to the coast. Heather dominated forests of birch and pine are common, in addition to planted forests of spruce (Puschmann, 2005). The climate becomes colder with a reduction in precipitation in the inner parts of the fjords. Larger areas consisting of pine are typically to be found here, normally on top of shallow soil or gravel deposits (Puschmann, 2005). Planted spruce are commonly seen at hillsides along the fjords or up the valleys. Regarding the tree line, it increases from the coastal areas towards the inner part of the region.

A comprehensive part of the region consists of bedrocks from the Pre-Cambrian period. These rocks are forming a complex called Vestre Gneisregionen and consist mainly of granite, gneiss and migmatite (Nordgulen and Andresen, 2013). Migmatite is commonly found with layers and lenses of mica and amphibolite. The coastal areas have great zones consisting of Devonian sediments with conglomerate and sandstone as the most frequent type. They descend from the wear-down of the Caledonian mountain range (Nordgulen and Andresen, 2013). The quaternary map presented in figure 18 shows a thin disjointed layer of soil that is covering the bedrock of most of the region. Certain areas are covered by glacial deposits like

thick moraine, glacio-fluvial or glacial-lake deposits and melt-out till. Deposits from previous landslides are also widely distributed in the region while some smaller areas are covered by unspecified fluvial deposits and thick layers of oceanic and fjord-deposits. Some organic material of peat or mud can be found as well.

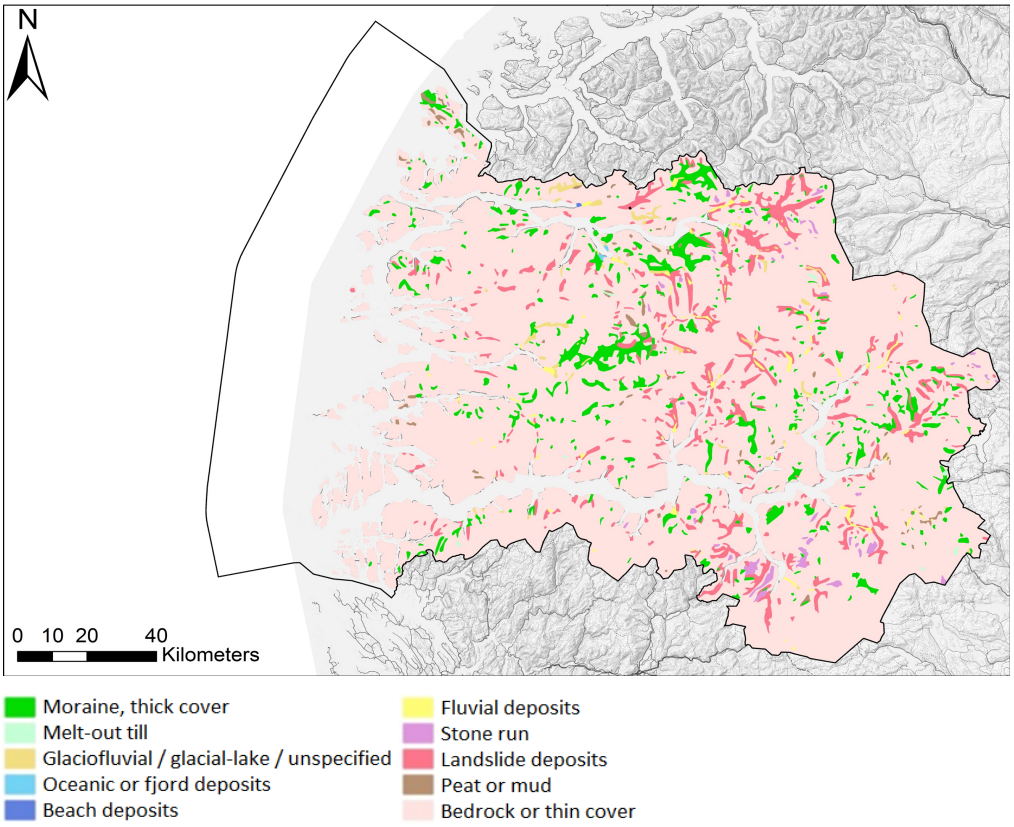

Figure 18. The quaternary map shows the distribution of different deposits for the region. Quaternary map was downloaded from NGU at: http://www.ngu.no/emne/datasett-og-nedlasting

3.2 Climate

3.2.1 Precipitation and Temperature

The annual precipitation in the region, normalized from 1961-1990 (www.senorge.no), is presented in figure 19. The climate in the region is widely controlled by the mountains and their effects on the large-scale wind currents (Barstad and Grønås, 2005). Wind currents bring moist air from the ocean, which is forced upwards and cooled down when it hit the mountains that causes it to condensate (Førland, 1979). This orographic effect, due to elevated terrain features, will intensify the precipitation especially during autumn and winter (Førland, 1979). A sample of gauge stations along Sognefjorden and Nordfjord were also chosen to visualize the spatial and temporal differences in received amount of precipitation within the region (figure 20). The gauges are all located below 100 meters a.s.l. and are thought to represent the

different geographic features in the region, from coastal areas towards the innermost areas.

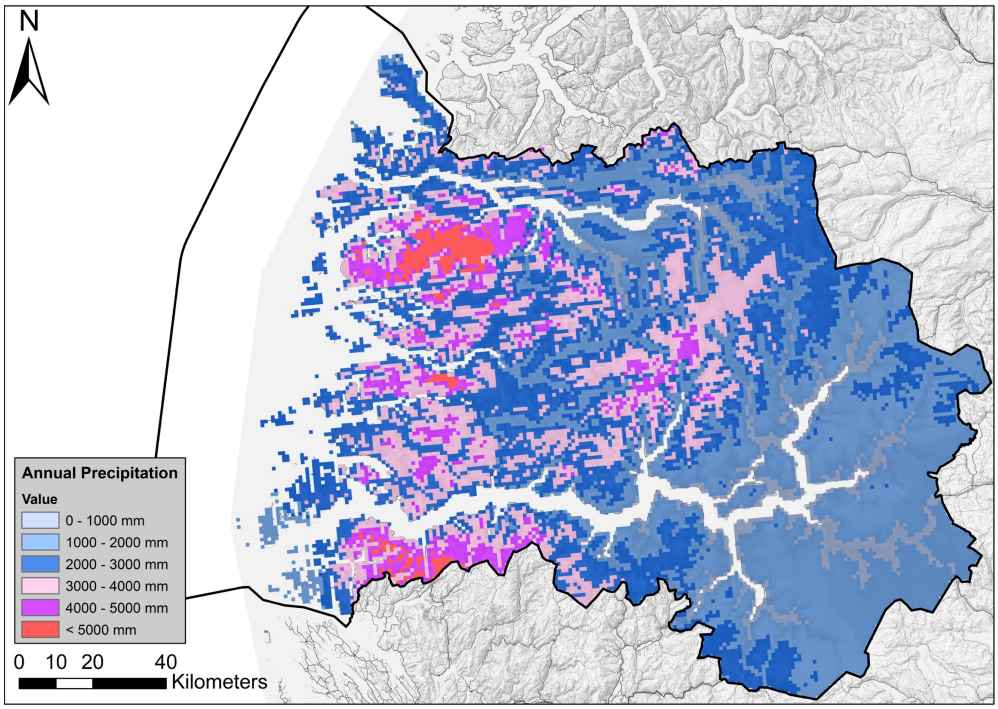

Figure 19. The annual precipitation for the region normalized from 1961-1990. Extracted from www.senorge.no.

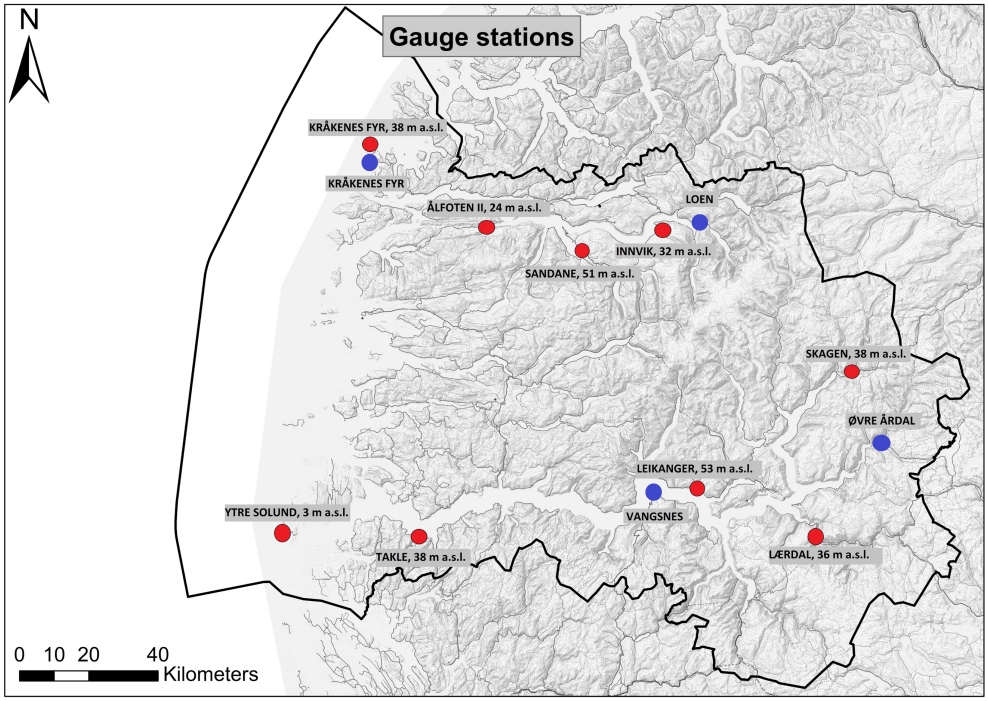

Figure 20. Data of precipitation (red color) and temperature (blue color) were collected from a sample of gauge station in the region with some of them located along Sognefjorden and some along Nordfjord. Both temperature and precipitation are normalized values from 1961-1990.

The analysis of climatic data presented in figure 21 and 22 shows that coastal areas, represented by gauges at Ytre Solund and Kråkenes Fyr, receive 1000–2000 mm of precipitation a year. The amount of precipitation increases greatly the following kilometres

inland as also observed in figure 20. The gauge station "Takle" is located within this region and receives approximately 3200 mm a year. The precipitation is found to decrease further inland with the gauge "Lærdal" receiving about 500 millimetres a year. Regarding seasonal differences, the precipitation is greatest during autumn and winter while spring and summer are drier. There is slightly more precipitation in coastal areas in the south compared to the north when considering differences in precipitation with change in latitude. However, the opposite is seen when considering gauges further inland where the stations along Nordfjord is found to collect a bit more precipitation throughout the year than the stations along Sognefjorden. The innermost station at "Skagen" in the municipality of Luster receives an annual amount of 735 millimetres compared to Lærdal`s 500 millimetres.

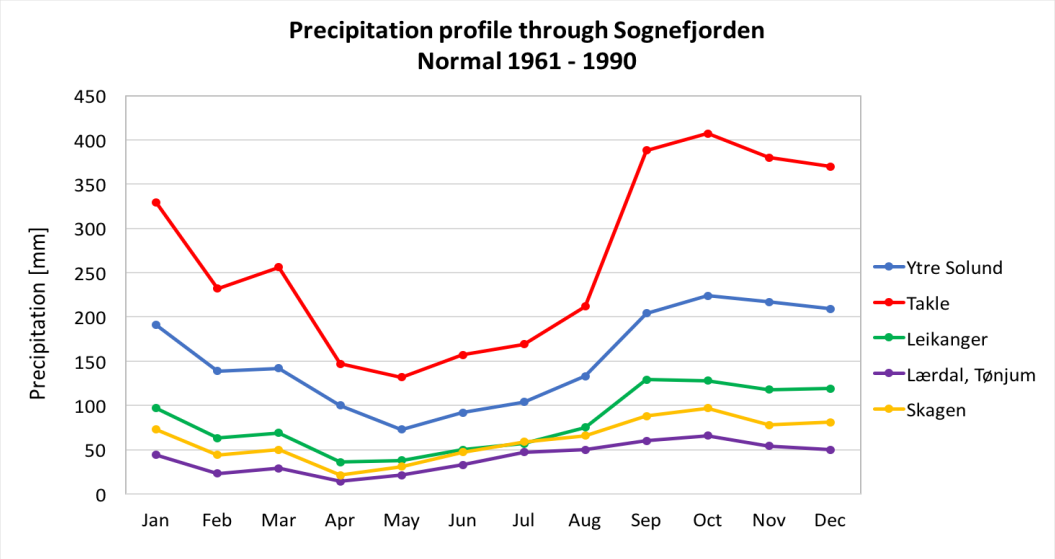

Figure 21. A sample of gauge stations along Sognefjorden presents normalized precipitation values from 1961-1990. Data extracted from: www.eklima.no.

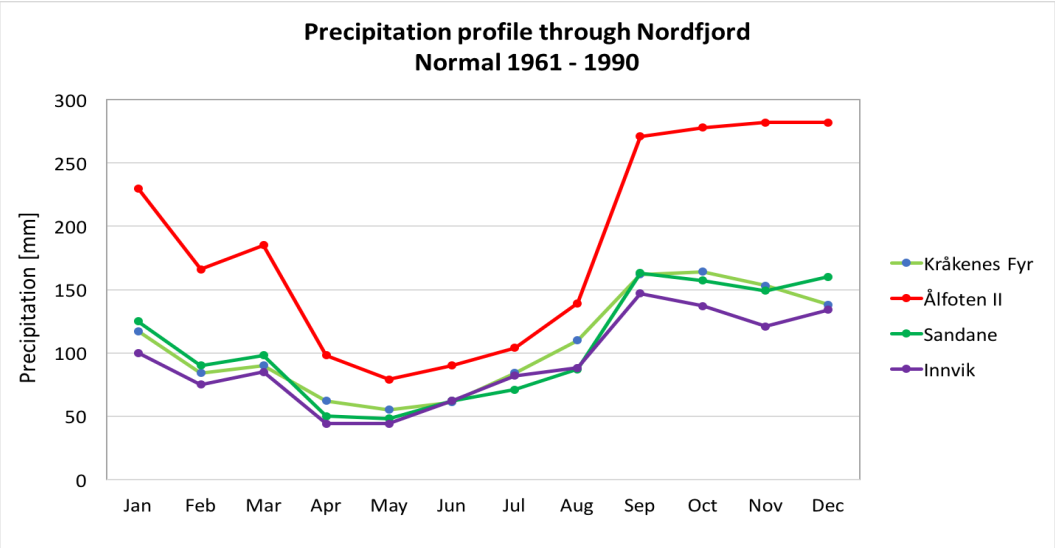

Figure 22. A sample of gauge stations along Nordfjord presents normalized precipitation values from 1961-1990. Data extracted from: www.eklima.no.

Most of the intensive precipitation falls within the range between 150-300 metres a.s.l. in the region (Førland, 1979). However, the study by Førland (1979) claims the distance to the coastal line to better explain the variation in precipitation that can be seen from my previous plots. The innermost areas (distances above 45 kilometres from coastal line) will be spared from the most intensive precipitation as a natural respond to the drying of air when it condensates over the mountain peaks.

Estimates of temperatures in the region, normalized from 1961-1990, were gathered from a sample of stations as seen from figure 20. The temperature varies from the coast to the innermost fjords. From figure 23 it is seen that the coldest month in the innermost parts are January with an average temperature of -3° to -6° Celsius. Coastal and near-coastal areas have the coldest temperatures in February with an average temperature of 1° to 2° Celsius while august is the warmest month with an average temperature of approximately 14° Celsius. The innermost areas have their highest average monthly temperature in July at 14 - 17° Celsius. The seasonal variations are therefore greater for the innermost areas compared to the coastal and near-coastal areas. Observations of temperature and precipitation for the region correlate well with findings from Hisdal et al. (2017) who claims coastal areas to have a maritime climate while it changes to a more continental climate towards east. Coastal areas are therefore mild and receive a lot of precipitation while the continental areas experience greater differences in temperature with less annual precipitation.

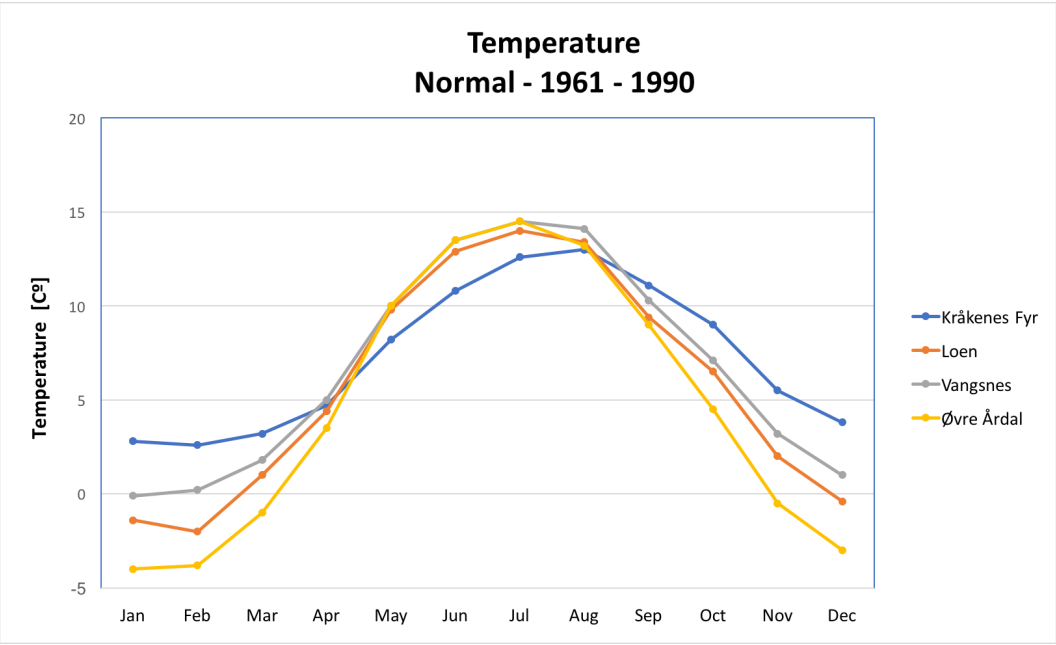

Figure 23. A sample of gauge stations in the region presents the normalized temperature in the period from 1961-1990. Data extracted from: www.eklima.no.

3.2.2 Climate change

Landslides are strongly linked to climatic conditions with intensive rainfall, melting of snow and temperature being components that play an important triggering role (Hungr et al., 2001). These components are expected to change in respond to climate change and are therefore thought to increase the number of people being exposed to landslide risk (Gariano and Guzzetti, 2016). Stability of both natural and engineered slopes are one crucial component that are thought to change (Seneviratne et al., 2012). However, it is still difficult to determine where, and if the landslide risk will increase or decrease as a direct or indirect respond to the change in climate (Gariano and Guzzetti, 2016).

The following scenarios from Hisdal et al. (2017) describes the expected change of precipitation and temperature in the region by comparing the period from 1971-2000 to 2071-2100. The annual temperature will increase with approximately 4.0° degrees. The increase is found to be greatest for autumn, winter and spring but less prominent during summer. Moreover, there will be fewer days with considerably low temperatures during winter. It will result in a reduced amount of snowfall as well as fewer days with snowfall. The effect will be more prominent in areas with winter temperatures already varying around 0° Celsius. Regarding summer, there will be more frequent days with mean temperatures above 20° Celsius. The annual precipitation is thought to increase with approximately 15 % in the region. Summer and autumn are expected to have an increase of 15% while winter and spring have about 10 % of increase. The increase is primarily thought to comprehend the near-coastal areas that already receive the greatest amounts of precipitation. The number of events with extreme precipitation is thought to increase, both in intensity and frequency. Table 3 summarize the most important findings from expected change in climate and its influence on precipitation and landslide behaviour.

Table 3. Table summarizes the most important findings of change in precipitation and landslide behaviour (Hisdal et al., 2017).

Event type	**Explanation**
Extreme precipitation events	An increase in number of events with intensive rainfall, both in frequency and intensity.
Rainfall- and snowmelt-induced landslides	Increased frequency due to frequent days with intensive precipitation.
Rock fall and rock avalanches	More frequent events due to frequent days with intensive precipitation

3.3 Landslide activity

My region is known to be prone to landslides. One way of improving the landslide EWS in my region is to produce susceptibility maps. These maps aim to identify potential slopes that may initiate a landslide, based on topographic parameters and hydrological models (Bargel et al., 2011). It exists many national maps that shows the landslide susceptibility for my region and two of them are presented in respectively figure 24 and figure 25. The first one presents susceptible areas on local scale (Fischer et al., 2012). It shows specifically where landslides may occur by indicating their source area, track and runout distance (Krøgli et al., 2018). Topographic and hydrological settings are considered to point out source areas while a runout model is used to estimate the maximum runout distances. The map is useful in the communication-phase in the EWS by presenting landslide susceptibility together with warning zone and warning level at varsom.no (Krøgli et al., 2018). Susceptible areas are seen to be located over the entire county, with the highest density observed in the innermost valleys and fjords and with a lower density observed for coastal and near-coastal areas.

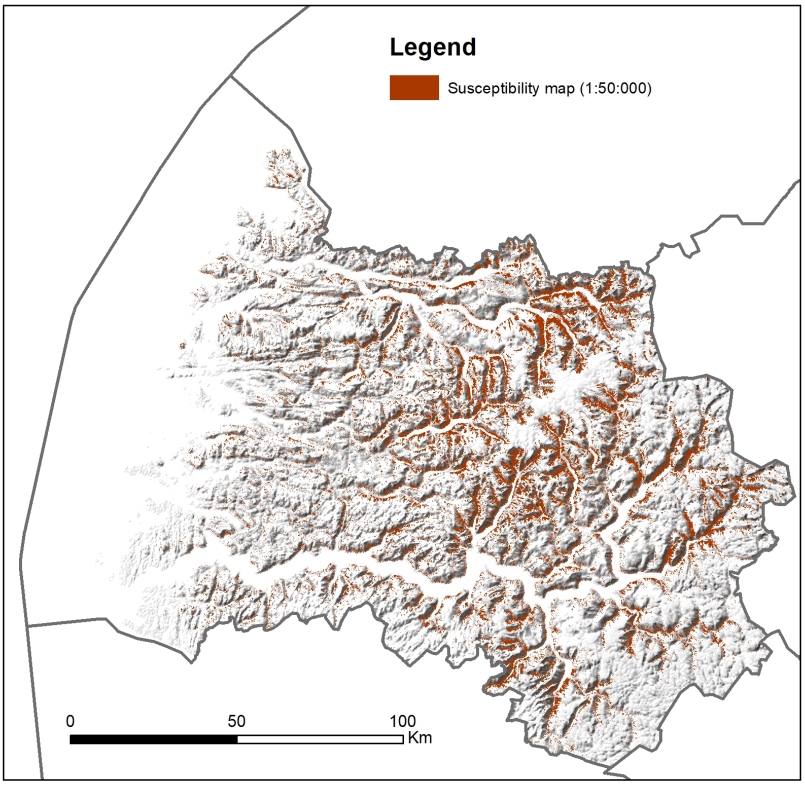

Figure 24. Landslide susceptibility map for the region. Available from (Fischer et al., 2012)

The second susceptibility map, from Cepeda and Bell (2014), classifies the landslide susceptibility at a catchment level as either very high, high, moderate or low for the region

(figure 25). Some of the components that are used are quaternary deposits, land cover data, slope angle, average yearly rainfall data and various water runoff variables (Cepeda and Bell, 2014). This map have been used to improve a threshold map that are used by forecasters in the initial phase of the EWS to perform more accurate assessments (Bell et al., 2014). Great zones of very high susceptibility are located over the entire county, especially in the innermost areas.

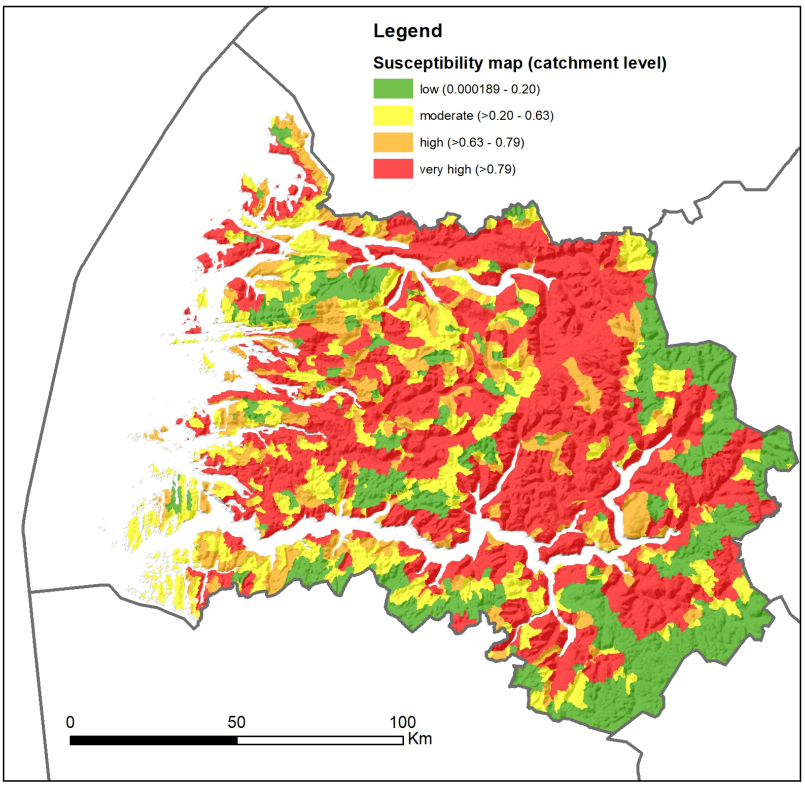

Figure 25. Susceptibility map on catchment level for the region. From Cepeda and Bell (2014).

4 Data

Reliable analysis of risk and hazard in relation to landslides requires a systematic registration of historical and recent landslide events. The national mass movements database NLDB contains all registered historical and recent landslides and snow avalanches in Norway. They are given as point coordinates together with event-information organized in an attribute table. The database can be used to perform hazard and risk evaluations. However, the quality of data and amount of information varies considerably. Improving data quality has therefore become important due to the increased interest of performing hazard analysis. It needs to be accomplished before any type of analysis is undertaken, as also indicated in (Sokalska et al., 2015). Better quality will lead to more reliable and accurate results for prospective analysis.

Since year 2000, NGU started the process of coordinating a gathering of mass movement data into one single database. Since then there has been a collaboration between several institutions. The institutions that participate to its development are the Norwegian Public Road Administration (SVV), the Geological Survey of Norway (NGU), the Bane NOR, the Norwegian Geotechnical Institute (NGI) and Norwegian Water Resources and Energy Department (NVE) (Sokalska et al., 2015). The NGU has registered historical landslides by looking through church books, old newspapers and periodicals to find all events that have caused damage to humans, properties or cultivated land (NVE, 2017b). The Bane NOR has the responsibility of registering landslides that affect the railroads in the country (NVE, 2017b). Likewise, the Norwegian Public Road Administration (SVV) has the responsibility to register landslides or flood events that affects the roads in the country. Employees from the regional office at NVE and the forecasters of landslides and snow avalanches at NVE have been collecting daily data more or less since 2013. The data can be registered through the application www.skredregistrering.no or through regobs.no and can be visualized through several portals like, NVE atlas.no, xgeo.no or kartkatalog.nve.no.

The responsibility of further developments and management of the database was given to the NVE in 2014. The NVE is also in charge of the web portals (Colleuille et al., 2017). The digital platform of the NLDB, www.skredregistrering.no, can in general be used by municipalities, consultants and public to perform registrations. Registrations may also be performed through regOBS that is an open platform where public can share their observations. It is used to send and share field-data for any observation, warning-sign or

events that are used for warning and preparedness purposes (Colleuille et al., 2017). This data is transferred to the NLDB within 48 hours (NVE, 2017b). The version of the NLDB applied herein is from 30.08.2017 and was extracted from the open-access web portal of the NLDB at www.skredregistrering.no. It contains data for 61639 events from the entire country, ranging from year 800 until 24.08.2017.

Table 4 shows an example of how particular events in the NLDB are organized in an attribute table. The amount of information can for some events be great, which is why the information is sorted in different columns (date of event, name of location, typology etc.). Each event has its own landslide-ID and point coordinates. These coordinates point out the location of the event which has been decided by the responsible institution of the registered event. The coordinates do most often represent the location where the landslide caused harm or damage to infrastructure or population. However, some of them are located in the source area or at its deposit (Sokalska et al., 2015). Moreover, the coordinates are not necessarily correct, which is why another column indicates the accuracy of the coordinates in relation to the true location of the event (e.g. 10 meters, 100 meters, 10000 meters, etc.). Another accuracy-indicator shows the time of initiation (12 hours, 30 minutes, unsure, etc.). Information in the NLDB that were especially valuable for this research include: name of landslide, typology, damage, weather condition, responsible institution, comments and quality level. The landslides in the database have one of the following typology: debris flow, debris avalanche, debris slide, landslide in clay, rock fall, rock avalanche (different magnitudes), slushflow, snow avalanche, icefall, unspecified slide in soil and unspecified.

Table 4. Example of the attribute table from the national database. It shows some of the data and how it is organized within different columns.

OBJECTID_1 *	Shape *	skredTidsp	OBJECTID	skredID	skredType	skredNavn	stedsnavn	noySkredTi	noyPosis	persBerort
2	Point	24.07.2017	288	{173A9592-23D4-4309	142	Utvik		4 timer	1000 m	Nei
15	Point	24.05.2017	1139	{FF92E897-E7C1-4074	190			Ikke registrert	Ikke reg	Ukjent
4	Point	19.05.2017	364	{C8BA37CF-59A4-472	142	Kråkagjelet, Aurlandsdalen	Kråkagjelet, Aurlandsdalen	4 dager	100 m	Nei
9	Point	09.05.2017	670	{3B9A277A-406E-47C	190	Grasdalen	Grasdalen	Ikke registrert	500 m	Ukjent
3	Point	05.05.2017	323	{FE75F384-C59E-4208	190	Grasdalen infralydanlegg	Grasdalen infralydanlegg	Ikke registrert	500 m	Ukjent
337	Point	12.04.2017	16704	{BC3D1239-F101-4825	190	Napen	Napen	Ikke registrert	Ikke reg	Ukjent
336	Point	08.04.2017	16685	{B94DB713-EEB1-445	190	Napen	Napen	Ikke registrert	Ikke reg	Ukjent

The NVE has the recent years worked to assign a quality level to each record. Criteria have therefore been proposed depending on the accessible information and documentation regarding the event. The information can be derived from field observations, pictures from media, newspaper articles or any other observation or report from institutions. The levels and their requirements are presented in table 5. The quality is given as A, B or C, being A the best

quality. However, this is not being systematically assigned to all registers yet, therefore not all events have a quality designation.

Landslide data was also obtained from other sources of information beside the national database. Data was achieved from newspaper articles, summary reports from NVE, photos, aerial photos, satellite images among others.

Table 5. There are three levels of landslide quality: A, B and C. The quality is based on the knowledge of the landslide event. Modified from (Devoli et al., 2015).

A	B	C
Date: Accuracy +/-1 day or better, or when time of day are unknown. **Position**: Requires either 1) release- and depositional area drawn as polygon or 2) Accuracy of landslide location at +/- 50 metres AND runout area with accuracy of +/- 50 metres or better AND accuracy of release area at +/- 500 metres Correct **Landslide type** **No duplicate**	**Date**: Accuracy +/-1 day or better, or when time of day are unknown. **Position:** Accuracy of landslide location at +/- 50 metres or better. **No duplicate**	Requires that the registration represent a true landslide event and not a false event.

5 Method

The methodology for the research aimed firstly to obtain a first landslide dataset from the national database to explore the regional characterization of rainfall-induced landslides. A dataset of 61639 landslide events was downloaded with 16011 of the data located within my region. The distribution of data is presented in figure 26.

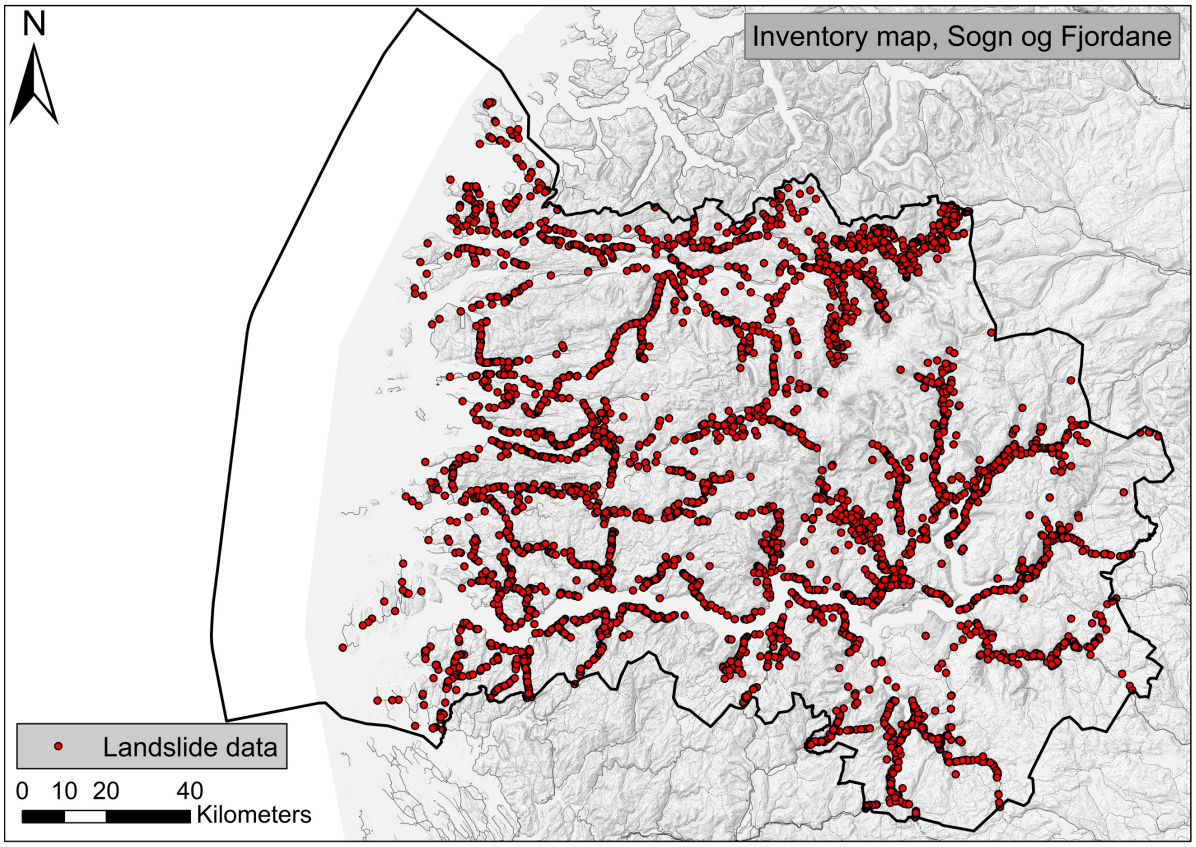

Figure 26. The distribution of data in my region with a total of 16011 landslide events. Extracted from the national landslide database.

Figure 27 presents the work chart that was applied to achieve my objectives. The great number of events and the quality of data in the database led to the necessity of performing different types of filtration due to limited time for the research. A quick selection from a first quality control was achieved where regional characteristics of the landslides were investigated. Then a second quality control was accomplished to complete a landslide inventory map on the extent of landslides to investigate landslide parameters and magnitude. A magnitude-frequency analysis was performed to find typical and frequent magnitudes as well as evaluating the landslide EWS performance and incorporating magnitude into the

warning levels. A threshold-analysis was at last performed, based on the same landslide inventory map. No field work was accomplished due to the fact of the study being a regional research for the entire county. It was not a purpose to visit and do field work for all these events.

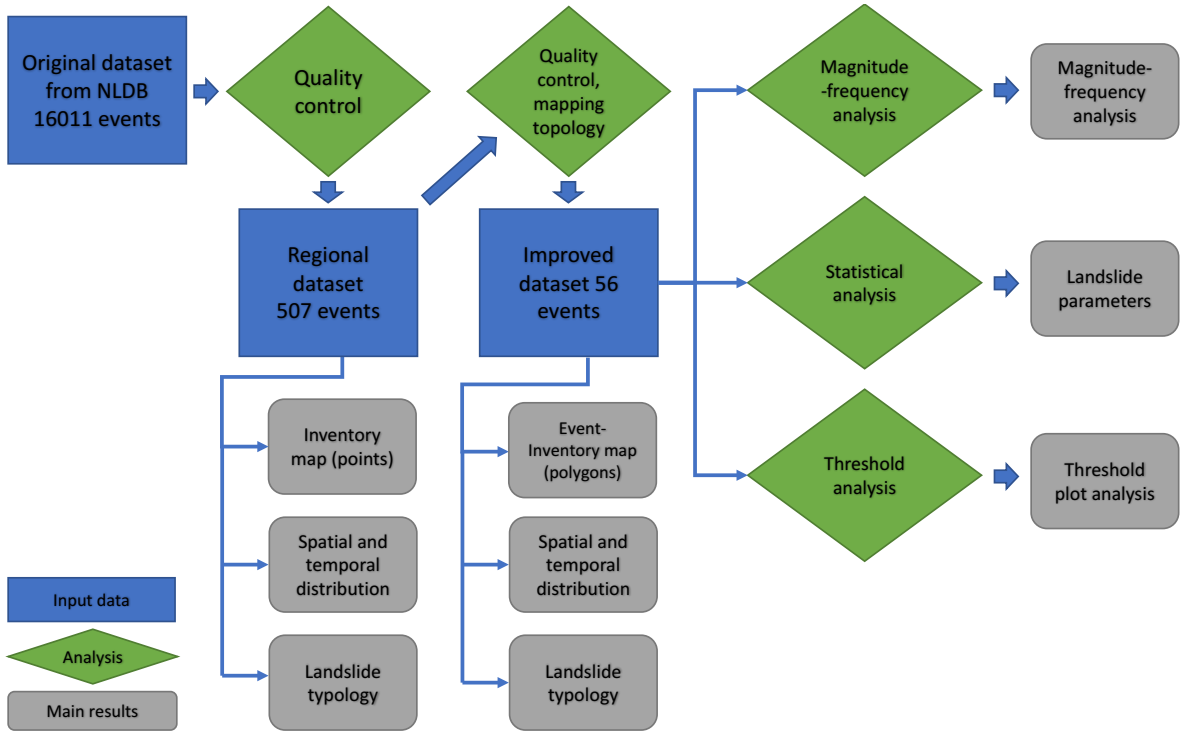

Figure 27. The flow chart show the input data, analysis and main results that were achieved from the analysis.

5.1 Applying the 1`st quality control

All events that occurred before 2011 were first selected away, including events defined with "no date". The following process was to exclude all unwished types of landslides that were not classified as rainfall-induced. Rock fall, rock avalanches and icefall were taken away. Events classified as snow avalanches were evaluated to have a likelihood of being a slushflow. However, it was difficult to evaluate whether some of these rather should have been classified as slushflow due to the poor quality of data. By also considering the great sample of snow avalanches led to the decision of only including data already classified as slushflows. Events classified as "unspecified landslides in soil" or "unspecified" were considered. Some events were later experienced to have wrong typology. An event registered as e.g. rock fall could in fact be a debris avalanche. That is why there is a great chance of selecting away events of interest during this quality control. The resulting dataset had a total

of 507 events. The aim was now to map as many events as possible from this dataset (dataset 1) by investigating them closer from different sources of information. These sources were summary reports from NVE, aerial photos, newspaper articles, satellite images and information from the national database. It was quickly experienced that too much time was applied for such careful investigations in the dataset for one single event and it was not possible go through all the data within the research period. It led to the necessity of creating a way of highlighting certain events that could help prioritizing events with the highest likelihood of being mapped.

5.2 Second quality control and mapping topology using different sources

The NVE's landslide forecasters on duty summarize what has happened during the week through simple reports. These reports have been created every week since the establishment of the landslide EWS in 2013, but they are not publicly available. These reports summarize the warning levels that were issued the previous week, as well as including the most important landslide observations in a way of validating their issued warning-levels. Such observations could be pictures from events, extracts from newspaper articles or any evaluation from NVE forecasters themselves. It was decided to highlight landslide events that occurred on dates (+/- 1 day) at which a landslide warning above 1 had been issued. It became an efficient way of classifying events that should be evaluated more closely in addition to limit the dataset even more. These reports did not exist for the years 2012 and 2011. It was therefore necessary to go through all events for these years more carefully. Investigations that brought up new documentation or information regarding an event was used to modify or add data in the attribute table in the first selected dataset. The following new attributes were created to the dataset to maintain structure and a good system while sorting out interesting events: available images, landslide quality, warning level and thickness of deposit.

There were still a lot of data and time-consuming work to do, even though summary reports now were consulted. Investigations revealed frequently multiple registrations of the same event, while some events had wrong typology. The same was observed by Sokalska et al., (2015) whom suggested possible sources of errors due to the following causes: 1) multiple registrations from the same institution/person, but with different locations, or 2) registrations from different institutions (often resulting in different type of attached information), or 3)

registrations by different persons, on the same location, but with different typology. It was therefore important to go through all registrations from the same event, before excluding the redundant registrations to assure that valuable information was kept.

The information organized in the attribute table was used in a way of prioritizing events that had a higher likelihood to become mapped by its landslide extent. This was necessary because too much time still was applied by investigating each event in the derived dataset. The prioritizing was especially handy for the year 2011-2012 due to lack of summary reports from NVE these years. The attributes "size" and "comments" were experienced as good indicators to pick out events with potential of being mapped. Considering size, one example could be "small rock, $<1m^3$ in the road cut", that led to the decision of not considering the event. The column "comments" was experienced to frequently contain valuable information regarding events with great magnitude.

My focus on rainfall-induced landslides made me look at specific dates when rainfall events occurred in the region that triggered more than 1 landslide. As expected, some dates had an extraordinary high number of initiated landslides like under the storms Dagmar in 2011 and Hilde in 2013. Investigations revealed that landslide data in the derived database from such events were generally poorly described. Despite the fact of these events being barely documented, it was decided that they should be investigated carefully. It turned up that some of them were very well-documented events through media that allowed me to map its extent. It was therefore decided to pay close attention to events triggered on dates with an unusual number of events without considering the amount of information.

The next process was to draw polygons and calculate magnitudes and other characteristic parameters for every possible landslide, aiming to characterize landslide parameters. These events constitute to my second selection dataset (dataset 2). Some events were generally well-descriptive with available pictures of the event, that made it possible to draw their extent immediately. However, most events required further investigations. For this purpose, it was necessary to use different sources of information. These were aerial photos, newspaper articles, google street view and satellite images. Aerial photos are known to be a good source for this type of approach. However, during my research I discovered that it was more efficient to begin searching through newspaper articles. It allowed me to get an idea of the type of landslide that was involved, its extent and location, before trying to spot the landslide through aerial photos. A four-step procedure was created to investigate the events in an efficient way.

5.2.1 Newspaper articles

Landslides affecting infrastructure or society are known to be written about and reported in the newspapers (Sokalska et al., 2015). Newspaper articles were frequently found to cover events with a certain magnitude or that had caused harm to roads, people or infrastructure (figure 28). They were often found to have pictures of the landslide, in addition to a description of the location (road number, name of river etc.). These pictures were typically found to be taken right after the event, sometimes under rainy and dark conditions with the purpose of giving the media a briefly description of the damages. Consequently, these pictures could have varied resolution and bad quality as seen from figure 29. A large landslide was commonly found to be documented by multiple newspaper articles, which led to the necessity of looking through all articles that covered the event. However, landslide events were sometimes experienced only to be documented by a single road-message with poor information of the event. The NVE`s weekly summary reports had luckily collected some screenshots from articles, which made it more efficient to search up the events. The articles were sometimes experienced to contain wrong scientific term regarding the landslide. A title as "debris avalanche" was often used, even though the actual landslide was a debris flow. Another problem occurred when several events had been triggered on the same day leading to articles mixing landslide pictures and event-information.

Figure 28. Example of a picture derived from a newspaper article. The debris avalanche from Krundalen in the municipality of Luster (2015) killed several sheep and crushed some of the farmers outhouses (Farsund, 2015). Photo: NRK.

Figure 29. Example of a picture derived from a newspaper article with poor quality. The event is from the municipality of Vågsøy, 2011. Photo: Arnfinn Henden.

5.2.2 Aerial photos

Aerial photos were collected from the online service www.norgeibilder.no. The digital tool allowed me to search through orthophotos to detect landslide traces that could help drawing accurate polygons for the full extent of the landslide. The availability of aerial photos were apparently great, with several imagery projects covering the study area, as shown in figure 30. Unfortunately, it was experienced that some landslide sites had lack of available aerial photos within my period of interest. It was therefore difficult to display traces after certain events. The example from Årdal in figure 31 enlightens the problem by orthophoto Sogn 2010 being the last available image from the location. Aerial photos from landslides younger than 2016 were rarely found.

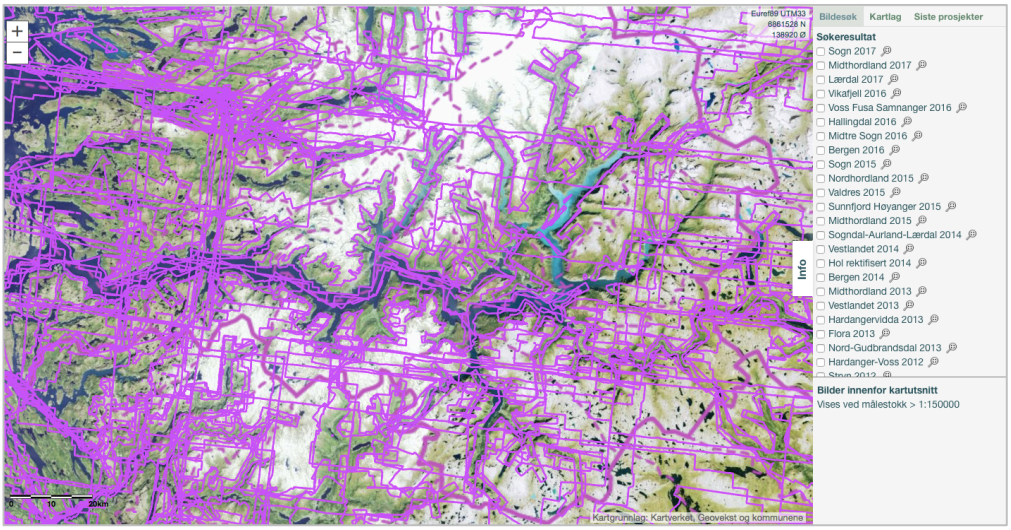

Figure 30. Distribution of available imagery projects within a section of my study area. The most recent imagery projects are listed on the right-hand side. Available from www.norgeibilder.no.

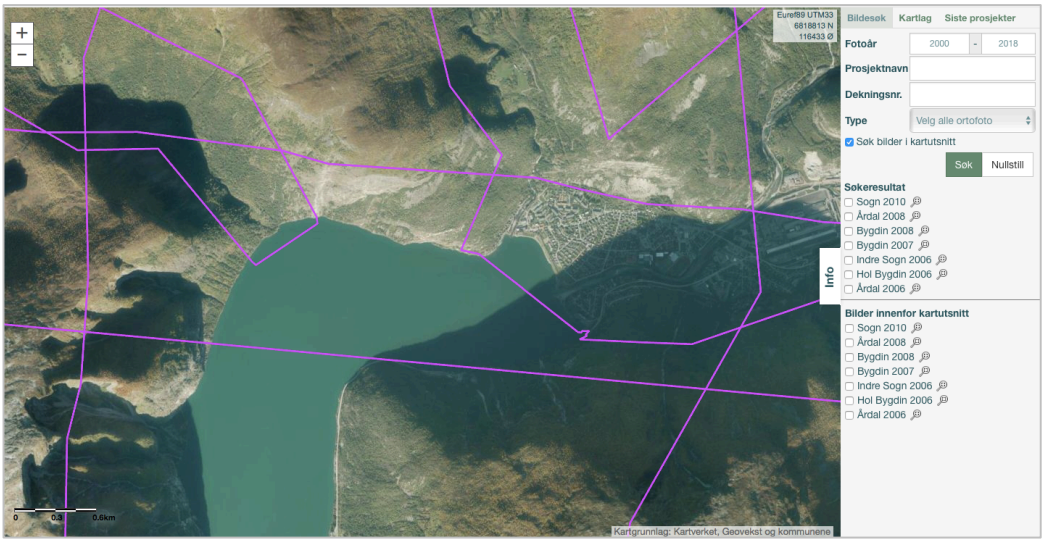

Figure 31. Distribution of available imagery projects in the municipality of Årdal. The most recent imagery project is from 2010. Available from www.norgeibilder.no.

Landslide sites were typically covered by orthophotos, but taken at different time-steps. Trails from the landslide would confirm its location, as well as indicating its extensiveness. It can be detected by e.g. looking after different colours within the soil and if there is any disturbed vegetation (Sokalska et al., 2015). The tool can therefore ascertain initiation zone and track and deposit for mapping purposes if the trail is clear enough as shown from figure 32. However, changes within the landscape can occur between the moment of initiation and date of photography. Interpretation should be accomplished carefully to map the landslide in a proper way. The use of images from articles to complement the understanding of its extent were therefore applied. Aerial photos can also be used to indicate the type of mechanisms that is involved (Sokalska et al., 2015). The landslide type can from this be classified. A channelized landslide could for example lead to the interpretation of being a debris flow.

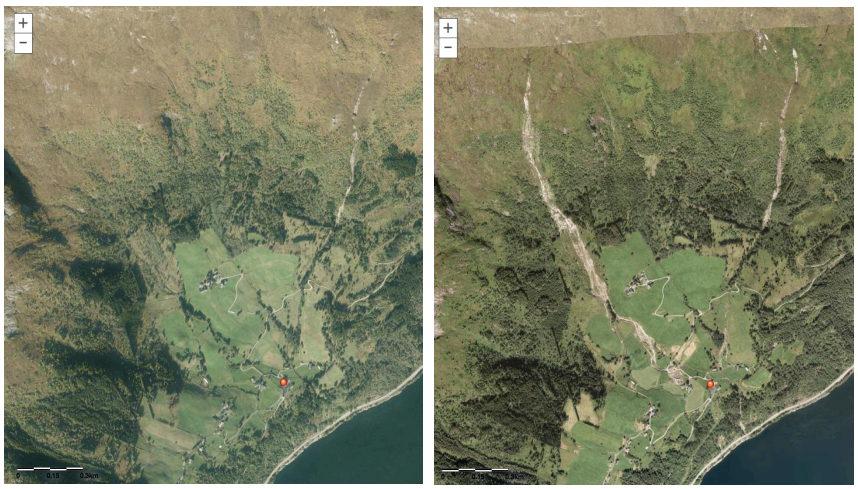

Figure 32. Available orthophotos from Berge in the municipality of Høyanger shows landslide traces from an event that was triggered 26.12.2011. Image to the left is taken before the event (2010), while the image to the right is taken after the event (2015). Available from www.norgeibilder.no.

5.2.3 Google Street View

Google Street View is a tool from www.googlemaps.no that allows the viewer to visit almost any location along the roads in the country. It was used to detect the correct location for landslide events that had inaccurate point coordinates or where there was lack of aerial photos. Coordinates could be located hundreds of meters from the true location and sometimes seemingly at the spot of observation. The tool was commonly applied for the most recent landslides after August 2017 as these point coordinates were not included in the downloaded version of the database. Pointing out the exact location was especially challenging for debris flows where pictures from newspaper articles commonly were found to only cover the channel-outlet together with its deposit. There could be plenty of river outlets within the area of the event and similarities with the surrounding landscape made it difficult to point out the correct location. Comparison of pictures from various sources together with Google Street View became handy. Matching landscape features in the background could help to prove the exact location of the landslide. One example is shown while comparing figure 29 to figure 33.

Figure 33. Example of how Google Street View can be used to match landscape features to prove correct spot of landslide. Compare the image to figure 29 to see the similarities. Available from www.google.no/maps.

5.2.4 Satellite images

Investigation of satellite images were accomplished through Copernicus, Earth Explorer and Google Earth. These sources were applied when it was desirable to look closer at events with lack of aerial photos and images from the other sources. The available images that were found had a varied resolution though, depending on the area of interest. A portion of luck was

needed to get an informative image after the event. Nevertheless, it worked very well for one specific event, contributing to an accurate polygon for a comprehensive debris avalanche in Krundalen as shown in figure 34.

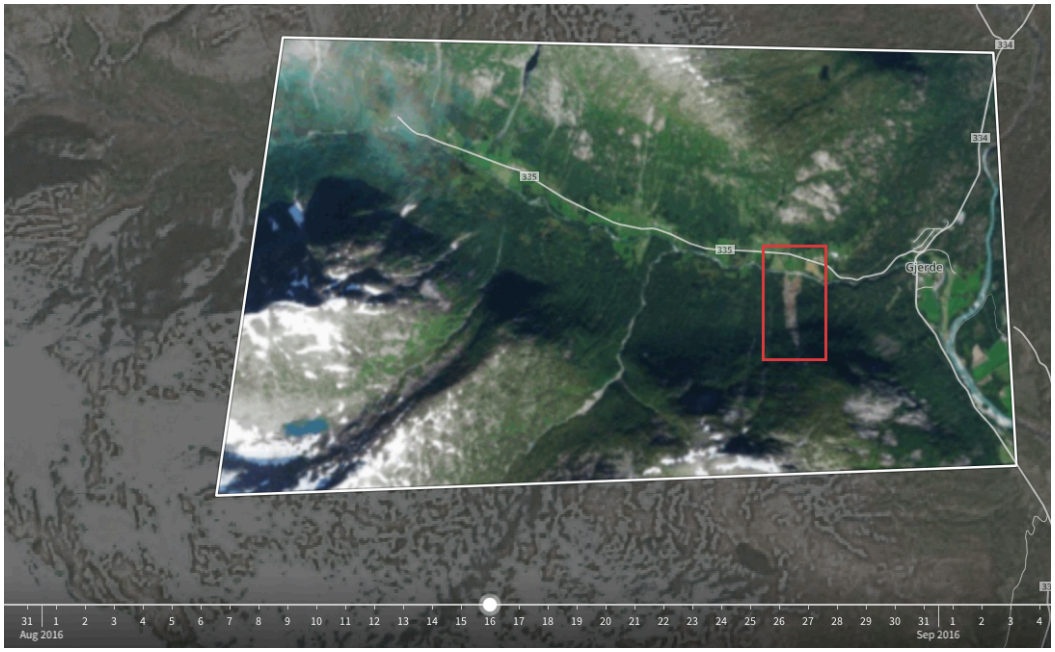

Figure 34. Example of a satellite image from Google Earth that showed landslide traces from the event at Krundalen in the municipality of Luster, 2015. Satellite image is from August 2016. Available from Google Earth.

5.2.5 Creating polygons

Geographical Information System (GIS) is a software that allows the user to perform spatial analysis on geographical referenced information. ArcMap was used to display layers of GIS-datasets within the study area that polygons could be drawn from. It was possible to calculate magnitude and other statistical landslide parameters from these polygons as well as creating different types of maps. A background layer consisting of images of high-resolution orthophotos was downloaded as a WMS-server from www.geonorge.no with coordinate system GCS WGS 1984. This background image was used for drawing the polygons. A WMS of topographic and hybrid data were also downloaded and came in handy when additional topographic information was needed to interpret the extent of an event. Moreover, the following layers of data contributed to the analysis: bedrock and quaternary deposits from NGU and a digital terrain model from Kartverket.

Some requirements were needed to be fulfilled to draw a polygon from an event. Exact location was needed to be proved. It was necessary to have an illustrative image(s) that could indicate its extensiveness and broadening. There were few landslides (usually the larger ones)

that had images showing the full extent from the source area towards the deposit. Some interpretations were therefore applied while drawing their extent. These interpretations were later discussed with my supervisor Graziella Devoli to ensure that the most likely extent was mapped to achieve most reliable results. Debris avalanches were in general the easiest landslide type to map due to their open-slope appearances and that they frequently were found to leave plenty of landslide traces in the terrain, as seen from figure 35 and figure 36. The necessity of interpreting their extent was low compared to debris flows.

Figure 35. Pictures from newspaper articles could display traces of landslide events that were not visible from available aerial photos. These pictures were used to draw the polygon in figure 36. Event from Tynning in the municipality of Gulen, 2011. Photo - Left: Private. Right: 2211-TIPSER.

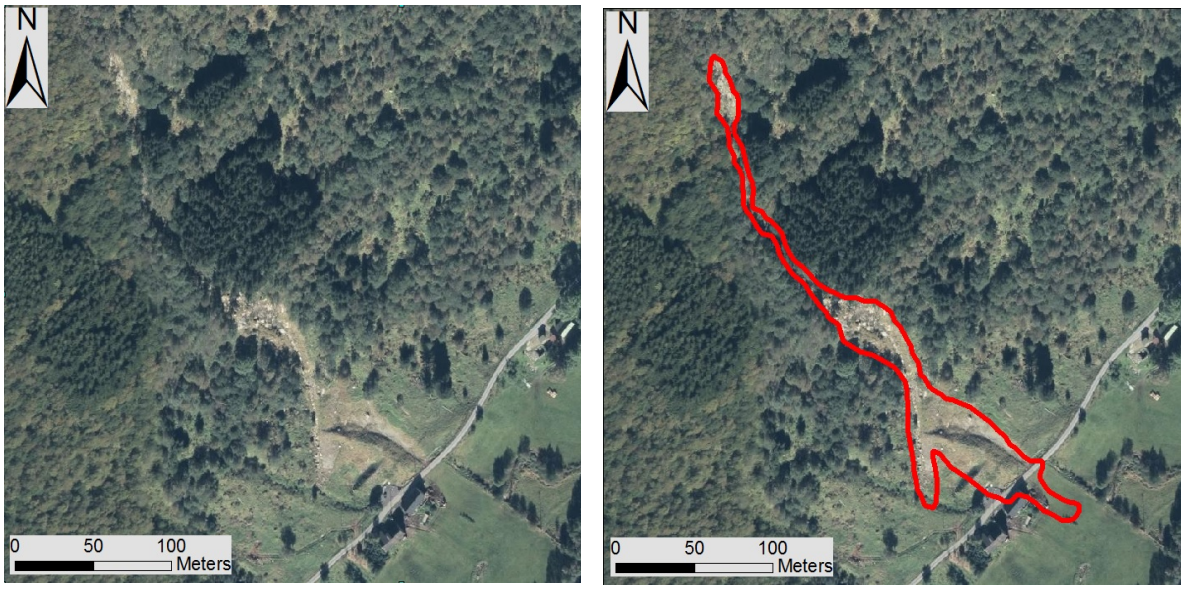

Figure 36. Example of how aerial photos are used to draw the extent of a landslide. Pictures from newspaper articles were used in addition to make it as accurate as possible (figure 35). Event is from Tynning in the municipality of Gulen, 2011. Available from www.norgeibilder.no.

The extent of debris flows was easily mapped for the depositional area with help from pictures together with their channelized-dependency of occurrence. However, pictures did

barely exist further upslope for these events and their channelized behavior caused the landslide traces to become less-visible. Jakob (2005) support this observation by claiming that vegetation may prohibit identification of debris flows as well as vegetation surviving the debris flow, depending on flow velocity, flow depth and the boulder size. Interpretations were therefore frequently applied do decide its starting point as it could be hard to distinguish between the landslide traces and former landslide traces. It was decided that these events were drawn upwards in the channel until the surroundings became doubtful for representing a starting point. Such circumstances could be a sudden increase in steepness, or that the channel entered an area without supply of loose soil. These starting points are therefore considered as vague compared to debris avalanches. An example from figure 37 shows how a polygon is interpreted based on a single picture from the depositional area of a debris flow.

Figure 37. Example of how a polygon was interpreted based on a single picture from the deposit. Arrows indicate the deposits. This debris flow event is from Undredal in the municipality of Aurland, 2014. Aerial photo available from www.norgeibilder.no. Photo: Unknown.

Another example from figure 38a shows the polygon that was created for a debris slide. Debris slides were in general hard to spot due to their low magnitudes. Those that were mapped had preserved its landslide traces well for mapping purposes. Slushflows turned out to cause the same problems for mapping purposes as for debris flows. Figure 38b shows one example of a mapped slushflow event. The magnitude of a landslide was estimated based on the area (m^2) of the polygons and hence interpretations play an affective role on the magnitudes.

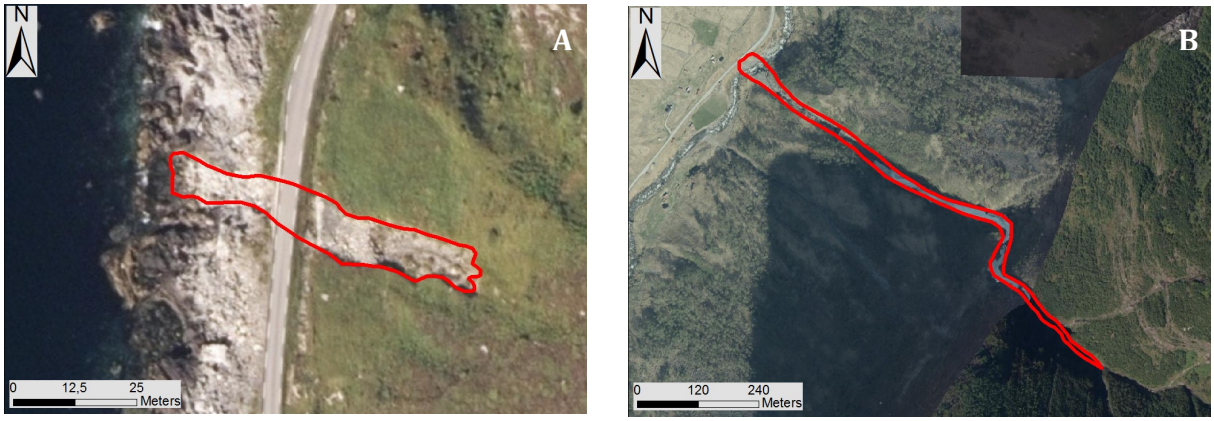

Figure 38. A: A polygon from a debris slide event from Vågsøy municipality, 2011. B: A polygon from a slushflow event from the municipality of Hornindal, 2015. Available from www.norgeibilder.no.

5.2.6 Parts of a landslide and notions

The dynamics of a landslide will change from the starting point until it reaches steady state in the depositional area. Mechanisms and characteristics of the dynamics are different for each part. A useful way of analyzing and describing the involving processes was by dividing the landslide into separate parts and by using different notions. The upper edge is called the scar, which is left exposed after the mass have been transported downslope (Cruden and Varnes, 1996). Source area is located as an area in the upper part of the landslide that indicates where the mass has loosened from. Further downslope you'll have the travel path or track which is where the mass has been transported along. The mass will slow down and accumulate at the bottom, which is called the deposit or runout area. Runout distance is the total length of the landslide from source area towards the depositional area (Effendy et al., 2016). Figure 39 and figure 40 shows the interpreted parts of landslides from respectively a debris avalanche and a debris flow. The example from the debris flow visualizes the challenge of interpreting its source area. It could also have started further upslope as a slushflow in one of the two darker channels. Figure 41 illustrates how the landslide may be divided while mapping the extent in GIS.

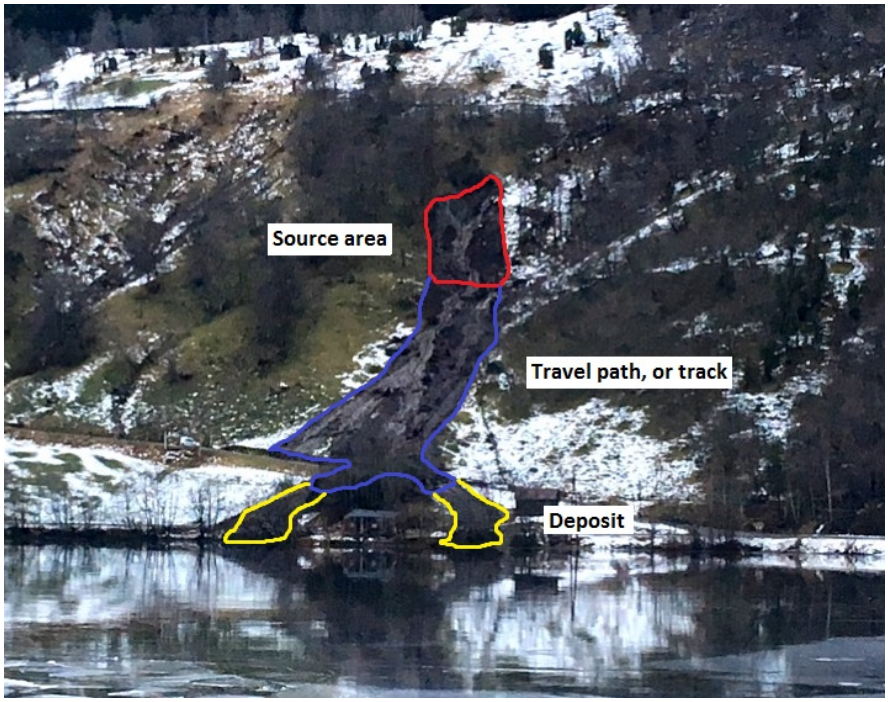

Figure 39. Example of dividing a debris avalanche into separate parts that simplifies the description of involving processes at each stage. Event is from Bell in the municipality of Gaular, 2017. Photo: NRK-Tipsar.

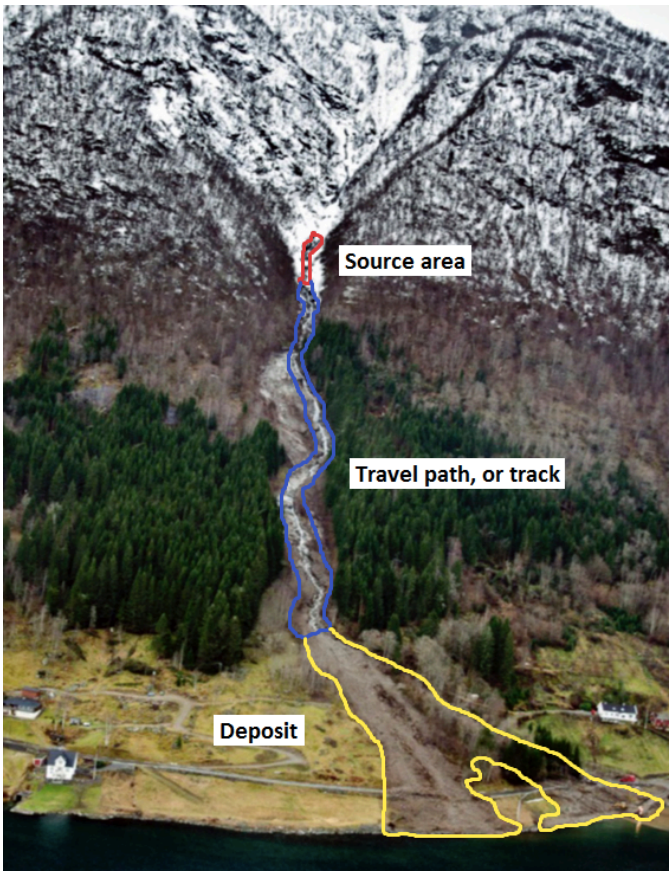

Figure 40. Example of dividing a debris flows into separate parts that simplifies the description of involving processes at each stage. Event is from Skrednes in the municipality of Balestrand, 2011. Photo: Unknown.

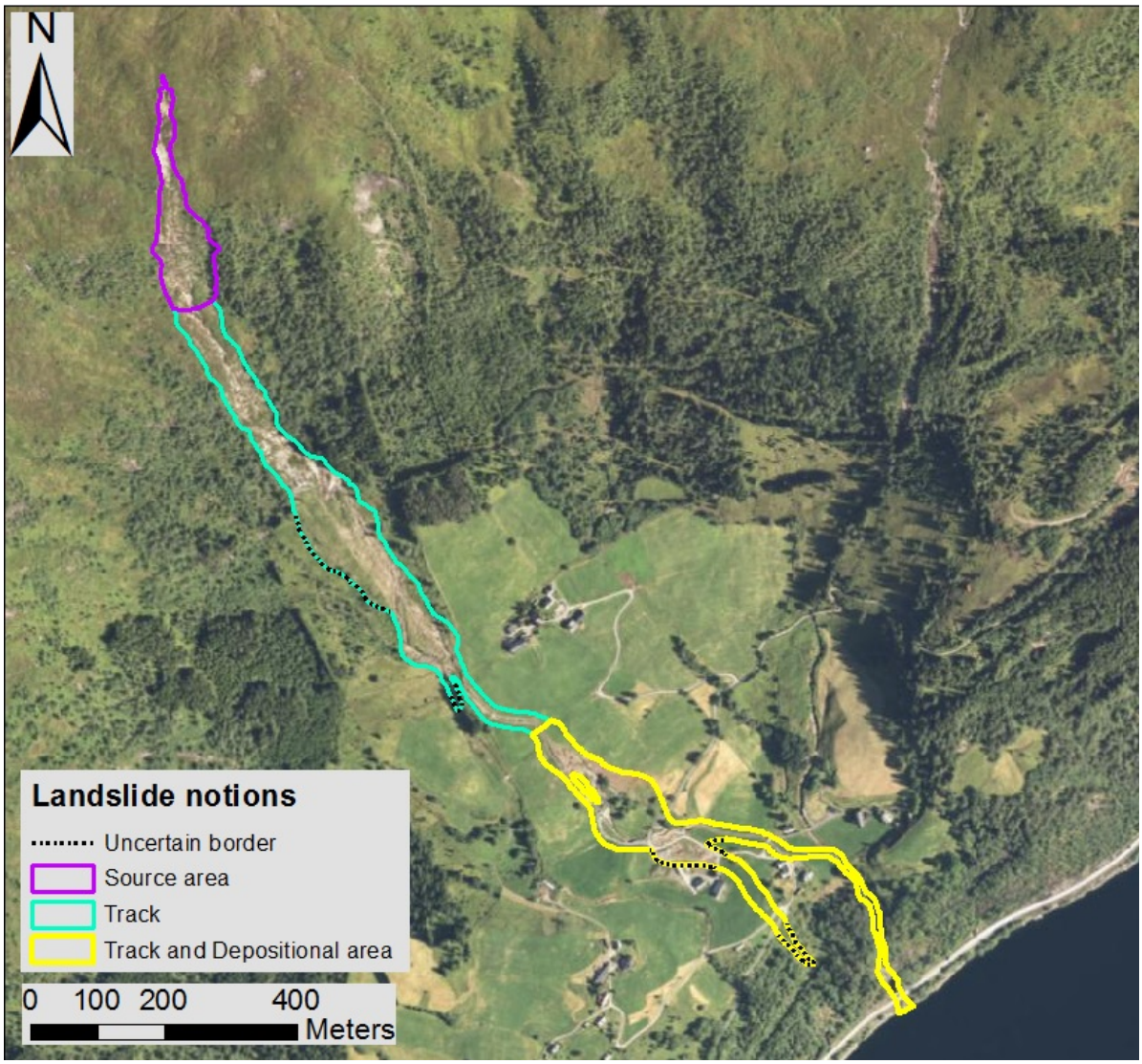

Figure 41. Example of how a landslide may be dividing into separate parts while mapping the extent in GIS. Event is from Berge in the municipality of Høyanger, 2011.

5.3 Statistical calculations

Statistical calculations in ArcMap were performed at all polygons to investigate the main landslide parameters and characteristics in the region. Calculations were first performed on the DTM raster dataset. Range in elevation and maximum height were calculated through the function "zonal statistics" as well as mean and standard deviation. Runout distance was manually calculated for each polygon by line-measurements in ArcMap. The DTM was applied to create a map of slope gradients. The resulting raster dataset contained slope values down to a cell size of 10 meters. Slope values in the starting point for the landslides were manually extracted from the raster dataset. Calculations of statistical parameters as mean slope value and standard deviation were accomplished through the function "zonal statistics". Bedrock and the quaternary deposits were investigated through the bedrock and quaternary

maps from NGU. Information was derived from the map by manually zooming into each polygon and by observing the type of bedrock or quaternary deposit at the zone of initiation.

It was desirable to investigate if there were any typical orientation for the landslides in the region. Aspect was therefore calculated by using the method from Lilleøren and Etzelmüller (2011). Mean aspect, or mean vector direction was calculated from

$$\bar{\theta} = \tan^{-1}\left(\frac{\sum_{i=1}^{n}\cos\theta_i}{\sum_{i=1}^{n}\sin\theta_i}\right) \quad (1)$$

and the vector strength was calculated from

$$\bar{R} = \frac{\sqrt{\sum_{i=1}^{n} cos\theta_{ir}^2 + \sum_{i=1}^{n} sin\theta_{ir}^2}}{n} \quad (2)$$

Number of observations is given as "n". Vector strength close to 1 would indicate that there's little spread within the data. Vector strength close to 0 would indicate that there's large spread in the data (Lilleøren and Etzelmüller, 2011).

5.4 Magnitude-frequency analysis

The magnitude characterization of landslides was accomplished when the mapping process was completed. Landslide magnitude for an event were automatically calculated in ArcMap while finishing a polygon. The relation between magnitude and frequency of landslides were determined by creating a magnitude-cumulative frequency curve (MCF). The method was accomplished in the same way as Dahl et al. (2013) did for his landslide magnitude analysis for the Faroe Islands. All mapped landslides were ranked in an order of decreasing magnitude. Individual landslide frequency f_i was determined as

$$f_i = \frac{1}{T} \quad (3)$$

with f_i as the landslide frequency and T as the registration period (7 years). The calculated landslide frequencies were added up using the following equation

$$F_i = \sum_{i=1}^{n} f_i \quad (4)$$

with F_i as the annual landslide frequency of a minimum landslide area. The annual landslide frequencies F_i and their corresponding landslide area [m^2] were then plotted together in a graph on a log-log scale.

5.5 Threshold analysis

Data for threshold analysis was gathered for each landslide event in dataset 2 from the online platform xgeo.no. Historical data of relative water supply and relative soil water content were extracted by searching at the date of event and then by picking the grid value at which the polygon started in as shown in figure 42. Data extracted from one specific day represent the mean value between 07:00 at the date of interest, until 07:00 the following day. The time of initiation, when the landslide was triggered, is therefore crucial to extract correct data that correspond with the event of interest. However, a great number of events had a time-accuracy of several hours, but often with time of registration in the early morning. It was mostly presumed these landslides occurred during the night. One problem turned up while extracting data from xgeo.no. The grid values that were extracted seemed to visualize the data for the following day. This bug was reported to NVE and was quickly fixed (S.Boje, oral communication). Finally, all the data were plotted in the established threshold plot, previous presented in figure 12 in chapter 2.3.2.

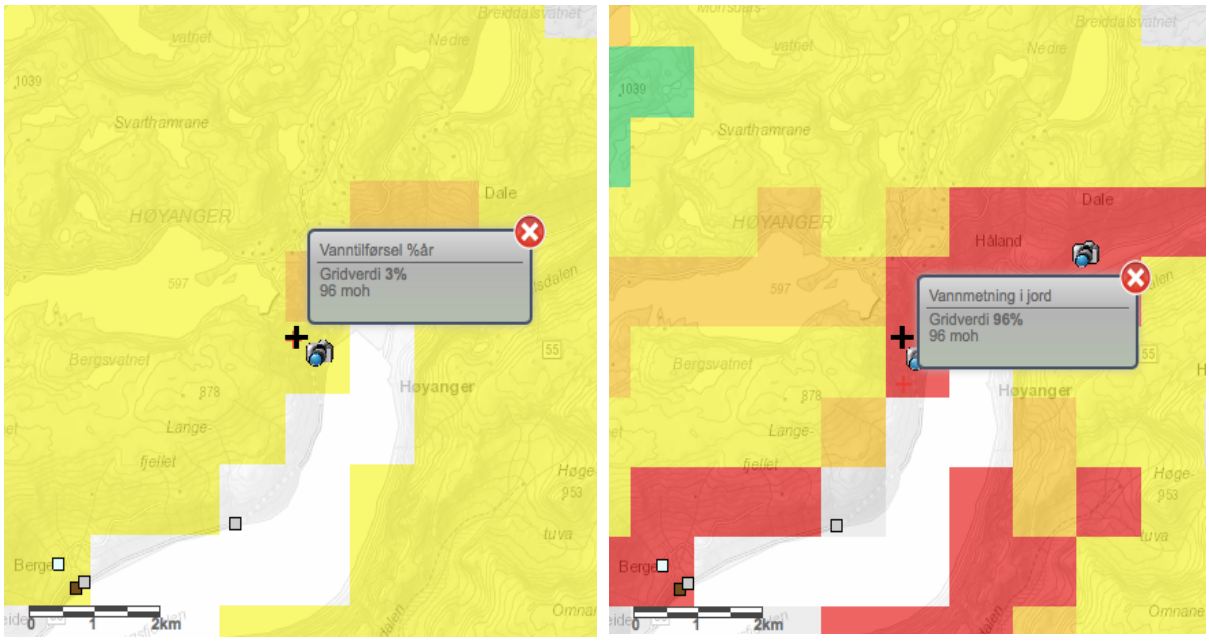

Figure 42. Example of how data of relative water supply (left) and relative soil water content (right) were extracted from grids at xgeo.no. Cross indicate point of initiation. Data extracted from www.xgeo.no.

6 Results

Two datasets have been analyzed to better characterize rainfall- and snowmelt-induced landslides in the region Sogn og Fjordane.

6.1 Regional characterization

The analysis of landslide events recorded in the national database after applying the first quality control shows that a total of 507 landslides have been reported in the region from 01.01.2011 until 24.07.2017. This dataset (dataset 1) was used to characterize the spatial and temporal distribution at regional level and to analyze landslide typologies. The spatial distribution of the events is shown in figure 43. The figure shows that landslides have been reported over the entire region, close to the coast as well as in the innermost areas. It cannot be observed any special area with more density then others. However, a great number of events are located along the fjords in the county.

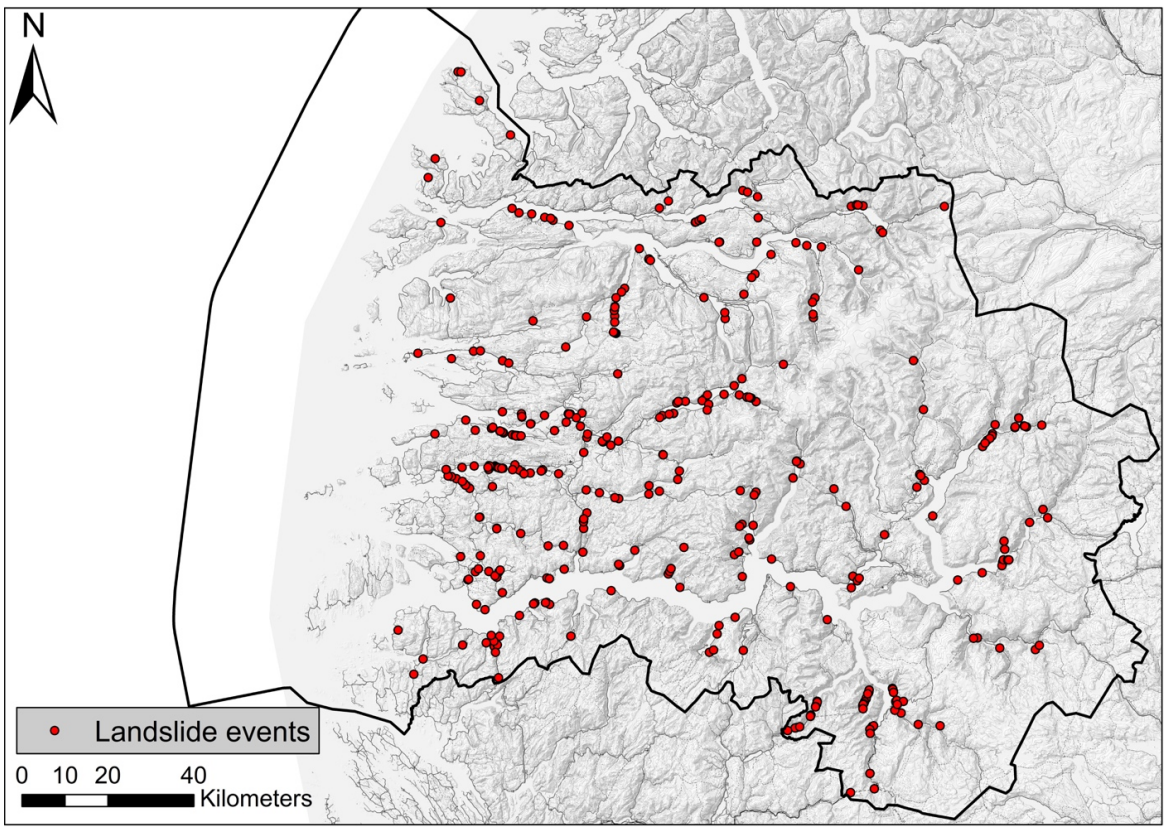

Figure 43. The distribution of landslide events in the region from dataset 1. Total number of events are 507.

Their temporal distribution, presented in figure 44, shows that rainfall-induced landslides have been reported in all years analyzed, however, with a varying number of events. The year with the highest number of events was 2011 with a maximum number of 185 landslides recorded, while 2012 was the year with the lowest number of events with 16 events recorded. In two occasions the total number of landslides was influenced by the fact that there was an extreme weather event like Dagmar in 2011 (82 events) and Hilde in 2013 (42).

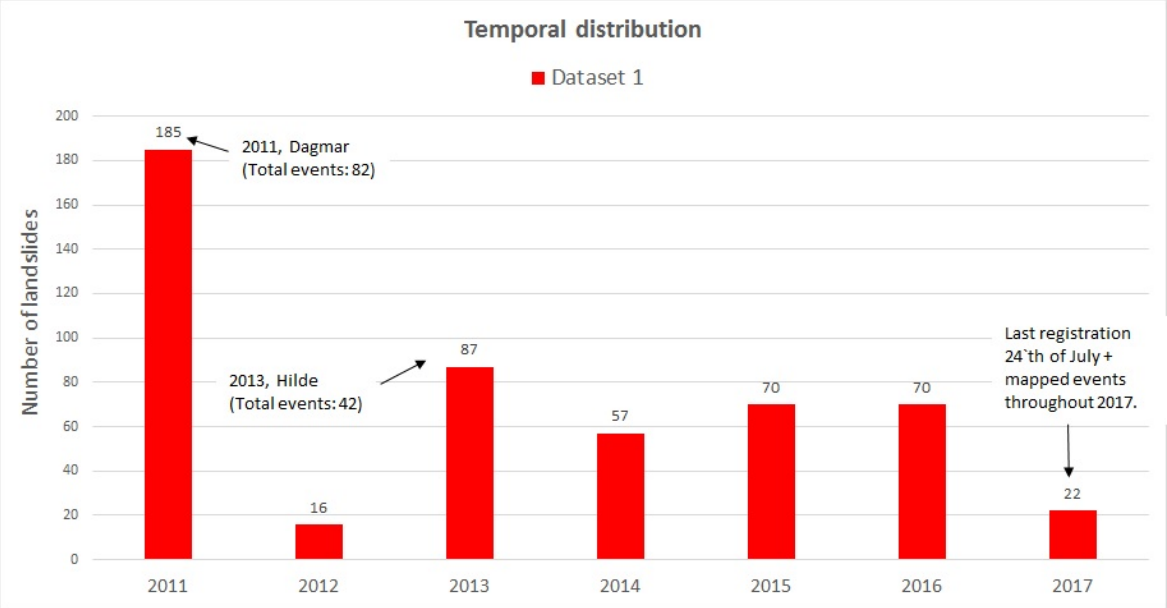

Figure 44. Yearly number of landslide events from dataset 1. The total number of events are 507.

Table 6 present all the hydro-meteorological events (e.g. rainfall and/or snowmelt episodes) that reached the category of extreme events in the period investigated. The number of associated initiated landslides are given as well. The extreme event Dagmar in 2011 is associated with the highest number of events with 82 and with a maximum 24h rainfall intensity of 40-60mm. The extreme event Hilde is following behind with 42 events and a rainfall intensity of 80-100mm. The other events have a total number of initiated events ranging from 8-2 events and with rainfall intensity of typically 40-60mm, locally up to 60-80mm. All events occurred either November, December or January.

Table 6. Table presents hydro-meteorological events characterized as extreme events in the study area from 2011-2017. The total number of associated rainfall-induced landslides are indicated, as well as maximum 24h rainfall intensity for the region (extracted from www.xgeo.no).

Area	**Year**	**Date**	**Name of Extreme Weather**	**Triggering cause**	**Max. 24h rainfall intensity in SF (from xgeo.no)**	**Approx. number of rainfall-induced landslides events in SF**
Sogn og Fjordane	2011	December (26 - 27)	Dagmar	Intense rainfall	40-60mm (locally up to 60-100 mm)	82 events
Sogn og Fjordane, Møre og Romsdal, Trøndelag	2011	November (25-26)	Berit	Intense rainfall	40-60 mm	12 events
Sogn og Fjordane, Hordaland, Møre og Romsdal, Trøndelag	2013	November (15 - 16)	Hilde	Intense rainfall	80 - 100 mm (locally up to 100-150 mm)	42 events
Sogn og Fjordane, Hordaland, Rogaland, Agder	2015	December (4 - 6)	Synne	Intense rainfall	40-60 mm (locally up to 60-80 mm)	8 events
Sogn og Fjordane, Hordaland, Rogaland	2016	January (29 - 30)	Tor	Intense rainfall	40-60 mm	4 events
Sogn og Fjordane, Hordaland, Rogaland	2017	December (7 - 8)	Aina	Intense rainfall	40-60 mm (locally up to 60 - 100 mm)	2 events
Sogn og Fjordane, Hordaland, Rogaland, Møre og Romsdal	2017	December (22 - 23)	Birk	Intense rainfall	60 - 80 (locally up to 80-150 mm)	4 events

Figure 45 presents the monthly distribution of landslides in the years analyzed. As observed in previous works for Western Norway (Jørandli, 2016) this analysis confirms that the autumn months and March are the ones when more events are registered. Three distinct peaks with a high number of landslides are observed in October, November and December. Another clear peak is seen for March. A peak can be seen for April and June that most likely are linked to late melting of snow or torrential rain.

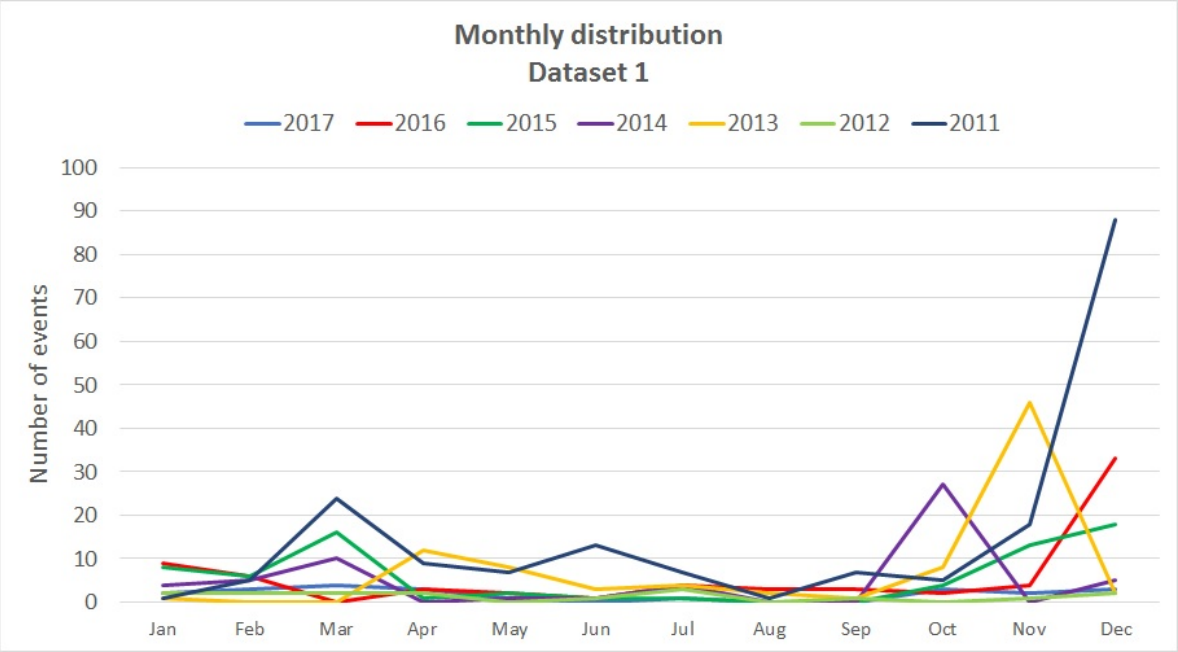

Figure 45. Monthly distribution of landslide events from dataset 1 differentiated by year. The total number of events are 507.

The distribution of landslide typology within dataset 1 is presented in figure 46. Most of the landslide events recorded in the database had an unspecified typology. A total number of 389 events in our dataset were therefore recorded as "unspecified" (in Norwegian "løsmasseskred, uspesifisert"). Sixty-nine events have been recorded as debris avalanches, 25 events as debris flows, 14 events classified as slushflows, and 10 defined as debris slide.

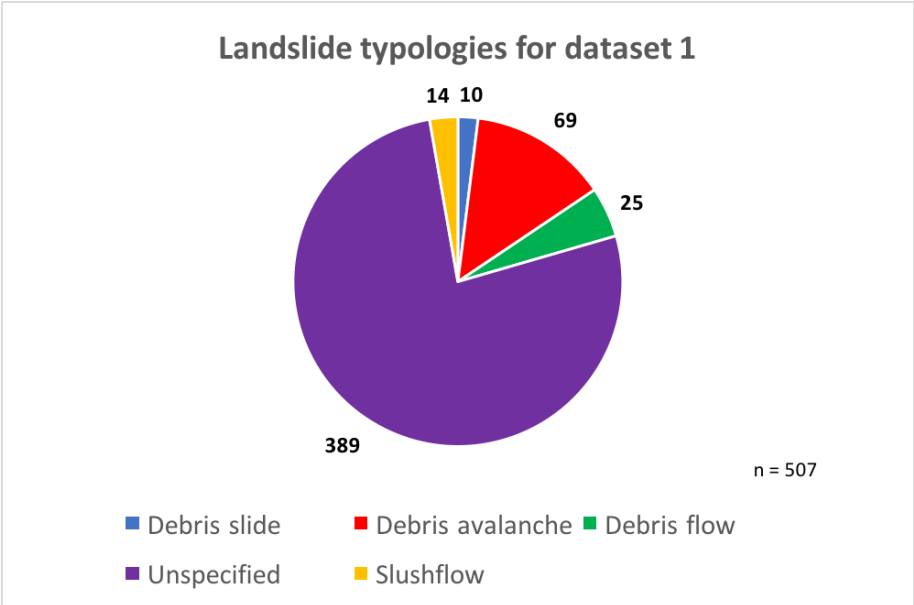

Figure 46. The distribution of landslide typologies for dataset 1. The total number of events are 507.

The landslide events were plotted against annual normal precipitation, landforms, and susceptibility maps to see if it was possible to find a specific pattern and cluster of data. Comparing events with annual normal precipitations, it was found that landslides occur over the entire region both in low-precipitation zones as well as in the most intensive zones (figure 47). A vague clustering of events can be seen in the mid-west part of the county in a zone with high annual precipitation.

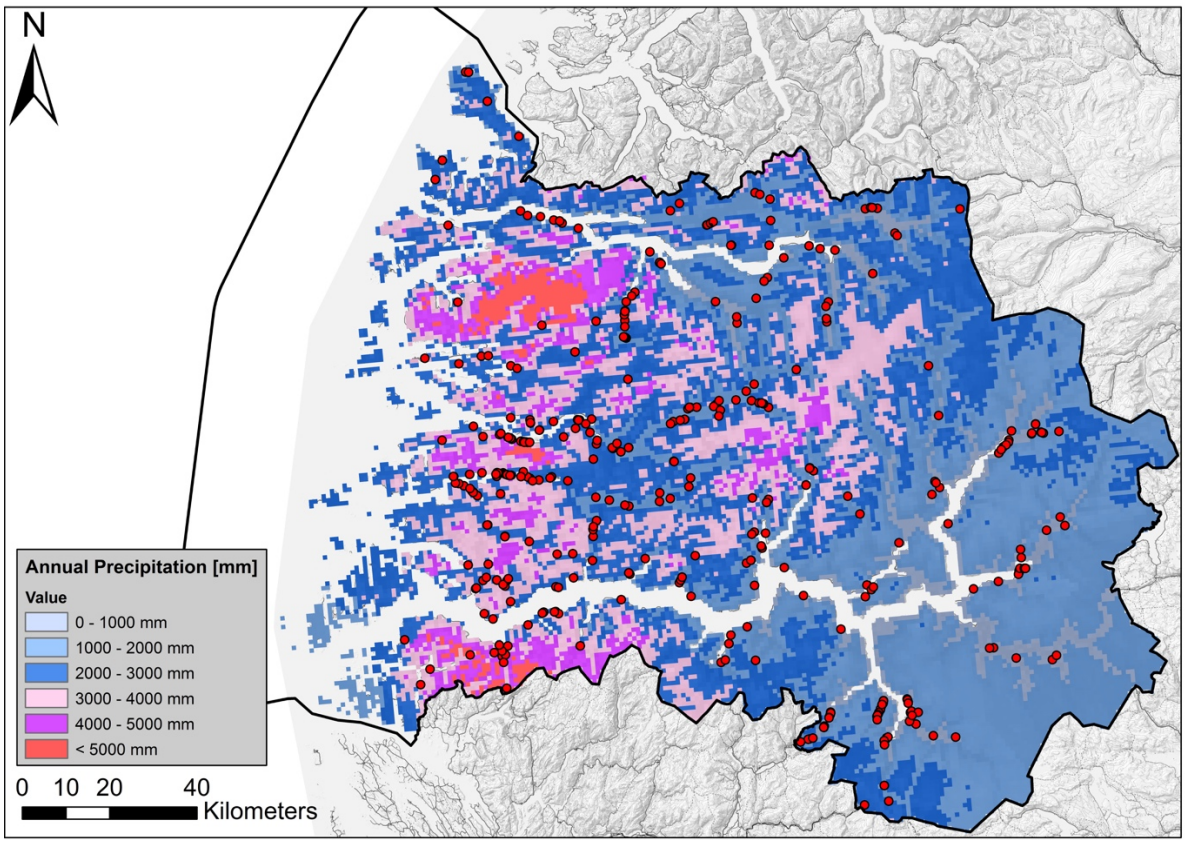

Figure 47. Annual precipitation in the region, normalized from 1961-1990 (extracted from www.senorge.no), is shown in addition to landslide events from dataset 1. Total number of events are 507.

While considering landforms, it is seen from figure 48 that most landslide events in coastal and near-coastal areas occur in glacially-scoured low mountains and valleys. Landslide events located further inland appears mostly in alpine relief or glacial relief. Some few events are located at hills with accentuated relief with moderate slopes and in high paleic mountains with moderate slopes. When comparing events with susceptibility it is found from figure 49 that landslide events occur in susceptible valleys and along fjords over the entire county. Some valleys in the innermost areas are observed to have many susceptible areas but with few registered events. It is observed a great number of registered events in near-coastal areas where there apparently are fewer susceptible valleys. Considering the susceptibility at

catchment level from figure 50 it is found that most events are located at areas classified with very high susceptibility, followed by some events in areas of high or moderate susceptibility.

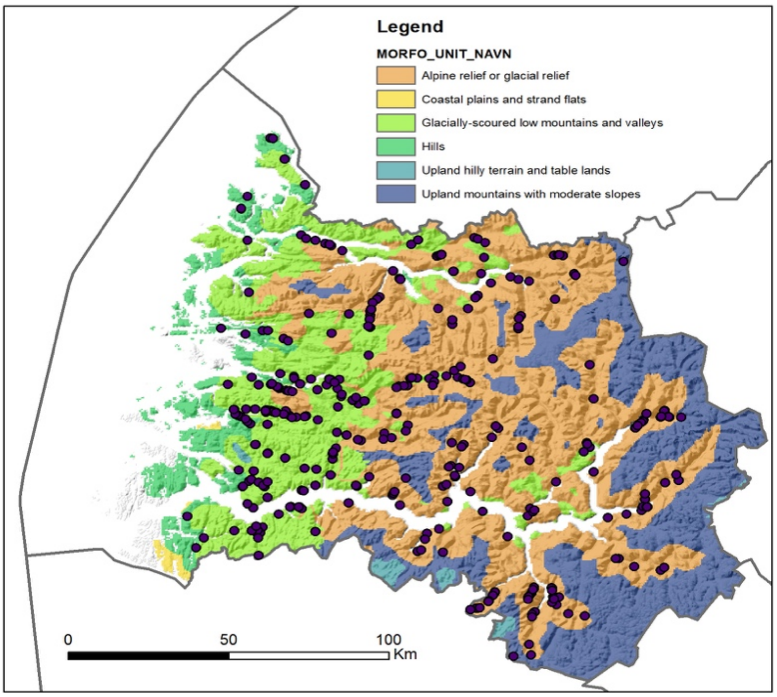

Figure 48. The relation between landforms and landslide events from dataset 1 are presented. The total number of events are 507. Landform map is modified from Etzelmüller et al. (2007).

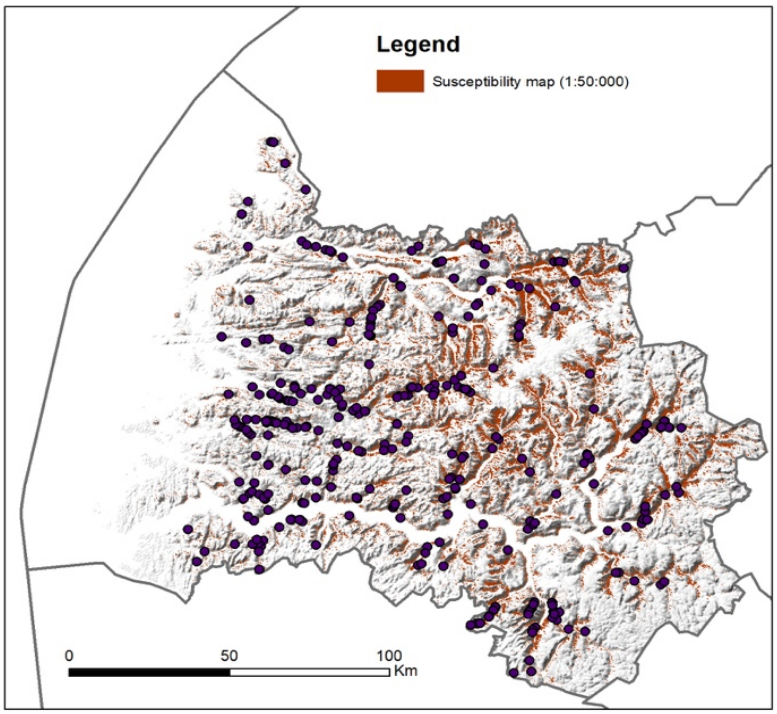

Figure 49. Susceptibility map on local scale for my region in addition to landslide events from dataset 1. Total number of events are 507. Susceptibility map modified from Fischer et al. (2012).

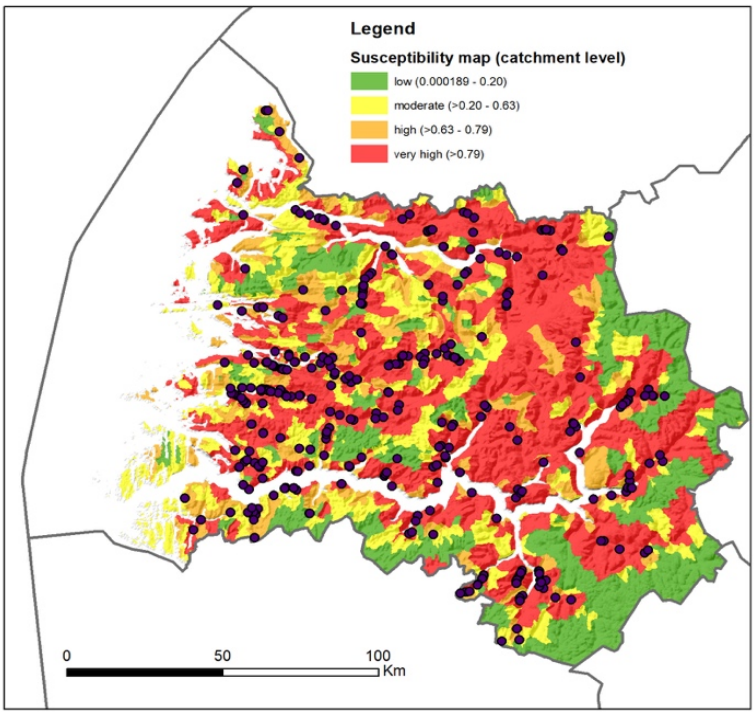

Figure 50. Susceptibility map on catchment level for my region in addition to landslide events from dataset 1. Total number of events are 507. Susceptibility map modified from Cepeda and Bell (2014).

6.2 Mapping of landslides and landslide characteristics

One of the objectives of the thesis were to improve the knowledge on landslides by a new quality control and by mapping the real extension of these events. The analysis of my sources of information (national database, aerial photos, satellite images, newspaper articles and summary reports) allowed me to improve the quality of 56 events by mapping landslide area and by collecting new event-information. Figure 41 found in chapter 5.2.6 shows an example of a polygon that was mapped. As already indicated in chapter 5.2, the lack of available aerial photos and poor landslide quality was the main cause for not allowing me to map more events. My new dataset (herein called dataset 2) consists of polygons of landslide events with high quality and were therefore used for further analysis. The spatial distribution of these 56 landslide events are shown in figure 51 together with the distribution of landslide events from dataset 1 (507 events). The inventory map of dataset 2 is presented in figure 52 with the landslide events differentiated based on landslide typology. The spatial distribution shows that both debris flows and debris avalanches are spread over the entire region. However, debris flows tend to be located slightly further inland then debris avalanches. It is not possible to reveal any trend in the distribution for debris slide or slushflows due to their low sample. Two of the events in dataset 2 were discovered by a coincidence through aerial photos while

performing API for a different landslide event. These two events were not registered in the applied version of the national database. The downloaded version of the national database from 30.08.2017, as mentioned in chapter 4, did not include events occurring from 30.08.2017 until 01.01.2018. A total of eight events was mapped during this period which are included in dataset 2.

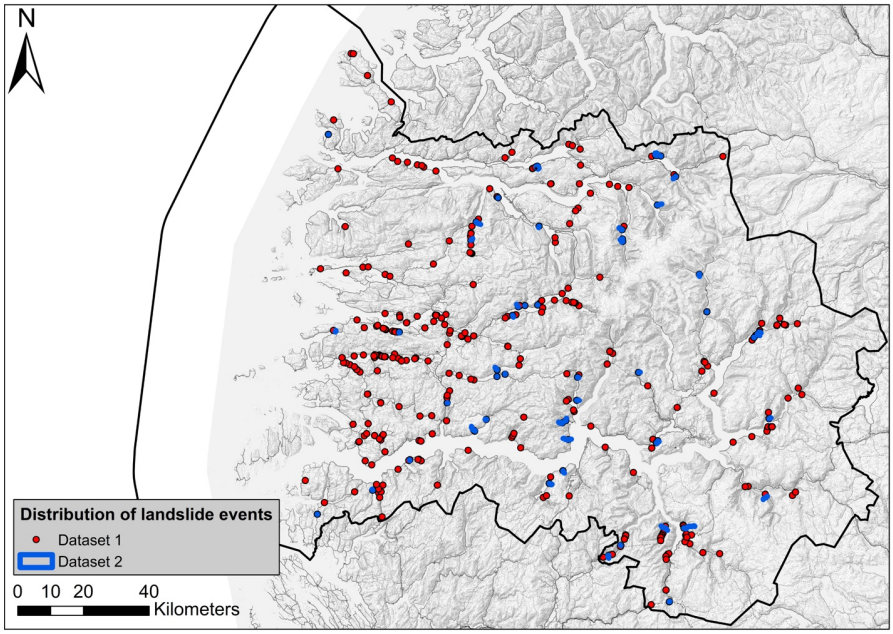

Figure 51. The distribution of landslide events from dataset 2 (56 events), together with dataset 1 (507 events). Dataset 2 consists of 21 debris avalanches, 20 debris flows, 6 slushflows, 4 debris slides and 6 unspecified landslides.

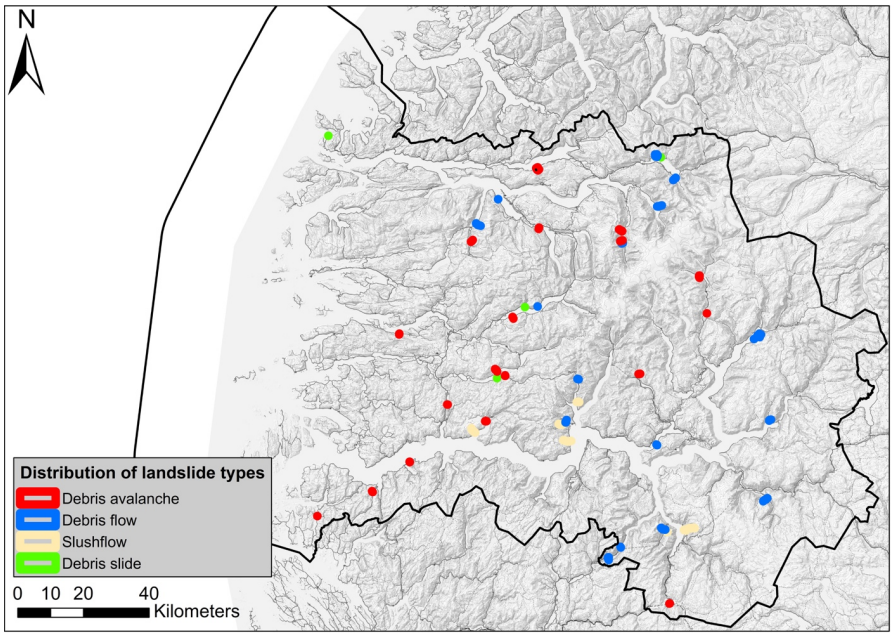

Figure 52. The spatial distribution of landslide events based on landslide typology from dataset 2. There are 21 debris avalanches, 20 debris flows, 6 slushflows and 4 debris slides. Unspecified landslides were not considered.

The analysis of the temporal distribution of landslides from dataset 2, presented in figure 53, reveals that landslides have occurred each year from 2011-2017. A total of 23 events were mapped from 2011 with 16 of them triggered by the extreme event Dagmar in 2011. A total of 8 events were mapped for 2013 with the extreme event Hilde triggering 7 of them. Eight events were mapped for year 2017, followed by six events for year 2016, 5 events from both year 2014 and year 2013 and with 1 event from year 2012.

Figure 54 shows the typologies of the 56 landslide events from dataset 2. Debris flows and debris avalanches are the type of process that dominate in the area with a percentage of respectively 37 % and 36 %. Moreover, there were 11 % of slushflows and 7 % of debris slides. Even though a better control was applied, it was still difficult to define the typology for 9 % of them that were classified as "unspecified". These events showed characteristics from at least two typologies, and could have a complex character by changing failure mechanisms during the movement. It was therefore difficult to classify these and later to use in the statistical analysis.

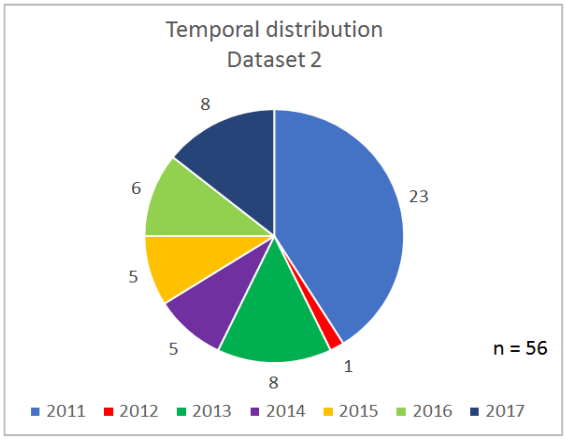

Figure 53. The distribution shows number of landslides differentiated by years for dataset 2. The total number of events are 56.

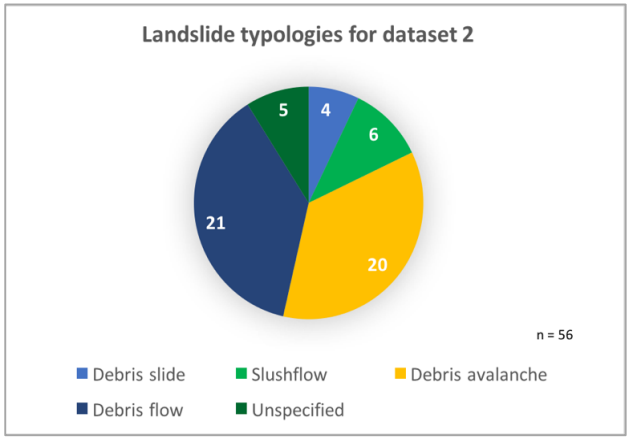

Figure 54. The distribution of landslide typologies for dataset 2. The total number of events are 56.

The release area of each event from dataset 2 was analyzed to identify in which type of bedrock and quaternary deposits the landslides started in. The NGU maps (bedrock and quaternary deposit map) were used for this purpose. The results of quaternary deposits are presented in figure 55 and indicate that most of the recorded landslides have occurred in slopes covered by a "thin, or no cover" with a total of 22 landslide events. Some events were in previous colluvial deposits left by previous landslides (12 events) and some in moraine material (7 events). The analysis show that debris flows have initiated in "thin, or no cover"

and in colluvial deposits. One event was in "peat and bog" deposit. Debris avalanches occurred in different types of quaternary deposits. The majority was in "thin, or no cover", but had a greater variety regarding the other deposits with 5 events in moraine material, 4 in landslide deposits and 2 events in weathered material. In terms of bedrock, it was found that most events started in areas with diorite- to granite gneiss, together with migmatite, with a total of 20 events, followed by 12 events occurred in monzonite and quartz monzonite (figure 56). Few events, less than 5, were found to occur for the other bedrock types. Debris avalanches have a peak of 11 events in diorite, to granite gneiss as well as 4 and 3 events for respectively monzonite and augen gneiss. Debris flows had 7 events in both monzonite, quartz monzonite and diorite- to granite gneiss. The other debris flow events had a great variety of underlying bedrock.

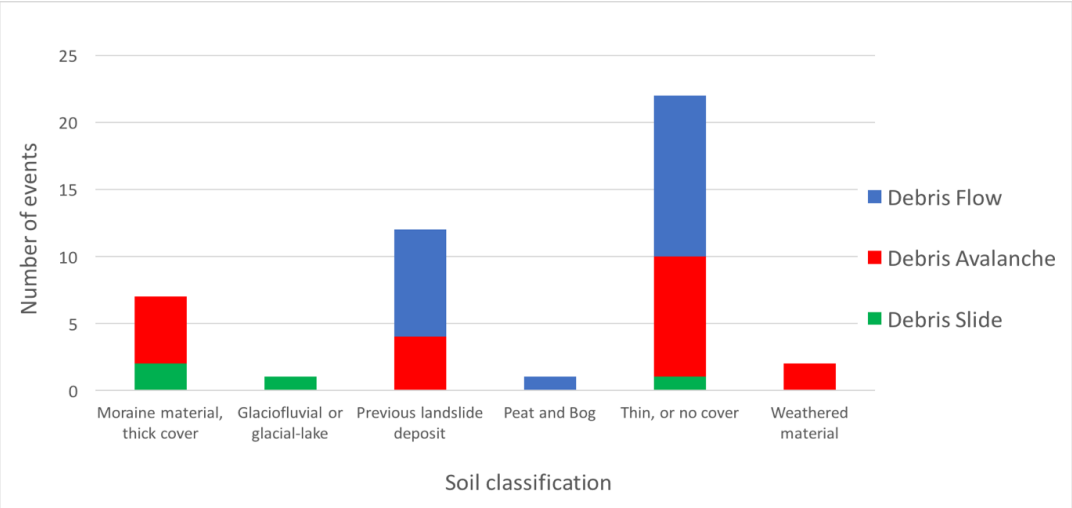

Figure 55. Distribution of soil type located at the initiation area of landslides from dataset 2. Slushflows and unspecified landslides was not considered. Total number of events: 45.

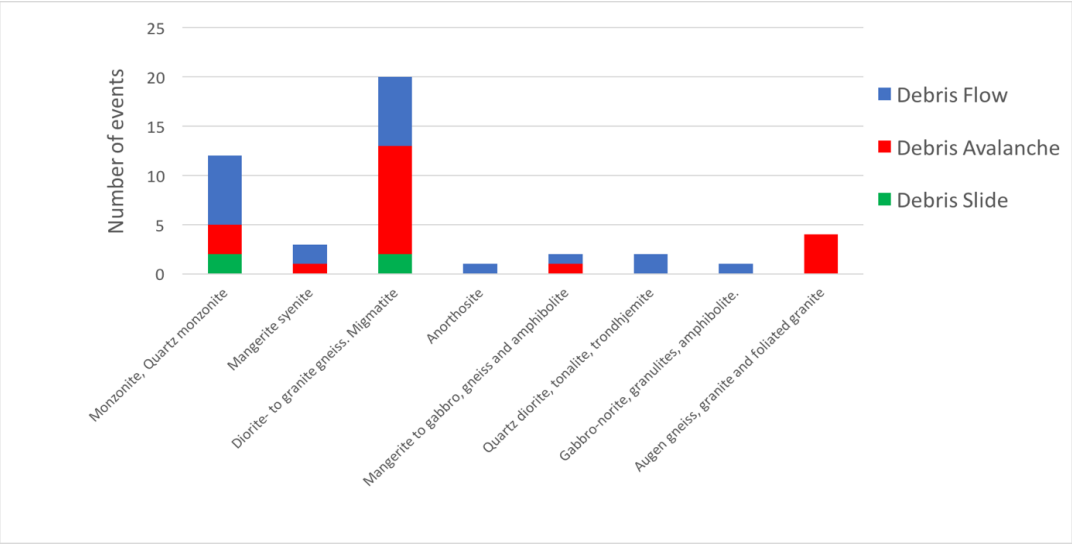

Figure 56. Distribution of bedrock type located at the initiation area of landslide events from dataset 2. Slushflows and unspecified landslides was not considered. Total number of events: 45.

6.3 Characterization of geometrical parameters for the mapped events

The dataset of mapped landslides was further used to statistically derive landslide parameters and to better characterize landslides in the region, especially debris avalanches and debris flows. The main landslide characteristics are summarized in table 7. Landslide parameters for debris slides and slushflows are considerably low and their statistical estimates are therefore considered as weak and not further presented.

Table 7. Different types of topographic information are presented from dataset 2. Mean values are calculated as well as standard deviations (found below). R- value close to 1 indicate no spread in aspect, and R- value close to 0 indicate no significant trend in aspect.

Data	n	Elevation Max (m a.s.l.)	Elevation range (m)	Slope Angle, Release Point (°)	Aspect (°)	R-	Area (m^2)	Runout Distance (m)	H/L
All data	56	453	369	37,3	287,4	0,12	22 463,1	754,4	0,518
		274	273	11,5			28 175,5	673,2	0,206
Debris flows	21	423	374	36,9	229,3	0,10	12 251,9	774,1	0,486
		246	237	11,0			10 511,1	508,1	0,158
Debris avalanches	20	437	300	37,5	352,6	0,22	24 835,6	526,9	0,573
		235	191	8,9			29 319,8	333,7	0,203
Slushflows	6	714	684	33,7			61 126,8	1 924,2	0,402
		385	398	18,8			42 317,0	1 104,5	0,201
Debris slides	4	114	16	31,1			510,8	42,2	0,314
		86	14	11,8			427,8	21,9	0,206
Unspecified	5	599	748	47,1			26 747,9	747,8	0,731
		164	208	10,3			26 747,9	254,7	0,210

Debris avalanches are found to start at a mean height of 437 meters a.s.l., followed by debris flows at 423 meters a.s.l. and debris slides at 114 meters a.s.l. The analysis of range in elevation shows debris flows to have a mean range of 374 meters and debris avalanches at 300 meters. Debris flows are found to initiate at a great variety of elevation ranges, from approx. 100 – 900 meters, followed by debris avalanches with a range from 50 – 700 meters. The analysis shows that debris avalanches have the greatest mean slope angle at release point with 37.5° degrees. Debris flows are following right behind with a mean of 36.9° degrees. Mean aspect for debris flows were calculated to be 229.3° degrees with a R- value of 0.12.

Debris avalanches had a mean aspect of 352.6° degrees with a R- value of 0.22. The low R-values indicate that there is no significant trend in aspect for these landslide types. From the table, it can be observed that the mean landslide magnitude (area) of all events is 22463.1 m^2. A closer view shows debris avalanches to have a mean magnitude of 24835 m^2 and debris flows with a mean magnitude of 12251.9 m^2. The analysis of the runout distance shows that debris flows have a mean runout of 774.1 meters followed by debris avalanches with a mean runout of 526.9 meters. Considering the results of the H/L ratio, it turns out that debris avalanches have the greatest ratio with a value of 0.573, followed by debris flows at 0.486.

The values of runout distance [L] and the elevation range [H] (from release point to deposit) can be combined in an empiric way and used to predict the runout distance of future events. These values were plotted in figure 57. The figure confirms debris flow to have a longer runout distance then debris avalanches in the region, reaching distances of 1.7 kilometers. An empirical relationship was obtained for debris flows and debris avalanches by the standard deviation regression method. The best interpolation that was obtained for debris avalanches were H = 0.5407 L + 15.061 with a coefficient of variation r^2 of 0.8942. Debris flows were found to have an empirical relationship of H = 0.4282 L + 42.805 with a r^2 of 0.8412. The coefficient of variation indicate that debris avalanches are better described by the empirical relationship then debris flows.

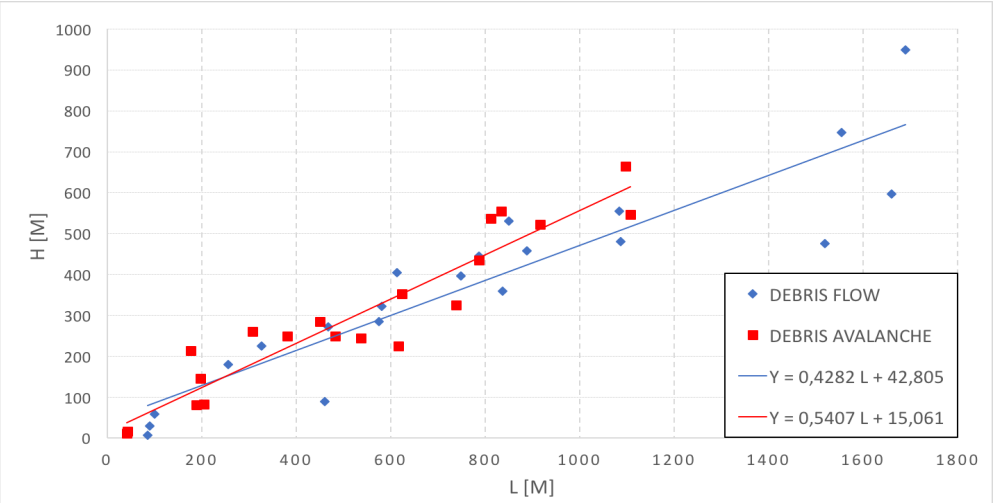

Figure 57. The relationship between range in height [H] and runout distance [L] for debris flows and debris avalanches are given. Data is acquired from the dataset 2 with a total of 41 events.

The relationship between range in height [H] and range divided by runout length [H/L] can also be used to estimate the mobility of landslides and therefore the friction angle that can be used in runout models. This relationship is presented in figure 58. The figure shows that

debris avalanches and debris flows have similar H/L values ranging typically from 0.4-0.8 and therefore similar mobility. Two debris avalanches differ greatly with values of 1.206 and 0.851 (less mobile) while debris flows have two events with distinctly lower H/L values with 0.194 and 0.082 (high mobile).

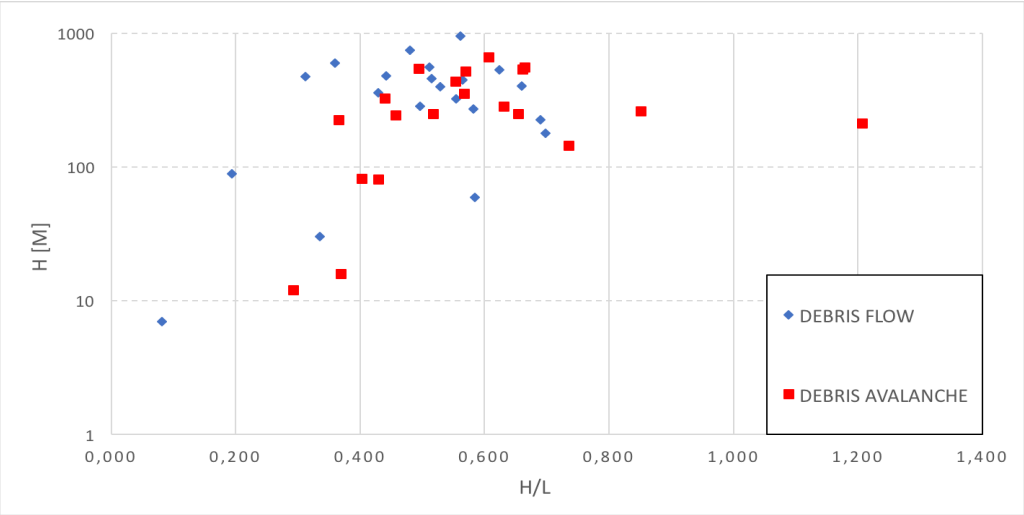

Figure 58. The relationship between range in height [H] and [H] divided by runout distance [L] for debris flows and debris avalanches. Data is acquired from dataset 2 with a total of 41 events.

Figure 59 shows the results of the slope angle analysis. A total of 10 debris flows were found to initiate from 40°-50° degrees, while 4 were found to initiate at both 20°-30° and 30°-40° degrees. There were 9 debris avalanches initiating at a slope angle of 40°-50° degrees, followed by 6 events from 30°-40° degrees and 3 events from 20°-30° degrees. However, both debris flows and debris avalanches were observed to initiate at angles below 20° degrees and above 50° degrees.

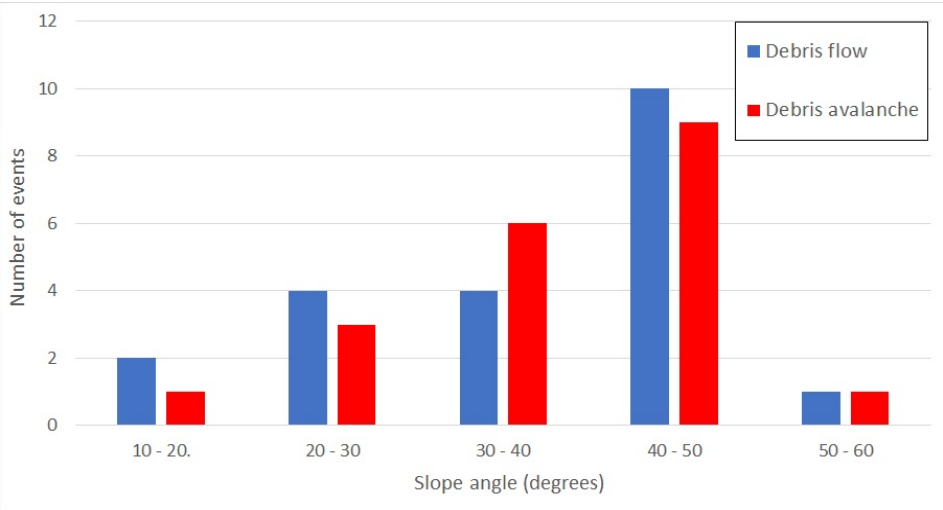

Figure 59. The observed slope angles for debris flows and debris avalanches from dataset 2. The total number of events are 41 events.

6.4 Characterization in terms of magnitude and frequency

6.4.1 Typical and frequent landslide magnitudes

The second dataset was used to perform a magnitude-frequency analysis. Figure 60 shows the result of the analysis. Landslides in the region have magnitudes ranging from 147 m2 - 124228 m^2 with most landslide magnitudes located within the range of 5000 m^2 – 25000 m^2. The cumulative landslide frequency is observed to decrease with increasing magnitude as expected. Regarding the landslide frequency, it is found that the region is likely to experience 7 landslides a year with magnitudes greater than 1000 m^2. A total of 4 landslides a year are expected with magnitudes greater than 10000 m^2 and one event is expected a year for landslides greater than approximately 65000 m^2.

A buckling point is observed for landslide magnitudes around 4000 m^2 – 5000 m^2, where the cumulative frequency increases its steepening trend. Another buckling point is observed around magnitudes of approximately 50000 m^2 where the cumulative frequency start to decrease rapidly with increasing magnitude.

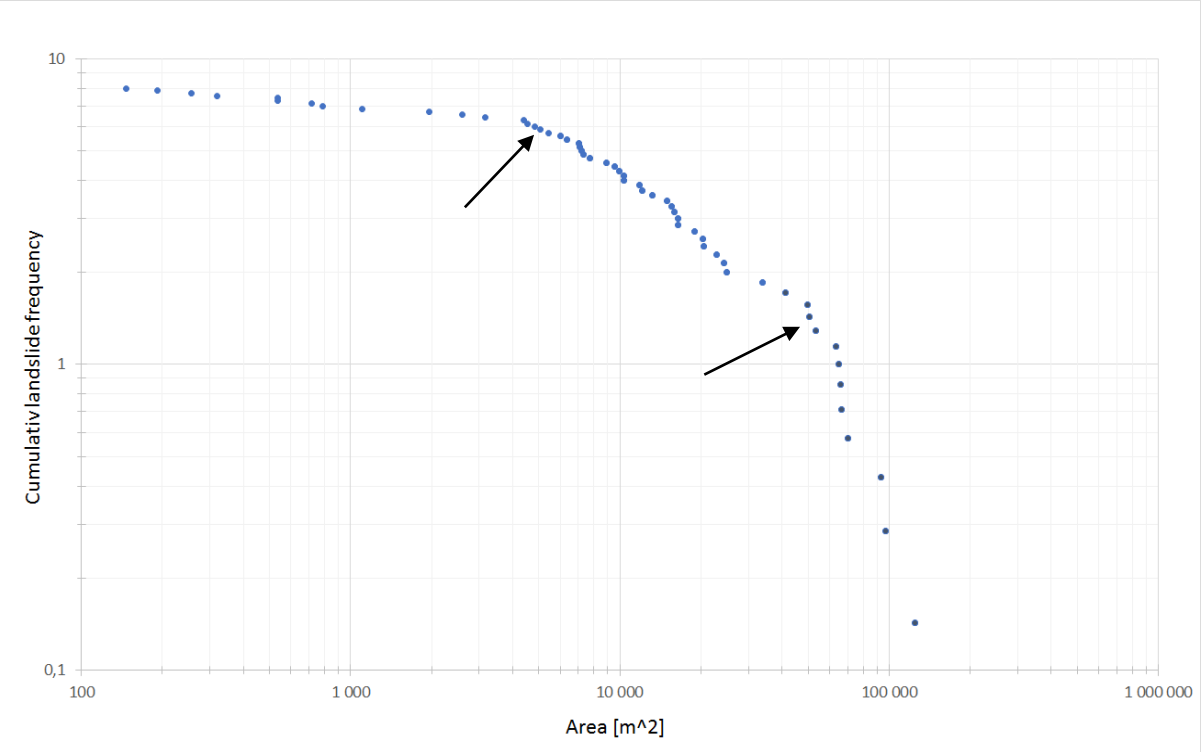

Figure 60. The magnitude-frequency curve for the region is presented. Buckling points are pointed out by arrows.

6.4.2 Landslide magnitudes differentiated between landslide typologies

Figure 61 presents the different magnitudes differentiated by landslide typologies. It can be seen that debris flows vary from 319 – 41201 m^2, but are more frequent in the range from approximately 4000 – 30000 m^2. The magnitudes for debris avalanches range from 191 m^2 to 96752 m^2 and represents six of the largest landslide magnitudes registered. Debris slides have a range of magnitudes from 146 m^2 – 1103 m^2 and slushflows varies from 18914 m^2 – 124228 m^2.

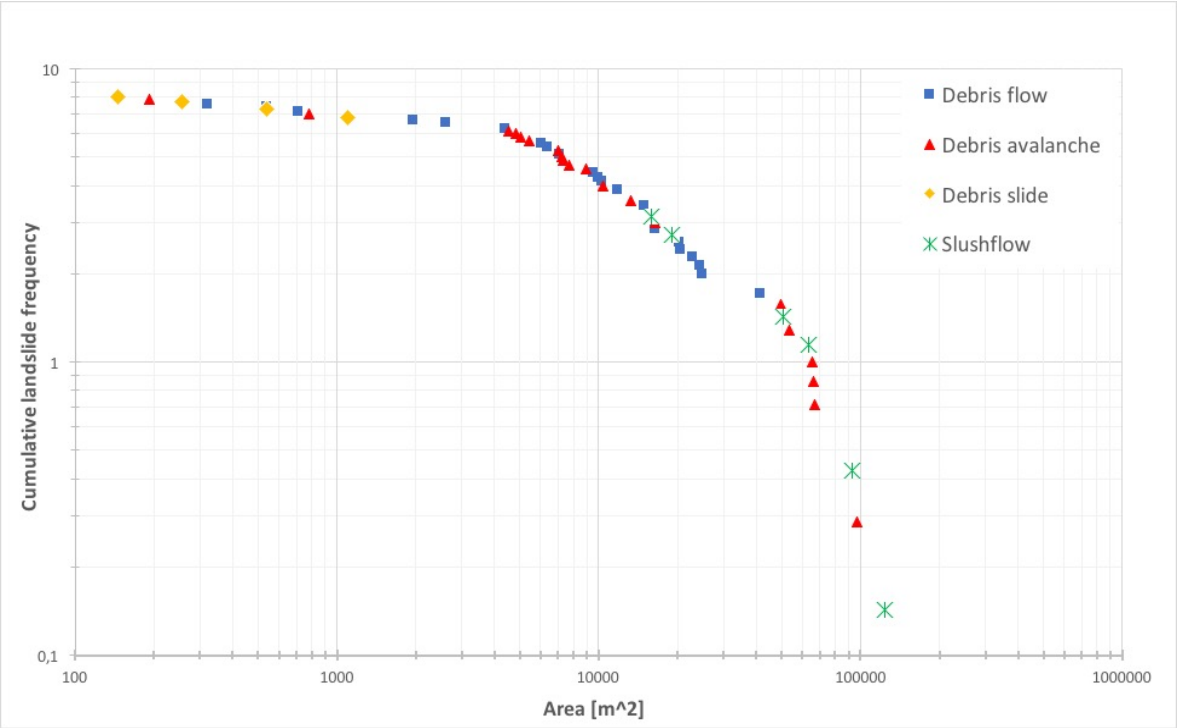

Figure 61. The magnitude-frequency plot visualizes the typical magnitudes differentiated by landslide typologies.

6.4.3 Landslide magnitudes for specific event inventories

Although the number of events were small, I tried to look at typical magnitudes associated with specific hydro-meteorological events as presented in figure 62. The events from 28.10.2014 are observed to have about the same magnitudes for all three events with a range from 16412 m^2 – 24438 m^2. However, the landslides associated with the extreme event Hilde in 15.11.2013 showed a greater variety of magnitudes from 6018 m^2 and up to 96752 m^2. The associated magnitudes from the extreme event Dagmar in 26.12.2011, presented in figure 63, shows the same tendency with a great variety from 256 m^2 – 93311 m^2.

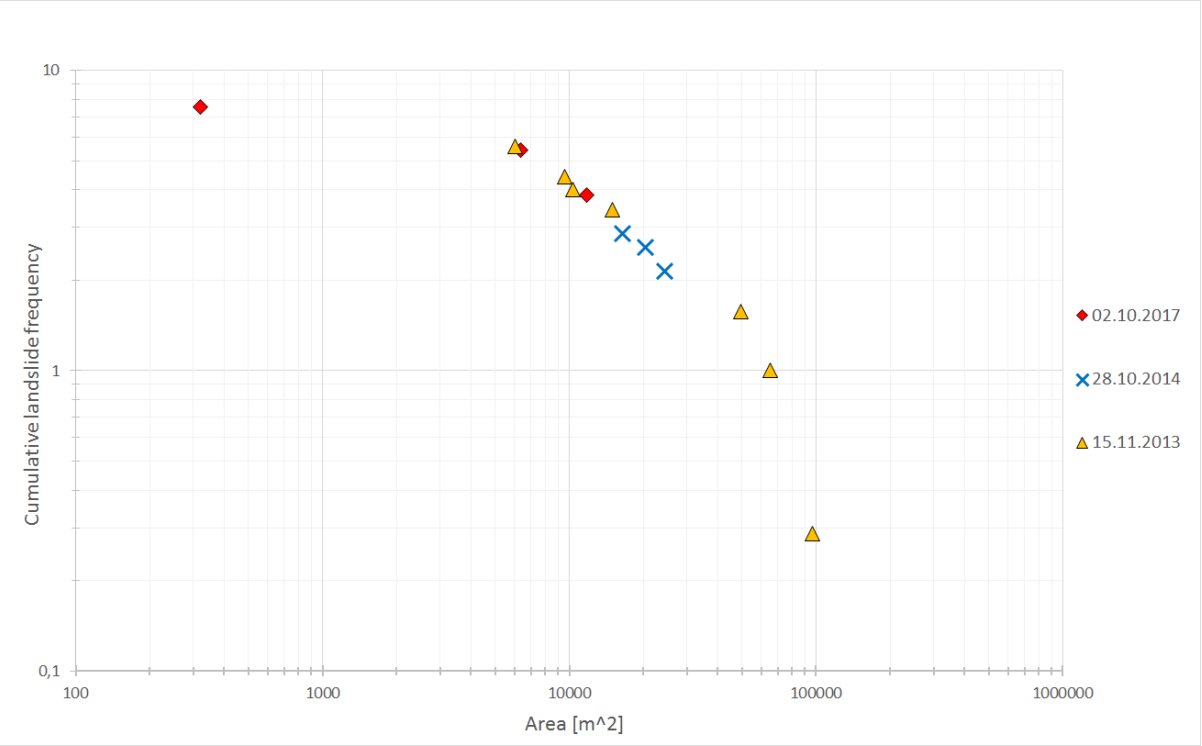

Figure 62. The magnitude-frequency curve shows landslide magnitudes associated with specific hydro-meteorological events. Number of events are: 02.10.2017 – 3, 28.10.2014 – 3, 15.11.2013 – 7.

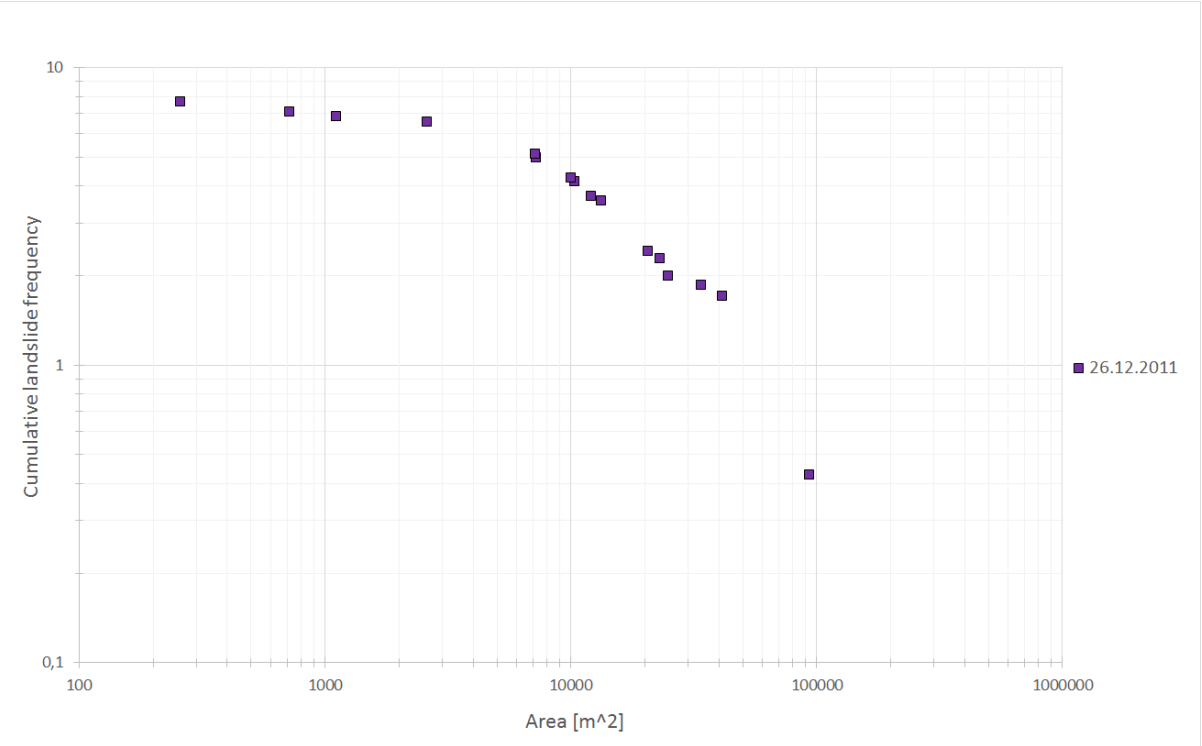

Figure 63. The magnitude-frequency curve shows landslide magnitudes associated with the specific hydro-meteorological event Dagmar in 2011. Number of events: 16.

6.5 Threshold analysis

Figure 64 presents observed values of relative water supply [%] and relative soil water content [%] for all landslide events from dataset 2, in comparison with the established threshold limits for the region. Eleven events are located within the orange (level 3) threshold limit (three observations are double), followed by 12 events inside the yellow (level 2) threshold limit (two observations are double). The rest are located outside this limit (level 1). The analysis shows a great number of events with 0 % of relative water supply, but with a high value of relative soil water content. Four events were, while extracting data from xgeo.no, found to have its starting point located in a grid with "NoData" of relative water supply or/and relative soil water content.

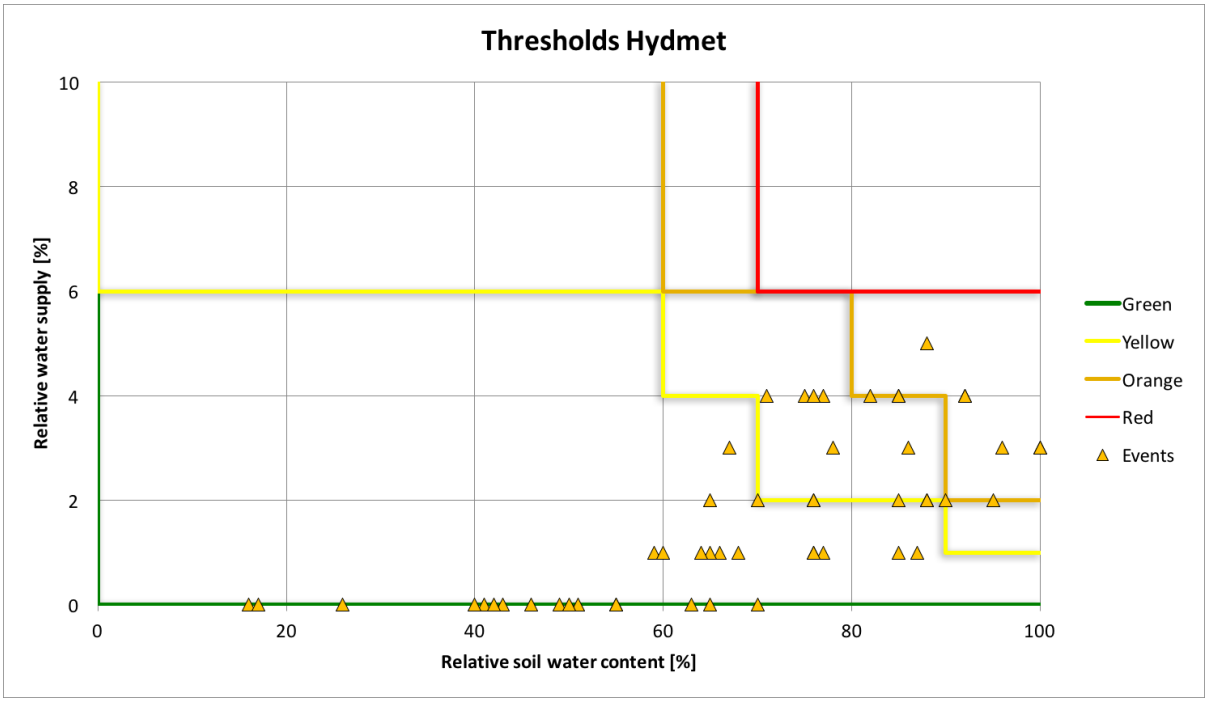

Figure 64. Threshold plot presents observed values of relative water supply [%] and relative soil water content [%] for landslide events in dataset 2. Total number of events are 52.

Figure 65 presents another threshold plot for events that occurred under a specific date and under certain hydro-meteorological conditions that initiated at least three landslides that were mapped. The extreme event Dagmar from 2011 has 3 events located within the orange threshold limit, followed by 6 events (one double registration) in the yellow limit. The extreme event Hilde from 2013 had 3 events in the orange level (one double registration) and 4 events in the yellow level. The event from 28.10.2014 had 2 events (a double registration)

in the orange level while the event from 02.10.2017 had all events located far away from the threshold limits.

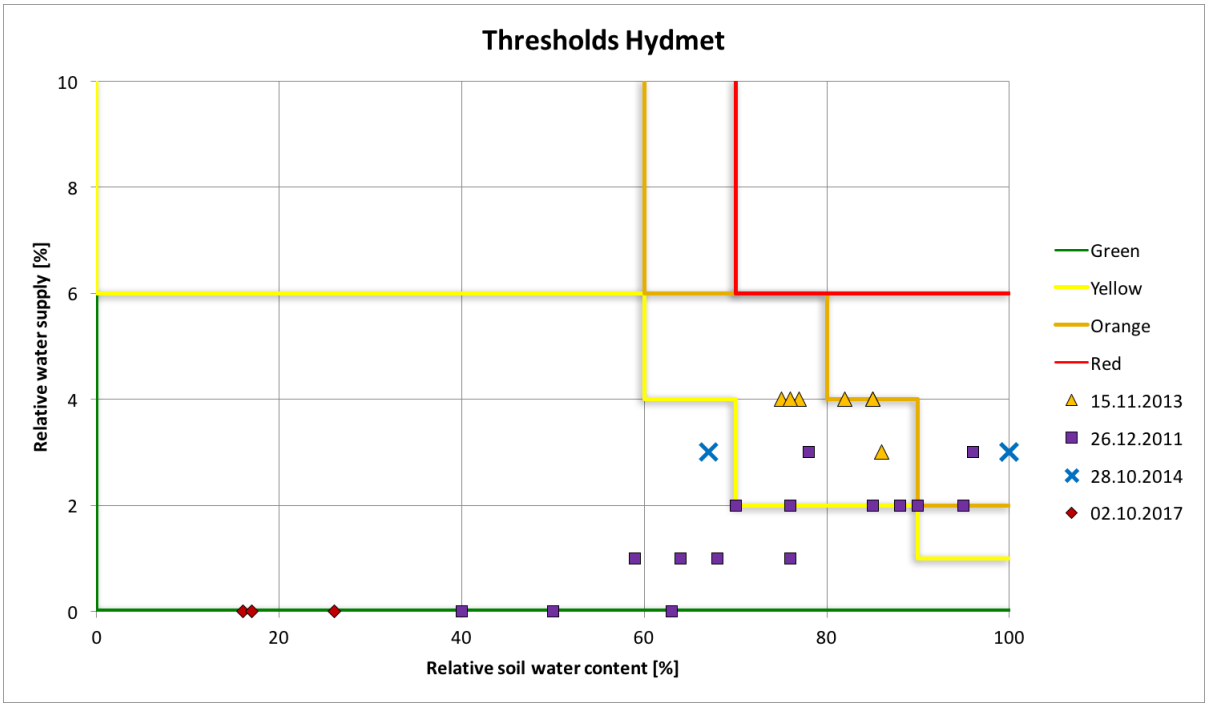

Figure 65. Threshold plot presents observed values of relative water supply and relative soil water content for landslide events associated with specific hydro-meteorological events. Total number of events are 29.

7 Discussion

The detailed study on rainfall-induced landslides in Norway has for now not been a priority and the knowledge of these types needs to be improved due to their occurrence of high frequency. A better knowledge and characterization is therefore mandatory, especially because an increase in frequency is expected in the future. This work is part of a national effort that started in 2011 (when the landslide EWS begun to be organized at NVE) and aims to better characterize these processes differentiated between the regions in Norway. My research has the purpose of analyzing landslides in terms of their magnitude and frequency, however, limitations and challenges were encountered. The low quality of landslide events recorded in the database and the lack of aerial photos or satellite images available after the events have strongly influenced the results of this work. The goal to map the extension of more than 500 events was not fully achieved.

7.1 Regional characterization

The spatial distribution of landslides confirms that landslides are a natural threat in the region, both in the coastal and near-coastal areas as well as in the innermost areas. However, the distribution is strongly influenced by the fact that landslides are recorded only when they made damage to infrastructure and buildings. This representation of landslides is therefore not realistic in the study area.

The topography confirms events to appear in slopes with slope gradients of 30° - 45° degrees as seen from figure 66. Rainfall-induced landslides are observed to initiate under such conditions in Norway (NVE, 2014a, Colleuille et al., 2017, Sandøy et al., 2017) as well as from international studies (Dai et al., 2003, Ortigao and Kanji, 2004, Hungr et al., 2014). A certain number of events, many located in near-coastal areas, are not clearly associated with steep slope gradients. Great amounts of annual precipitation are found in the same area that reaches values of above 3000 mm (figure 47). Precipitation is a crucial component for initiating landslides (Cruden and Varnes, 1996, Hungr et al., 2001, Dai et al., 2003, Dyrrdal, 2012). It is consequently thought to influence the number of events in these areas. However, it can be argued that a maximum zone of precipitation would presume an even greater collection of reported events here. An area located in the upper left corner (figure 47) are e.g. observed to have a low number of reported events even though there are much precipitation.

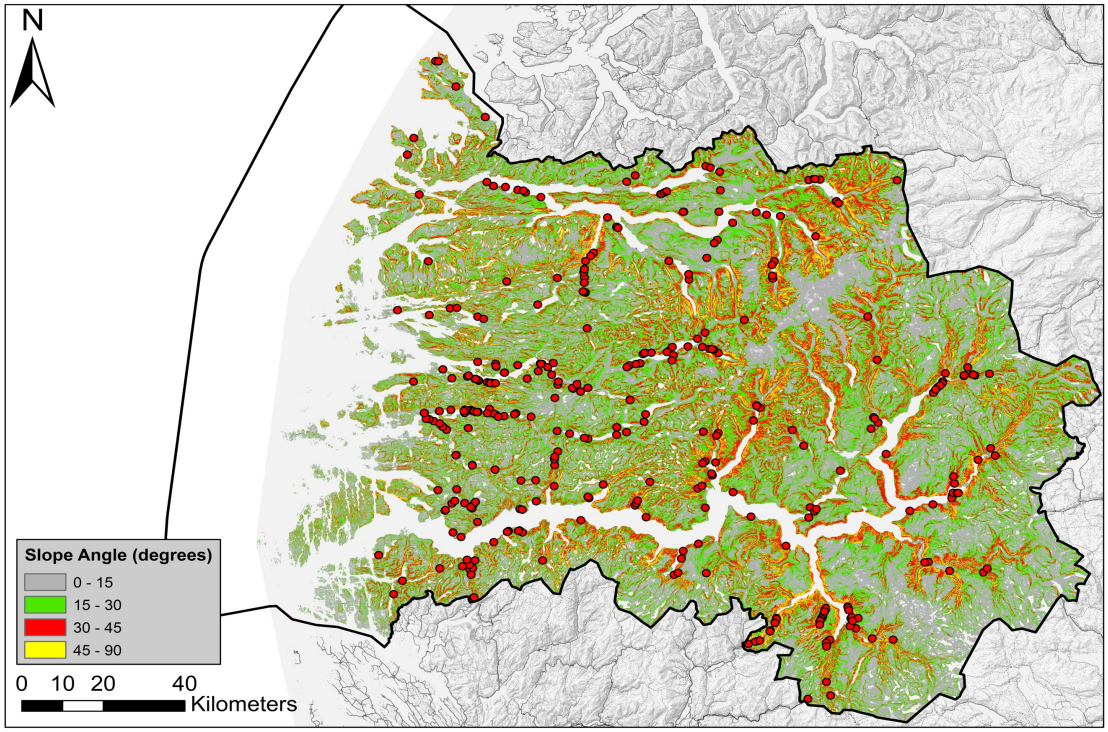

Figure 66. The distribution of landslide events (red circles) from dataset 1 compared to slope angles in the region. Total number of events are 507.

The comparison of landslide events and landforms (figure 48) confirms alpine relief or glacial relief to be a common landform for landslide initiation in the innermost parts of the region. The steepest slope gradients are also commonly seen within this landform. Coastal and near-coastal areas are more prone to landslides in landforms classified as glacially-scoured low mountains and valleys.

The landslide susceptibility analysis show that landslide events are registered in valleys with high density of susceptible areas as well as in valleys with low density (figure 49). It was also confirmed that most events appeared in areas classified with very high susceptibility. An area of mostly low and moderate landslide susceptibility is observed in the upper left corner in the region (figure 50), in the same spot where great amounts of precipitation are observed. The low susceptibility can be used as an indicator to explain the low number of triggered events here. However, the susceptibility map is limited on the landslide inventory input and lack of reported events will therefore affect the resulting landslide susceptibility (Cepeda and Bell, 2014). This area may therefore have a lower susceptibility than it should and cannot be used as the only explanation for the low number of events.

The temporal distribution in figure 44 show that landslides occur annually in the region. Extreme hydro-meteorological events are also common, but not annually. The great variations

in number of initiated events from these extreme events can be discussed from the maximum 24hour rainfall intensity (table 6). The extreme event Hilde in 2013 had a maximum intensity of 80 – 100 mm in the region and locally up to 100-150 mm. This is a bit higher compared to the other events which all had lower values of precipitation and lower number of landslide events (except Dagmar). The extreme event Dagmar had low precipitation intensity compared to Hilde, but were still associated with a high number of events. One explanation could be the extreme wind velocities from the event. Wind are known to cause an underestimation of precipitation in rain gauges (Dingman, 2008). Precipitation values from the event could in fact be closer to Hilde in 2013 then it seems. Wind effects can also lead to falling trees or removal of vegetation that may affect the slope stability (Antinao and Farfán, 2013). The number of initiated slushflows must also be considered as they do not depend on precipitation in the same way as debris flows and debris avalanches. Snow fall was registered the day before the event and the rate of snow melt was great due to the wind speed and mild temperatures under the event. Slushflows did therefore contribute to the high number of registered events. Another component could be the change in availability of loose material. An event like Dagmar removes a certain amount of loose material that could influence the number of landslide events from the next rainfall event.

Differences in temporal distribution for dataset 1 and dataset 2 are shown in figure 67. It shows the number of registered landslides compared to the number of events that were capable of being mapped. The number of mapped events are very low for all years, even though there are many landslides reported. It confirms that better quality of landslide data is needed which could help to achieve a greater dataset of mapped landslides.

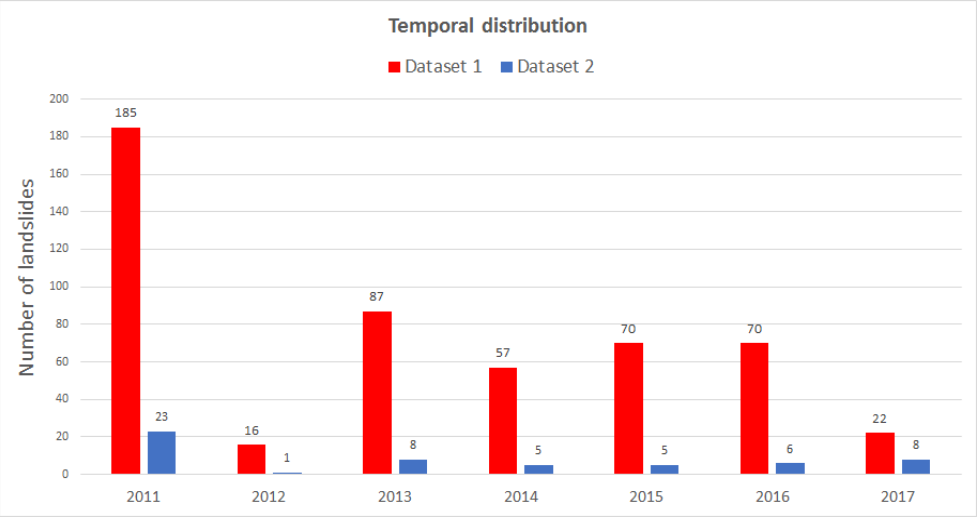

Figure 67. The temporal distribution of landslide events from dataset 1 (red color) compared to dataset 2 (blue color).

The analysis of the monthly distribution shows clearly that November and December are the months with the higher number of landslide events in deliberation with the annual precipitation patterns that Førland proposed in 1979. A study on extreme daily precipitation in coastal western Norway by Azad and Sorteberg (2017) share our findings by exploring that 60% of their events were associated with large-scale moisture transport occurring during November, December and January. The strong signal of December and November are, however, thought to be biased by the extreme-events from Dagmar in 2011 and Hilde in 2013 (table 6). A longer time of period are believed to clarify these months of being more vulnerable to landslides in the region and perhaps balance the number of events between these months.

The distribution of landslide typology enlightens the need of more careful classification and a systematic quality control of landslide data. A total of 77 % landslides were classified as "landslide in soil, unspecified". Some of these turned up to be debris flows, debris avalanches and debris slides while performing my analysis. The low number of mapped debris slides are believed to be underestimated. This type of landslide has a relatively low magnitude, as observed in my research. Landslide traces were therefore difficult to spot through aerial photos. The presence of shadow in some photos, caused by the topography, made it even harder. Surrounding vegetation could also cover the landslide traces (Stark and Hovius, 2001, Brardinoni and Church, 2004). Affected roads are also cleaned more quickly compared to larger events. The importance of these events having correct point-coordinates in the national database are therefore considered as high to spot them in aerial photos. Debris slides are also considered to feel less threatening due to its low magnitude and may consequently get less attention. This problem can lead to a potential lack of registrations from institutions or public. The Norwegian nomenclature and lack in tradition of studying this type of events are also believed to influence the low number of observed debris slides.

7.2 Landslide characterization

The objective for this part was to better characterize landslide typologies, their distribution and their physical parameters in the region, based on the regional dataset. Investigations through my sources of information allowed me to map the extent of only 56 landslide events. Lack in aerial photos, after the events, was the main cause for not allowing to map more events, together with poor quality on landslide data in the national database. A much greater sample is required to achieve strong and reliable results and to point out typical statistical

parameters. However, the lack on similar studies for my region makes my results valuable by pointing out important estimates for these landslides.

The landslide events were distributed over the entire region. However, a slightly difference between debris flows and debris avalanches are observed with debris flows tending to occur a bit further inland. The limited sample makes it difficult to conclude if this is a tendency worth considering or if its rather a coincidence. The temporal distribution of events was evenly distributed for all years except 2011 and 2012. Year 2011 had a great number of events associated with the extreme event Dagmar (table 6) that seemingly caused institutions and public to take pictures of events within the entire region. A great number of newspaper articles were found to cover these events and some of them were observed to encourage public to share pictures and stories from the storm.

The bedrocks monzonite, migmatite and gneiss of dioritic or granite origin were clearly the most frequent bedrocks located at our observed landslide sites in the region. However, quaternary deposits are considered with a greater importance. Soil classified as “thin, or no cover” or “colluvium deposit” were confirmed as most frequent in the region. Unfortunately, it is not possible to tell what type of thin cover that were present. A study by Bell et al. (2014) has also pointed out the quaternary map to have poor quality with certain areas having more details than others.

The typical elevations of the starting point of landslides were found in a range from 200–700 meters a.s.l. for debris flows and debris avalanches. Applied interpretations for deciding the source area, especially for debris flows, are thought to influence the results. The great variation in elevation from west towards east in the county is also believed to favour landslide initiation at different heights that may have influenced the values that is observed. A better approach could be to investigate typical heights separately for similar regions within the county. The typical elevation range were also similar between debris flows and debris avalanches. Precipitation has by Førland (1979) been proposed to influence typical heights of initiation. He found that the range from 150-300 meters receive the most intensive rainfall in the region. It could contribute to the initiation of landslides at these heights, regardless if they have potential of initiating further upslope. However, the observed events at heights up to approximately 950 meters could indicate that precipitation may maintain a certain intensity at higher elevations as well.

The typical slope angles of debris flows were found to range from 25°-45° degrees which correlates partially well with findings from Ortigao and Kanji (2004) who claims debris flows to initiate at angles above 20°-25° degrees. However, they propose debris flows to be less likely to initiate above 37° degrees due to the existence of rock scarps while Dai and Lee (2001) propose 40° degrees as an upper limit. As mentioned in chapter 5.2, there were several debris flows that were needed to be interpreted. An inaccurate starting point can have caused the wrong slope angle to be extracted from GIS. It can thus explain the observed uncharacteristic slope angles above 40° degrees. On the other hand, my study area does not necessarily represent the same conditioning and triggering components as for these comparative regions. A study by Fischer et al. (2012) mapped both regional and national susceptibility of debris flows in Norway by using slope angles from 25°-45° degrees, with the range in slope angle based on a landslide study by Dahl et al. (1983). These values correlate better with my findings. Considering debris avalanches there was a guide published by NVE in (2014b) that proposed this landslide type to initiate at slopes greater than 25° degrees in Norway. It correlates well with my findings, but with one of my events initiating at 16.7° degrees. This event was triggered in a road cut that explains its uncharacteristic slope angle (figure 68). No significant aspect was confirmed for debris flows and debris avalanches, neither for the whole dataset.

Figure 68. Example of a debris avalanche that occurred at a slope modified by humans. Event is from Dalsøyra in the municipalty of Gulen, 2017. Photo: Gulen Brannvesen

The observed trend of an increased runout distance with increased height of slope is supported by previous studies (Dai et al., 2003, Devoli et al., 2009, Qarinur, 2015). A study by

Corominas (1996) point out that a great height of fall is normally needed to obtain longer runout distances. The four most extreme debris flows for our dataset are found to have about the same runout distances, but with a great variety in range of height. The same observations are found on the debris flow data from Devoli et al. (2009) and Qarinur (2015). A trend line was confirmed for debris avalanches as well. A recent study in Norway on five large triangle-shaped debris avalanches by Sandøy et al. (2017) estimated runout distances that varied from 0.8 to 1.6 kilometres. The debris avalanches reaching the greatest distances in my dataset correlate well with this finding. However, most events reached distances below 800 meters and are believed as more typical values for my region.

Both debris flows and debris avalanches are confirmed to have about the same mobility in the region. However, two debris flows with H/L values of 0.082 and 0.194 stand out with a high mobility compared to the rest of the dataset while two debris avalanches have a distinctly lower mobility with values of 1.206 and 0.851. The mobility of landslides depend on several components like elevation, slope inclination, material properties, landslide volume, water-input and any topographic constraints (Devoli et al., 2009). The observed outliers can be a product of some of these components being uncharacteristic.

7.3 Magnitude-frequency

The characterization of rainfall- and snowmelt-induced landslides in terms of magnitude in the study area was accomplished by calculating landslide area (m^2) and by performing a magnitude-frequency analysis. A great variety of landslide magnitudes were observed in the region within the analysed period with the most typical size approximately of 10000 m^2. This magnitude was also concluded as most frequent from a study by Guthrie and Evans (2004), as shown in figure 11 in chapter 2.2, while they investigated landslides in British Columbia. However, it seems like landslides with low magnitudes are less frequent in their dataset as also observed in my research. An underestimation of landslides with low magnitudes have been pointed out by previous studies and can cause the wrong magnitude to apparently be most frequent (Stark and Hovius, 2001, Brardinoni and Church, 2004, Dahl et al., 2013). Dahl et al. (2013) claims low-magnitude landslides to be less frequent since a small potential slope failure is likely to be held in place due to supporting soil and roots. In other words, large potential slope failures are more likely to fail than small slope failures. The topography in my region is thought to, compared to other regions with less tremendous topography, favour a greater number of large landslides rather than small landslides. On the other hand, a large

landslide will have limited opportunities to become triggered compared to a small one as it requires preparatory factors to support that exact magnitude. The approach by looking through AP is, as mentioned in chapter 7.2, thought as another explanation for an underestimation. The applied quality controls in the national database are also thought to influence the underestimation by having a higher likelihood of undesirably selecting away low-magnitude events compared to large-magnitude events. However, the influence of this component is difficult to evaluate as there are lack on previous studies that has performed the same type of quality controls.

The magnitude-frequency plot from figure 60 confirms the expected decrease in cumulative frequency with increasing magnitude for our region. Another characteristic feature that has appeared in previous landslide magnitude-frequency studies (Guthrie and Evans, 2004, Guzzetti, 2005, Dahl et al., 2013) is the point of roll-over. Magnitude-frequency curves, regardless of the way magnitude is calculated (Dahl et al., 2013), seem to have a buckling point that separates data of low and large magnitudes in both non-cumulative and cumulative distributions (Guzzetti, 2005). The data consisting of large magnitudes can be described by a power-law relationship (Guzzetti, 2005). The point of roll-over was, however, not clearly seen from our M-F plot probably due to the unfortunate low sample size. Nevertheless, I propose a mathematical power-law as

$$Y = 21950\, X^{-0,925}\,, R^2 = 0,8977$$

in a way of indicating landslide frequency and magnitude for the study area. The power-law, presented in figure 69, covers approximately 70 % of the total dataset and is thought to be applicable for magnitudes greater than 6000 m^2. The power-law can be used to point out magnitudes that should be considered as large or small. It can also indicate the limitations of landslide magnitudes within the study area (Guthrie and Evans, 2004). However, the visual impression of my proposed power-law and its fit to the data are poor compared to similar studies Guthrie and Evans (2004) and Dahl et al. (2013). There's a need to improve the sample size to ascertain the point of roll-over so that large magnitudes can be better described.

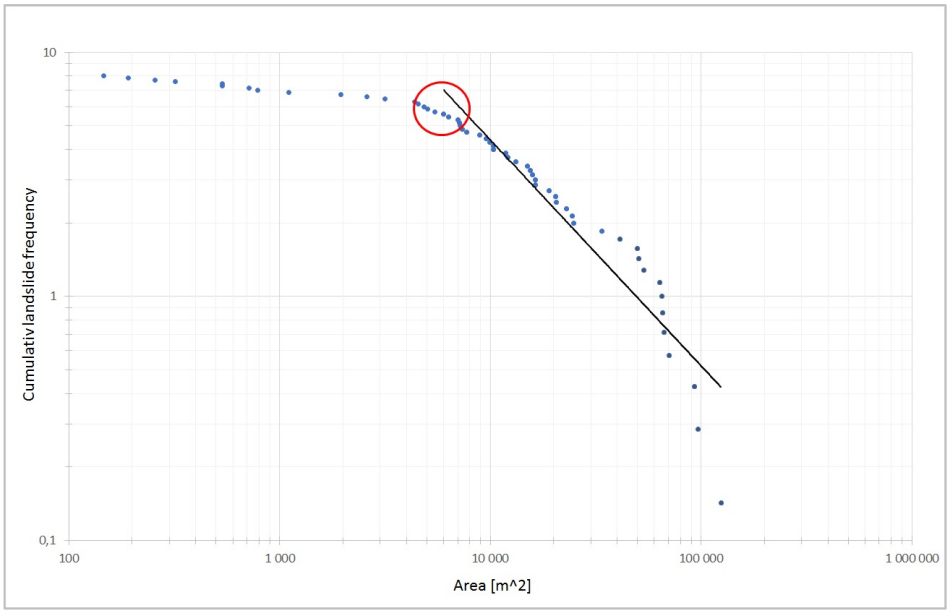

Figure 69. A proposed roll-over point is decided at approximately 6000 m² and the linear power-law is presented.

Some characteristics can be derived from the MF-curve differentiated by landslide typologies. It is observed that debris slides all have magnitudes smaller than 1500 m^2. This is in general lower magnitudes compared to debris flows, debris avalanches and slushflows as expected. It was also expected that debris avalanches showed a great variety of magnitudes, as well as representing some of the largest events from the record. Debris flows were expected to have lower magnitudes compared to debris avalanches due to their restriction to channelized slopes. All slushflow events from the M-F analysis were found to have a very high magnitude. Their long runout distances, range in elevation and ability to flow even at gradual slopes are thought as an explanation. However, their sample size forces me to await discussing these values as typically for the region. The data are still valuable by indicating that these may have a considerable magnitude that authorities and the landslide EWS should be aware of.

7.4 Incorporation of magnitude in landslide EWS

For the objective of incorporating magnitudes into the landslide EWS I looked at typical magnitudes associated with specific hydro-meteorological events, as well as associated warning levels gathered from summary reports from NVE.

User surveys have been performed three times in recent years to evaluate functions of the landslide EWS, aiming to investigate if users were satisfied or not (Colleuille et al., 2017). It turned out that several users, including SVV, enquired more detailed landslide information in

a way of evaluating the landslide risk on local scale (Colleuille et al., 2017). I believe that incorporation of landslide magnitude will work as a valuable estimate by allowing the users to perform more appropriate mitigation measures and to choose the correct state of preparedness. The users and especially SVV will e.g. have a better idea of the damages that should be expected at the roads and the following clean-up process that is needed afterwards. A proposal of how magnitude may be incorporated will now be discussed.

The incorporation of magnitude into the warning levels is based on observed landslide magnitudes from certain meteorological events by also considering their associated warning-level. The extreme meteorological event Dagmar in 2011 had an associated outcome of 82 landslide events as seen from table 6. This event occurred at a very early stage of the EWS (6 months after the system was initiated) and it was therefore not issued any warning level for this case. From my point of view, I suggest this event to be considered as a typical level 4 event due to the great number of landslides and the variety of observed magnitudes. This event is observed to have magnitudes above and below 10000 m^2. The criteria of warning levels in the landslide EWS have pointed out that large events are expected at this level as well as multiple small events. One event turned out to have a distinctly greater magnitude compared to the others of approximately 96000 m^2 and is therefore considered to refer as a "large magnitude". Observed events with magnitudes below 10000 m^2 are considered as referring to the expected small landslides.

Another meteorological event from 28.10.2014 had an associated level 3 warning. Three landslide magnitudes at approximately 20.000m^2 occurred during this event and are proposed to represent magnitudes in between large and small magnitudes. Some larger events were observed from the extreme meteorological event Hilde in 2013. This event was evaluated as a level 3 event by summary reports from NVE. Three events differed greatly with magnitudes above 50000 m^2 that confirms landslides to have relatively large magnitudes, as well as small ones at this warning level. Another finding is that the total number of initiated events in both level 3 and 4 can be very high, but with a higher number for level 4 events. However, it can be discussed if the extreme-event Hilde, that resulted in a total of 42 registered landslide events, rather should have been considered as a level 4 event.

No specific meteorological event was used to consider magnitudes for a typical level 2 event. However, my experience was that landslides occurring on days with few events, typically a total of 1-3 events, had rather random magnitudes ranging from relatively low to medium-

sized. I therefore expect a warning level 2 event to be less likely to initiate a large magnitude and that authorities should prepare for a medium-sized magnitude to prepare for the worst scenario.

The following terms of landslide magnitudes in Sogn og Fjordane are proposed:

- Small: 0 – 10.000m^2.
- Medium: 10.000 – 50.000m^2.
- Large: > 50.000m^2.

It is now desirable to connect landslide magnitudes and landslide EWS warning levels based on the proposed terms of small, medium and large. Figure 70 presents typical magnitudes associated with different warning levels. I suggest warning level 2 to consider landslide events with magnitudes up to 10.000m^2. There's also a likelihood of experiencing a single event with medium magnitude. Large landslides are unlikely to occur. Warning level 3 should expect multiple landslides with medium magnitude in a range from 10.000 – 50.000 m^2 with increased likelihood of dealing with a large landslide above 50.000m^2. Level 4 is thought to need an even higher state of preparedness due to expectation of an unusual high number of initiated events at all scales with likelihood of initiating several landslides of large magnitudes.

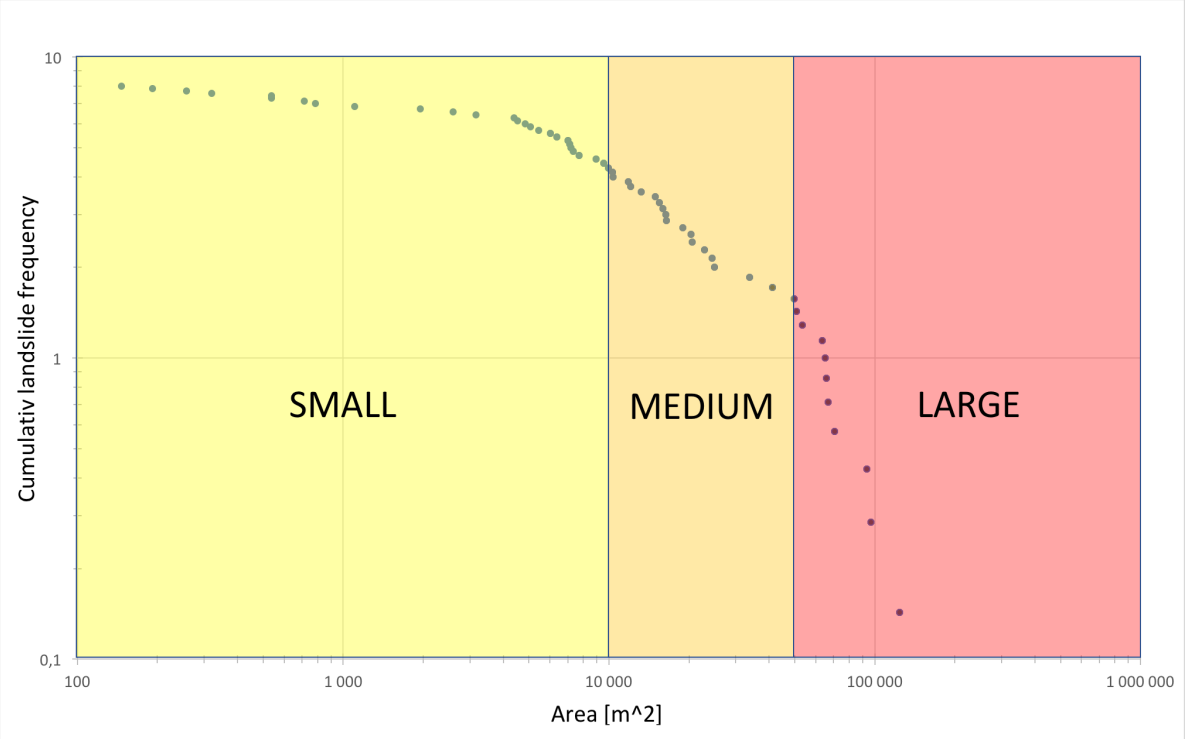

Figure 70. The magnitude-frequency plot presents a proposed relationship between landslide magnitudes and warning levels Proposed terms of magnitudes are given as well.

It is also important to assure that users of the landslide EWS are aware of the potential harm the magnitudes may cause in a way to reduce economical and human loss. Figure 71 visualizes the typical damages associated with a small landslide that was found in my region. They were commonly observed to cause some type of damage on roads like bringing material on top of the road which in some cases resulted in a road blockage. However, this magnitude is believed to have potential of causing more damage if location is unfortunate. Exposed roads, railways or any house may be partially destructed. The closing of roads is not thought as necessary at this warning level.

Figure 72 presents typical damages associated with a landslide of medium magnitude. Road blockages due to landslide deposits were commonly observed and could also destroy the road completely or partially. Roads may be closed for days due to time-consuming cleaning with need of repairing the damages. These magnitudes have also potential of causing severe harm to inhabitants by hitting any exposed house or infrastructure. I believe that authorities must evaluate whether exposed roads should be closed for the upcoming meteorological event to assure that no one will put themselves in danger.

Figure 71. A debris flow (approx. 6400m²) presents the typical outcome of a small landslide in the region. Event is from Almhol in the municipality of Luster, 2017. Photo: Left: Eirik Winge. Right: Tore H. Medgard, Statens Vegvesen

Figure 72. This event (approximately 34000m²) represent the likely outcome of a medium-sized landslide. Event is from Prestteigelvi in the municipality of Vik, 2011. Photos: Grunde Engan.

A possible outcome associated with a landslide of large magnitude is shown in figure 73. This type of magnitude is thought to have great potential of creating severe damage on roads, infrastructure or properties that can lead to serious harm to inhabitants. Authorities should encourage vulnerable population to stay home until the event has passed, as well as closing exposed roads when the event hits.

Figure 73. A debris avalanche shows the likely outcome of a landslide defined with large magnitude (approx. 97000m²). Event is from Skredestranda in the municipality of Eid, 2013. Photo: Jan Helge Aalbu

Each warning level in the landslide EWS has an associated general explanation of the upcoming event, as well as classification criteria that are used to evaluate its performance. The criteria have so far taken advantage of using the terms "large" and "small" magnitudes when considering the size of the expected landslide. Table 8 presents my proposal of incorporating my values of small, medium and large magnitudes into the warning levels. These terms are not thought as representative for other regions. The incorporation is thought to be helpful by diminishing subjective meanings in the process of evaluating the performance of the landslide EWS. It will also lead to the necessity of an immediate and systematic approach to map the extent of landslides as they occur. This is only thought to have positive outcomes by achieving landslide data with good quality and to finally start a systematic mapping of landslides in the region. It will also help to improve the national database.

Table 8. Warning levels are modified to include my proposed definitions of magnitudes and the associated outcome for these events as well as proposed mitigation measures.

Level	General Explanation	Classification Criteria used to Evaluate the Performance of the Landslide EWS
		Small: 0-10000m², Medium: 10000-50000m², Large: > 50000m²

4	• Extreme situation that occurs very rarely and that requires immediate attention.
	  ○ Exposed roads must be closed.
	  ○ Encourage population to stay home
	• Many landslide events are expected.
	• Consequences:
	  ○ Likely to cause severe damage on roads, infrastructure or people.
		• > 14 landslide events
		• Large landslides are expected, together with a high number of events having a great variety of magnitudes.
		• Several road blockings due to landslides.

3	• Severe situation that occurs rarely and requires preparedness.
	  ○ Consider closing exposed roads
	  ○ Inform population
	• Many landslide events are expected
	• Consequences:
	  ○ Considerable damage on roads or infrastructure.
	  ○ Clean-up process can be time consuming (days)
		• 6-10 landslides
		• Medium-sized landslides are expected in an area of about 10-15.000km².
		  ○ Large landslide might occur
		• Several road blockings due to landslides.

2	• Situation that requires vigilance. • Some landslide events are expected, certain large events may occur.	• 1-4 landslides • Small landslides are expected in an area of about 10-15.000km² ○ Medium-sized landslides might occur. • Flooding/erosion in streams
1	• Generally safe conditions	• No landslides are expected • 1-2 landslide may be triggered from local rain showers. • Man-made landslides may occur

7.5 Threshold analysis

The NVE is aware that thresholds present some inaccuracy and do not perform well in Sogn og Fjordane (S. Boje, oral communication). This is based on the 7 years of experience since the establishment of the landslide EWS. A warning message can consequently be issued even if the thresholds are not exceeded. To adjust thresholds, a dataset of landslides with a better quality is required. Since a better dataset was now available, it was decided together with NVE to perform threshold analysis and investigate how the observed values of relative water supply and the relative soil water content of my landslide events from dataset 2 fitted with the established threshold limits. Inaccuracy of data will be discussed to explore how we can adjust or improve threshold limits.

Quite many events seem to be underestimated regarding the relative water supply. A report by Boje (2017) explains that there are several errors related to both observed and simulated precipitation. The observed landslide events from 02.10.2017 is a great example of how the GWB-model fail to interpolate values of observed relative water supply within the region. These events were all located relatively close to each other with a nearby gauge stations named “Skjolden” that measured 37 mm precipitation as seen from figure 74. However, the relative water supply that was extracted from these events was 0 %. A quick inspection performed by NVE, after my findings, (S.Boje, oral communication) revealed the GWB-

model to not include this gauge station while interpolating precipitation. An underestimation was therefore present for these events and the observed values of relative water supply are clearly wrong. These landslides are examples of events being unsuitable by trying to use observed values to improve regional threshold limits. The use of hydro-meteorological events with a higher number of events or with events that are spread over a larger area are thought as a better approach for this purpose.

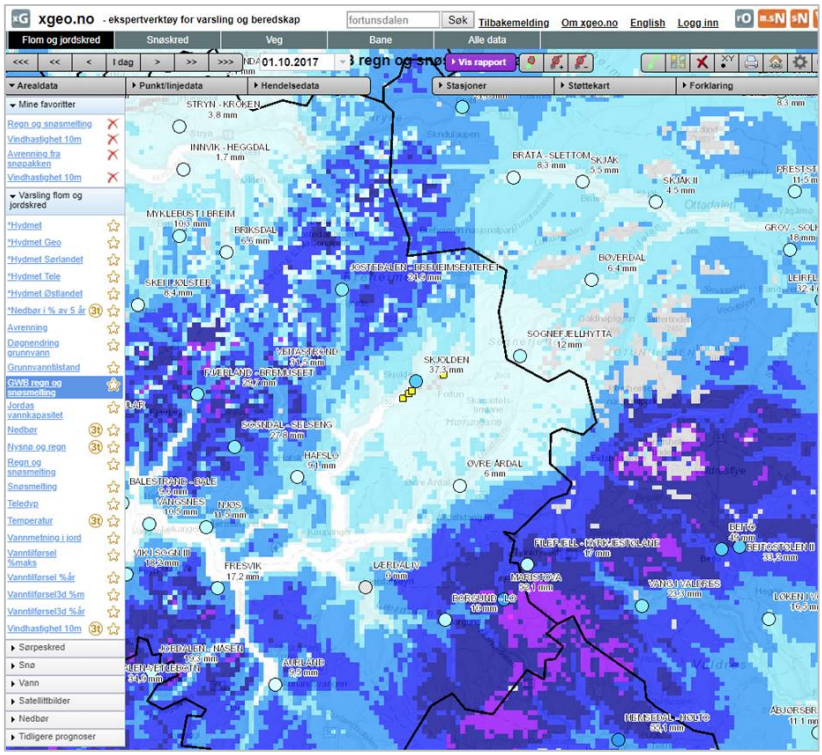

Figure 74. Screenshot from xgeo.no shows the gauge station "Skjolden" (slightly right of the blue marker) measuring 37.5 mm of precipitation at the event from 02.10.2017. Three debris flows, seen as yellow squares, were located nearby but observed to have only 0 % relative water supply.

Another challenge appears when the GWB-model interpolate precipitation in an area with temperatures varying around 0 degrees (S.Boje, personal communication). The model will interpolate the rainfall as snowfall if the mean temperature that day falls below 0 degrees. Another problem is pointed out by Boje (2017) if a precipitation event occurs in between two dates (e.g. 06:30-07:30). The proportion of precipitation from the triggering event may then be split between two days. The amount of precipitation that is extracted may consequently turn out to be lower than it should. A great number of my events had an uncertain time of initiation, but were confirmed to occur during the night and may therefore have been influence by this error. Landslide events are also typical to become initiated from torrential rain. These meteorological events can be limited in a small area and rain gauges do not necessarily measure the correct amount from such events (Boje, 2017).

I believe challenges are still present when extracting observed values of relative water supply. The data are likely to become more accurate when the errors pointed out are excluded or handled in a better way. Observed values are then believed to appear closer to the established threshold limits of warning levels.

7.6 Methodology and data

A magnitude-frequency analysis has never been performed in Norway. There are also lack of systematic mapping of landslide events in the region. It was therefore necessary to find a time-efficient way to map the extent of as many landslides as possible. Quality controls were performed in the national database with some elements not being observed from any previous study. The research was therefore expected to reveal weaknesses, as well as exploring clever and time-efficient methods to achieve my objectives. I will now discuss my approach to illuminate my experience so that prospective analysis can be performed in a better way.

I decided to not perform any field trips during my research. My regional research did not have any purpose of doing field work for all these events as mentioned in chapter 5. It could probably help to increase the number of mapped events with poor quality by visiting their landslide locations. Observation of landslide traces from field trips could have been used to ascertain the extent of landslides and by improving the landslide data quality. However, this approach was believed to require too much time to become accomplished within my study period.

The use of the national database as a starting point for my research allowed me to quickly collect landslide data on rainfall-induced typologies. However, some weaknesses of my approach were revealed while performing my quality controls. My first quality control assumes landslide data to have correct landslide typology, as well as correct year and date. Landslide events in the database were frequently observed to have wrong typologies and sometimes wrong date. These errors in the database did therefore cause my first dataset to become incomplete.

The next step was to map as many events as possible. Poor quality in the national database including inaccurate point coordinates, wrong typologies, multiple registrations and lack of event-information led to a time-consuming investigation of landslide traces in both aerial photos and newspaper articles. The approach by using aerial photos to map the extent of

landslides have commonly been used by several studies. The main problem was, however, that there were many landslide sites with lack of available aerial photos in my period of interest. A closer inspection on the availability of AP should have been performed in advance to prevent this error.

The registered events are, as already mentioned in chapter 7.2, strongly restricted to areas where events have performed damage on roads and infrastructure. Another weakness is therefore by not systematically going through AP for the entire region. It causes a probable loss of missing potentially useful events for the analysis. Dahl et al. (2013) did this for his research and later verified 30 % of his observations through media, field work or public. He therefore ensured that the whole region was closely investigated so that any landslide traces were revealed. However, the lack of AP in the region could make it difficult to complete the sample anyway. Nevertheless, it is clearly ideally that closer investigations of landslides should have been accomplished through analysis of accessible AP of the entire region to establish a more complete dataset.

Looking at prior events older than 2011 are thought as an alternative approach to achieve a sample of landslides and to estimate their magnitudes. It would increase the likelihood of landslide events being covered by at least one AP taken both before and after the event. However, a walkthrough of events older than 2011 is believed to be time-consuming in other ways. My experience was clearly that the most recent events were the best documented in the database and that the oldest events are more likely to contain more errors. The summary reports from 2013 allowed me to quickly highlight rainfall-induced events considering historical warning levels. It clearly helped me to map the extent of a great number of events in an efficient way.

My methodology has turned out as a good way of updating landslide data with poor quality. The approach allows to update attributes as landslide typology, adjust point-coordinates to correct location, adding valuable information and by eliminating errors in the database while performing the analysis.

8 Conclusion and summary

Sogn og Fjordane is prone to rainfall-induced landslides and it was desirable to investigate if these could be better characterized in terms of magnitudes, as well as other landslide parameters, based on an existing landslide dataset from the national database. It was also desirable to propose a way of incorporating magnitudes into the criteria for landslide EWS warning levels and to investigate how this information could be communicated to public and authorities.

My objectives were achieved through an analysis of the landslide database by a first quality control selection, aiming to perform a regional characterization. This first dataset contained 507 rainfall-induced landslides and regional analysis confirms these to occur annually and in the entire region, occurring most frequently during late autumn, winter and spring. However, extreme hydro-meteorological events are observed to strongly influence the temporal distribution. The distribution is believed to strongly rely on the dependency of events causing harm to society, as well as topography with slope angles of 30°-45° degrees, precipitation patterns and soil type. Areas classified as alpine- or glacial relief and glacially-scoured valleys must be considered with great caution in the region, as well as areas classified with very high susceptibility. The analysis of typology revealed great potential of improving the classification of landslide typology in the national database and debris slides are being underestimated due to errors of API.

My second dataset was used to improve the landslide quality by creating a landslide inventory map consisting of landslide polygons. This was accomplished by an analysis of different sources, like aerial photos, summary reports from NVE, newspaper articles, satellite images and google street view. The availability of aerial photos was poor as well as the landslide quality in the national database which only allowed me to map 56 events. Landslide characteristics differentiated by typology revealed debris flows and debris avalanches to occur over the entire region at a great variety of heights with typical slope angles of 25°-45° degrees. Both debris flows and debris avalanches were observed with similar mobility but with debris flows tending to have longer runout distances. The landslide magnitudes were used to perform a magnitude-frequency analysis that revealed landslide areas of 10000 m^2 for being most frequent in the region but with potential of reaching over 100000 m^2. Incorporation of magnitudes required to look at specific landslide magnitudes from specific

hydro-meteorological events associated with an issued warning level. Landslide magnitudes below 10000 m^2 should refer to a small landslide, magnitudes in between 10000 – 50000 m^2 should refer to a medium landslide while landslide magnitudes above 50000 m^2 are proposed as large magnitudes.

A level 4 warning event must expect large landslides as well as a high number of events occurring at all scales causing road blockages and severe damage on society. A level 3 event is also likely to experience a large landslide, but mostly medium-sized are believed to occur which also could cause considerable damage on roads and infrastructure. At last, a level 2 warning event are rarely associated with large magnitudes and should rather expect a medium-sized landslide. At last, it was desirable to investigate the fit of observed values of relative water supply and relative soil saturation to evaluate the established threshold limits of the landslide EWS. The relative water supply is still being underestimated due to errors of the GWB-model and from measuring errors at the gauge stations.

My results have clearly pointed out some of the typical magnitudes and frequencies for my region as I wished for, as well as the associated damages they may cause. My pioneering approach of incorporating magnitudes are therefore believed as valuable for the landslide EWS, with opportunities to improve my findings even more. Efficient ways of mapping the extent of landslides have been found and it also works very well for updating attributes of landslide events in the national database. Nevertheless, the results of my research are not as strong as I hoped for due to the low sample of dataset 2. Limitations of aerial photos and poor quality of data in the national database restricted my findings and the applied methodology did therefore not come up to my expectations. Another approach could have been to use LiDAR, performed investigation of events older than 2011 or by visiting landslide sites to accomplish a greater sample of mapped events. However, this work has a great importance by being part of an ongoing project by performing systematically mapping of landslide events and the lack of previous studies at these landslide in my region makes my results all valuable. I am therefore satisfied with my results.

Future work

Future work might include:

- A systematic approach to map the extent of all possible landslides in my region to produce stronger results and to ascertain my findings of typical magnitudes. I also encourage similar analysis in other regions since my results most likely are not representative for other counties.
- Perform magnitude-frequency analysis on volume and investigate if this is better to become incorporated rather than landslide area.
- Present magnitude-frequency analysis with a non-cumulative distribution when sample is considered as great enough to ascertain the point of roll-over and to derive a more accurate power-law relationship.
- Incorporate attribute of warning level in the national landslide database so that future work can easily select events associated with specific warning levels to improve the landslide EWS
- Capacity training to ensure users and institutions to classify and using correct terms of landslide typologies when performing registrations. It will increase the data quality and hence the quality on future analysis.
- A walkthrough of events in the national database that occurred under specific hydro-meteorological event to assure that all registered events are documented correctly and properly. My investigation revealed some of these to be poorly described, even though a lot of event-information was derived from my sources of information.
- Analysis that explores controlling components of the total number of initiated events occurring under specific hydro-meteorological events.

9 Literature

ANDREASSEN, M. L., ELVEHØY, H., KJØLLMOEN, B., ENGESET, V. R. & HAAKENSEN, N. 2005. Glacier mass-balance and length variations in Norway. *Annals of Glaciology,* 42**,** 317-325.

ANTINAO, J. L. & FARFÁN, L. M. 2013. Occurrence of landslides during the approach of tropical cyclone Juliette (2001) to Baja California Sur, Mexico. *Atmósfera,* 26**,** 183-208.

AZAD, R. & SORTEBERG, A. 2017. Extreme daily precipitation in coastal western Norway and the link to atmospheric rivers. *Journal of Geophysical Research: Atmospheres,* 122**,** 2080-2095.

BARGEL, T. H., FERGUS, T. Å., DEVOLI, G., ORVEDAL, K., PEEREBOOM, I. & ØYDVIN, K. E. 2011. Plan for skredfarekartlegging - Delrapport jordskred og flomskred. The Norwegian Water Resources and Energy Directorate

BARSTAD, I. & GRØNÅS, S. 2005. Southwesterly flows over southern Norway - mesoscale sensitivity to large-scale wind direction and speed. *Tellus A: Dynamic Meteorology and Oceanography,* 57**,** 136-152.

BAUM, L. R. & GODT, W. J. 2010. Early warning of rainfall-induced shallow landslides and debris flows in the USA. *Landslides,* 7**,** 259-272.

BELL, R., CEPEDA, J. & DEVOLI, G. Landslide susceptibility modeling at catchment level for improvement of the landslide early warning system in Norway. In Proceedings of World Landslide Forum 3, 02-06 June 2014 Beijing.

BOJE, S. 2017. Hydrometeorologiske terskler for jordskredfare på Sørlandet og Østlandet. The Norwegian Water Resources and Energy Directorate

BOJE, S., COLLEUILLE, H. & DEVOLI, G. 2014. Terskelstudier for utløsning av jordskred i Norge. The Norwegian Water Resources and Energy Directorate

BRARDINONI, F. & CHURCH, M. 2004. Representing the landslide magnitude-frequency relation: Capilano River Basin, British Columbia. *Earth Surface Processes and Landforms: The Journal of the British Geomorphological Research Group,* 29**,** 115-124.

CEPEDA, J. & BELL, R. 2014. Susceptibility map for debris flows, debris slides and soil slides in Western Norway. The Norwegian Geotechnical Institute.

COLLEUILLE, H., BOJE, S., DEVOLI, G., KRØGLI, K. I., ENGEN, K. I., SUND, M., SKASLIEN, T., HUMSTAD, T., FREKHAUG, M. & WIRÉHN, P. 2017. Jordskredvarslingen. Nasjonal varslingstjeneste for jord-, sørpe- og flomskredfare. The Norwegian Water Resources and Energy Directorate

COROMINAS, J. 1996. The angle of reach as a mobility index for small and large landslides. *Canadian Geotechnical Journal,* 33**,** 260-271.

COROMINAS, J. & MOYA, J. 2008. A review of assessing landslide frequency for hazard zoning purposes. *Engineering Geology,* 102**,** 193-213.

COROMINAS, J., VAN WESTEN, C., FRATTINI, P., CASCINI, L., MALET, J. P., FOTOPOULOU, S., CATANI, F., VAN DEN EECKHAUT, M., MAVROULI, O., AGLIARDI, F., PITILAKIS, K., WINTER, M. G., PASTOR, M., FERLISI, S., TOFANI, V., HERVÁS, J. & SMITH, J. T. 2014. Recommendations for the quantitative analysis of landslide risk. *Bulletin of Engineering Geology and the Environment,* 73**,** 209-263.

COSTA, J. E. 1984. Physical geomorphology of debris flows. *Developments and Applications of Geomorphology.* Berlin: Springer-Verlag.

CRUDEN, D. M. & VARNES, D. J. 1996. Landslides: Investigation and Mitigation. Chapter 3: Landslide types and Processes. *Special Report - National Research Council, Transportation Research Board*, 60.

DAHL, M.-P. J., MORTENSEN, L. E., JENSEN, N. H. & VEIHE, A. 2013. Magnitude–frequency characteristics and preparatory factors for spatial debris-slide distribution in the northern Faroe Islands. *Geomorphology,* 188, 3-11.

DAHL, S., BERG, K. & NÅLSUND, R. 1983. *Stabilitetsforholdene i skråninger med morene og lignende jordarter*.

DAI, F. C. & LEE, C. F. 2001. Terrain-based mapping of landslide susceptibility using a geographical information system: a case study. *Canadian Geotechnical Journal,* 38, 911-923.

DAI, F. C., LEE, F. C. & WANG, J. S. 2003. Characterization of rainfall-induced landslides. *International Journal of Remote Sensing,* 24, 4817-4834.

DECAULNE, A. & SÆMUNDSSON, T. 2006. Meteorological Conditions During Slush-Flow Release And Their Geomorphological Impact In Northwestern Iceland: A Case Study From The Bíldudalur Valley. *Swedish Society of Anthropology and Geography*, 187-197.

DEVOLI, G., BLASIO, D. V. F., ELVERHØI, A. & HØEG, K. 2009. Statistical Analysis of Landslide Events in Central America and their Run-out Distance. *Geotechnical and Geological Engineering,* 27, 23-42.

DEVOLI, G., TIRANTI, D., CREMONINI, R., SUND, M. & BOJE, S. 2018. Comparison of landslide forecasting services in Piedmont (Italy) and Norway, illustrated by events in late spring 2013. *Nat. Hazards Earth Syst. Sci.,* 18, 1351-1372.

DEVOLI, G., WASRUD, J. & JULIUSSEN, H. 2015. Registrering av nye skredhendelser i nasjonal skreddatabase. Etablering av kvalitetsnivå etter kontroll av skredhendelser. The Norwegian Water Resources and Energy Directorate

DINGMAN, S. L. 2008. *Physical Hydrology, Second Edition*, Long Grove, III. : Waveland Press Inc, 2008 @2002.

DYRRDAL, A. V. 2012. Estimation of extreme precipitation in Norway and a summary of the state-of-the-art. Norwegian Meteorological Institute.

EFFENDY, F., TOHARI, A., FERANIE, S. & LATIEF, E. D. F. 2016. Prediction of landslide run-out distance based on slope stability analysis and center of mass approach. *IOP Conference Series Earth and Environmental Science.*

ERIKSTAD, L., HALVORSEN, R., MOEN, R., THORSNES, T., ANDERSEN, T., BLOM, H. B., ELVEBAKK, A., ELVEN, R., GAARDER, G., MORTENSEN, B. P., NORDERHAUG, A., NYGAARD, K. & ØDEGAARD, F. 2009. Landformvariasjon (terrengformvariasjon og landformer). Naturtyper i Norge., 1-91.

ETZELMÜLLER, B., ROMSTAD, B. & FJELLANGER, F. 2007. Automatic regional classification of topography in Norway. *Norwegian Journal of Geology,* 87, 167-180.

FARSUND, S. H. 2015. *Bonden såg gigantraset ta uthusa og fleire sauer* [Online]. NRK Sogn og Fjordane. Available: https://www.nrk.no/sognogfjordane/sauebonden-sag-gigantraset-ta-uthusa-og-fleire-sauer-1.12442418 [Accessed].

FISCHER, L., RUBENSDOTTER, L., SLETTEN, K., STALSBERG, K., MELCHIORRE, C., HORTON, P. & JABOYEDOFF, M. 2012. Debris flow modeling for susceptibility mapping at regional to national scale in Norway. *In:* EBERHARDT, E., FROESE, C., TURNER, K. & LEROUEIL, S. (eds.) *Landslides and Engineered Slopes: Protecting Society through Improved Understanding.*

FLENTJE, P., STIRLING, D. & CHOWDHURY, R. 2011. Landslide Inventory, Susceptibility, Frequency and Hazard Zoning in the Wollongong and Wider Sydney Basin Area. *Australian Geomechanics,* 46**,** 41-50.
FØRLAND, E. J. 1979. Nedbørens høydeavhengighet. *Klima,* Nr. 2**,** 3-24.
GARIANO, S. L. & GUZZETTI, F. 2016. Landslides in a changing climate. *Earth-Science Reviews,* 162**,** 227-252.
GOKCEOGLU, C., SONMEZ, H. & ERCANOGLU, M. 2000. Discontinuity controlled probabilistic slope failure risk maps of the Altindag (settlement) region in Turkey. *Engineering Geology,* 55**,** 277-296.
GUDE, M. & SCHERER, D. 1998. Snowmelt and slushflows: hydrological and hazard implications. *Annals of Glaciology,* 26**,** 381-384.
GUTHRIE, R. H. & EVANS, S. G. 2004. Magnitude and frequency of landslides triggered by a storm event, Loughborough Inlet, British Columbia. *Natural Hazards and Earth System Sciences,* 4**,** 475-483.
GUZZETTI, F. 2005. *Landslide Hazard and Risk Assessment. Concepts, methods and tools for the detection and mapping of landslides, for landslide susceptibility zonation and hazard assessment, and for landslide risk evaluation.* Ph.D, University of Bonn.
GUZZETTI, F., CESARE, M., A, CARDINALI, M., FIORUCCI, F., SANTANGELO, M. & CHANG, K. 2012. Landslide inventory maps: New tools for an old problem. *Earth-Science Reviews,* 112**,** 42-66.
HESTNES, E. 1985. A Contribution To The Prediction Of Slush Avalanches. *Annals of Glaciology,* 6**,** 1-4.
HIGHLAND, L. M. & BOBROWSKY, P. 2008. *The landslide handbook - A guide to understanding landslides,* Reston, Virginia, U.S. Geological Survey Circular 1325.
HISDAL, H., VIKHAMAR-SCHULER, D., FØRLAND, E. J. & NILSEN, B. I. 2017. Klimaprofiler for fylker.
HUNGR, O., EVANS, S. G., BOVIS, M. J. & HUTCHINSON, J. N. 2001. A Review of the Classification of Landslides of the Flow Type. *Environmental & Engineering Geoscience,* VII**,** 221-238.
HUNGR, O., LEROUEIL, S. & PICARELLI, L. 2014. The Varnes classification of landslide types, an update. *Landslides,* 11**,** 167-194.
HUNGR, O., MCDOUGALL, S., WISE, M. & CULLEN, M. 2008. Magnitude-frequency relationships of debris flows and debris avalanches in relation to slope relief. *Geomorphology,* 96**,** 355-365.
INTRIERI, E., GIGLI, G., CASAGLI, N. & NADIM, F. 2013. Brief communication «Landslide Early Warning System: toolbox and general concepts». *Nat. Hazards Earth Syst. Sci.,* 13**,** 85-90.
IVERSON, M. R. 1997. The Physics Of Debris Flows. *Reviews of Geophysics,* 35**,** 245-296.
JAKOB, M. 2005. Debris-flow hazard analysis. *Debris-flow Hazards and Related Phenomena.* Berlin Heidelberg: Praxis. Springer
JOHNSON, K. A. & SITAR, N. 1989. Hydrological conditions leading to debris-flow initiation. *Canadian Geotechnical Journal,* 27**,** 789-801.
JØRANDLI, L. Ø. 2016. *Landslide occurrence as a response to large-scale synpotic weather types, precipitation and soil saturation in southern Norway.* Master of Science in Hydrology, University of Oslo.
KARTVERKET 2017. Høyeste fjelltopp i hver kommune. Kartverket.
KEAN, W. J., MCCOY, W. S., TUCKER, E. G., STALEY, M. D. & COE, A. J. 2013. Runoff-generated debris flows: Observations and modeling of surge initiation,

magnitude, and frequency. *Journal of Geophysical Research: Earth Surface,* 118**,** 2190-2207.
KRØGLI, K. I., DEVOLI, G., COLLEUILLE, H., BOJE, S., SUND, M. & ENGEN, K. I. 2018. The Norwegian forecasting and warning service for rainfall- and snowmelt-induced landslides. *Nat. Hazards Earth Syst. Sci. Discuss.,* 18**,** 1427-1450.
LARSEN, C. M. & TORRES-SÁNCHEZ, J. A. 1998. The frequency and distribution of recent landslide in three montane tropical regions of Puerto Rico. *Geomorphology,* 24**,** 309-331.
LARSEN, M. C. & WIECZOREK, G. F. 2006. Geomorphic effects of large debris flows and flash floods, northern Venezuela, 1999. *Zeitschrift fur Geomorphologie, Supplementband,* 145**,** 147-175.
LILLEØREN, S. K. & ETZELMÜLLER, B. 2011. A Regional Inventory Of Rock Glaciers And Ice-Cored Moraines In Norway. *Geografiska Annaler: Series A, Physical Geography,* 93**,** 175-191.
LUSSANA, C., SALORANTA, T., SKAUGEN, T., MAGNUSSON, J., TVEITO, O. E. & ANDERSEN, J. 2018. seNorge2 daily precipitation, an observational gridded dataset over Norway from 1957 to the present day. *Earth System Science Data,* 10**,** 235-249.
MCDONALD, A. J. W., O`CONNOR, E. A. & GREENBAUM, D. 1999. Rapid landslide susceptibility mapping.
NORDGULEN, Ø. & ANDRESEN, A. 2013. De eldste bergartene dannes. *Landet blir til. Norges Geologi.* Norsk Geologisk Forening.
NVE. 2013. Jordskred og flomskred. *Faktaark* [Online]. Available: http://publikasjoner.nve.no/faktaark/2013/faktaark2013_05.pdf [Accessed 25.10.2017].
NVE 2014a. Flaum- og skredfare i arealplanar. 22.05.2017 ed.
NVE 2014b. Sikkerhet mot skred i bratt terreng. Kartlegging av skredfare i arealplanlegging og byggesak. The Norwegian Water Resources and Energy Directorate
NVE. 2017a. *Glaciers* [Online]. The Norwegian Water Resources and Energy Directorate Available: https://www.nve.no/hydrology/glaciers/ [Accessed 24.01.2018].
NVE. 2017b. *Skredhendelser* [Online]. The Norwegian Water Resources and Energy Directorate Available: https://www.nve.no/flaum-og-skred/kartlegging/skred-og-flaumhendingar/skredhendelser/ [Accessed 13.11.2017].
NVE. 2018. *Aktsomhetsnivåer for flom- og jordskredvarsling* [Online]. Available: http://www.varsom.no/flom-og-jordskredvarsling/aktsomhetsnivaer-for-flom-og-jordskredvarsling/ [Accessed 29.05.2018].
ONESTI, J. L. 1987. Slushflow release mechanism: A first approximation. *Avalanche Formation, Movement and Effects (Proceedings of the Davos Symposium,* 162**,** 331-336.
ORTIGAO, J. A. R. & KANJI, M. A. 2004. Landslide Classification and Risk Management. *Handbook of Slope Stabilisation.* Springer, Berlin, Heidelberg.
PICIULLO, L., DAHL, M.-P., DEVOLI, G., COLLEUILLE, H. & CALVELLO, M. 2017. Adapting the EDuMaP method to test the performance of the Norwegian early warning system for weather-induced landslides. *Natural Hazards and Earth System Sciences,* 17**,** 817-831.
POPESCU, M. E. & SASAHARA, K. 2009. Engineering Measures for Landslide Disaster Mitigation. *Landslides - Disaster Risk Reduction.* Springer, Berlin, Heidelberg.
PUSCHMANN, O. 2005. Nasjonalt referansesystem for landskap. Beskrivelse av Norges 45 landskapsregioner. *NIJOS-rapport 10/2005.*

QARINUR, M. 2015. Landslide Runout Distance Prediction Based on Mechanism and Cause of Soil or Rock Mass Movement. *Journal of the Civil Engineering Forum,* 1**,** 29 - 36.
SANDØY, G., RUBENSDOTTER, L. & DEVOLI, G. 2017. Trekantformede jordskred - Studie av fem skredhendelser i Norge. 152.
SASSA, K. 1984. The Mechanism to Initiate Debris Flows as Undrained Shear of Loose Sediments. *Internationales Symposion INTERPRAEVENT***,** 73-87.
SENEVIRATNE, S. I., NICHOLLS, N., EASTERLING, D., GOODESS, C. M., KANAE, S., KOSSIN, J., LUO, Y., MARENGO, J., MCINNES, K., RAHIMI, M., REICHSTEIN, M., SORTEBERG, A., VERA, C. & ZHANG, X. 2012. Changes in climate extremes and their impacts on the natural physical environment. *Managing the Risks of Extreme Events and Disasters to Advance Climate Change Adaptation. A special Report of Working Groups I and II of the Intergovernmental Panel on Climate Change (IPCC).* Cambridge, Uk and New York, NY, USA: Cambridge University Press.
SILVA, F., LAMBE, W., HON, M. & MARR, A. W. 2008. Probability and Risk of Slope Failure. *Geotechnical and Geological Engineering,* 134.
SOKALSKA, E., DEVOLI, G., SOLBERG, I., HANSEN, L. & THAKUR, V. 2015. Kvalitetskontroll, analyse og forslag til oppdatering av historiske kvikkleireskred og andre leirskred registrert i Nasjonal skredhendelsesdatabase (NSDB). Norges vassdrags- og energidirektorat.
SOLENG, A., ØVERLAND, N. S., NAMORK, E., SCHWARZE, E. P. & OTTESEN, S. P. 2018. *Folkehelserapporten. Klimaendringer i Norge og helse* [Online]. Folkehelseinstituttet. Available: https://www.fhi.no/nettpub/hin/risiko--og-beskyttelsesfaktorer/klimaendringar-og-helse--folkehelse/ [Accessed 18.05.2018].
STARK, C. P. & HOVIUS, N. 2001. The characterization of landslide size distributions. *Geophysical Research Letters,* 28**,** 1091-1094.
STATISTISK-SENTRALBYRÅ. 2017a. *Folkemengd og areal, etter kommune (SÅ 57)* [Online]. Statistisk Sentralbyrå. Available: https://www.ssb.no/befolkning/nokkeltall/befolkning_oversiktstabeller [Accessed 15.05.2018].
STATISTISK-SENTRALBYRÅ. 2017b. *Tettsteder med minst 10 000 innbyggere. Folkemengde og areal (SÅ 54)* [Online]. Statistisk sentralbyrå. Available: http://www.ssb.no/302725/tettsteder-med-minst-10-000-innbyggere.folkemengde-og-areal-sa-54 [Accessed 15.05.2018].
STOFFEL, M. 2010. Magnitude-frequency relationships of debris flows - A case study based on field surveys and tree-ring records. *Geomorphology,* 116**,** 67-76.
UNISDR 2009. Terminology on Disaster Risk Reduction. 30.
VORREN, O. T. & MANGERUD, J. 2013. Istider kommer og går. *Landet blir til. Norges Geologi.* Norsk Geologisk Forening.
VÆRINGSTAD, T. & DEVOLI, G. 2012. Flom og jordskred i Trøndelag mars 2012. The Norwegian Water Resources and Energy Directorate

Attachment/Appendix

APPENDIX I: Dataset 2

List of the 56 landslide events that were mapped during the research and constitute to dataset 2. The following landslide parameters are given in this table: bedrock, quaternary deposits, applied sources of information and any valuable comments in relation to the mapping process. Language: Norwegian.

Date	Location	Landslide-ID in applied version of NLDB	Landslide-ID in dataset 2	Soil	Bedrock	Data source	Comments
2017-12-23	Mellom Fagersand og Klåbekkgrovi, rv.214	998	55	Bart fjell	Gabbro-noritt, granulitt, amfibolitt, de fleste steder forgneiset	Xgeo, regobs og Google Street View	Kun bilder fra avsetningsområde. Avsetningene tyder på et flomskred, men noen større stener.
2017-12-23	Mellom Vines og Fagersund, rv.214	997	54	Bart fjell	Gabbro-noritt, granulitt, amfibolitt, de fleste steder forgneiset	Xgeo, regobs, Google Street View	Sedimenter har hopet seg opp i vannrennen under veien. Lite bilder fra path og ingen fra source
2017-12-07	Bell, Viksdalen	996	53	Morenemateriale, sammenhengende dekke, stedvis med stor mektighet.	Diorittisk til granittisk gneis, migmatitt	Bilder fra media, regobs.	Relativt ok polygon. Bildet tatt noe langt unna, så mulig å gjøre mer presis med bedre bilder.
2017-11-09	Dalsøyra, Gulen	995	52	Forvitringsmateriale, ikke inndelt etter mektighet.	Diorittisk til granittisk gneis, migmatitt	Bilder fra xgeo, regobs og media. "Gulen 2009" fra Norgeibilder nyttig til	Source area tydelig fra bilder. Noe vanskelig å se hvordan løsmassene er utbredt ved naustet.

						sammenligning av objekt	
2017-11-09	Matbjøra, Gulen	994	51	Breelvavsetning (Glasifluvial avsetning)	Monzonitt, kvartsmonzonitt	Bilete fra xgeo, regobs og media. "Askvoll og Gaular, 2003" fra Norgeibilder nyttig til stedfesting.	Skal være et ganske godt tegnet polygon. Mulig den skal forskyves noe vest eller øst.
2017-10-02	Almhol, Luster	991	48	Skredmateriale, sammenhengende dekke, stedvis med stor mektighet	Diorittisk til granittisk gneis, migmatitt	Bilder fra regobs og media	Godt dronebilde ovenfra avsetningen. Ingen bilder visualiserer skredløpet og utløsninsområdet.
2017-10-02	Kviteskredneset, Luster	992	49	Skredmateriale, sammenhengende dekke, stedvis med stor mektighet	Kvartsdioritt, tonalitt, trondhjemitt	Regobs	Noe dårlig oppløsning på dronebildet. Vanskelig å se utbredelsen ved vegetasjonen i deposit.
2017-10-02	Skjoldateigen, Luster	993	50	Skredmateriale, sammenhengende dekke, stedvis med stor mektighet	Kvartsdioritt, tonalitt, trondhjemitt	Regobs	Flomskred over overbygg på veg. Godt dronebilde. Dårlig med bilde fra path og source
2016-12-30	Hyestranda	186	10	Humusdekke/tynt torvdekke over berggrunn	Diorittisk til granittisk gneis, migmatitt	elrapp@svv, regobs, 30.12.2016. Mulig bilde fra planet Explorer Beta, 07:2017.	Usikkert om erosjonen har startet over eller under den første vegen.
2016-12-30	Ommedalsvatnet	188	11	Bart fjell	Øyegneis, granitt, foliert granitt	Planet Explorer Beta, 07/2017. elrapp@svv.	Litt usikker posisjon på path pga dårlig satellitbilde
2016-12-08	Mellom Hammar og Strand ved Jølstravatnet	692	46	Morenemateriale, sammenhengende dekke, stedvis med stor mektighet.	Diorittisk til granittisk gneis, migmatitt	Firda. Planet Explorer Beta, 06/2017.	Source area er ikke angitt, men ligger trolig noen meter ovenfor polygonstart.
2016-11-25	Viksdalen	308	13	Bart fjell	Monzonitt, kvartsmonzonitt	Firda, drift@svv, regobs	Nedre del av polygon noe mer usikkert da dette ikke kom like godt frem på bilde.
2016-09-03	Øksland	231	12	Morenemateriale, sammenhengende dekke, stedvis med stor mektighet.	Diorittisk til granittisk gneis, migmatitt	Bilder fra media.	Ingen flybilder etter hendelse. Polygon må muligens forskyves noe nord/sør
2016-01-	Mastenes	117	7	Bart fjell	Diorittisk til granittisk	Norge i bilder: Etter,	Muligens to uavhengige skred,

29					gneis, migmatitt	Midtre Sogn 2016, 16/08. Før: Vestlandet 2013, 28/09.	men kan se ut som de henger sammen fra bildene.
2015-12-05	Brukaskreda	111	6	Bart fjell	Diorittisk til granittisk gneis, migmatitt	Firda, privat foto.	Godt foto fra skredhendelse skildrer skredløpet presist.
2015-12-05	Helgabakken	174	9	Bart fjell	Mangerittsyenitt	Bilder fra regobs	Ser ut til å være mye snø i avsetningene i skredet
2015-07-05	Krundalen i Jostedalen	155	8	Bart fjell	Diorittisk til granittisk gneis, migmatitt	Planet Explorer Beta, 19.08.2015. NRK. xgeo.no, jostein@nve	Mer presist polygon kan tegnes med høyere oppløsning på satelittbilder.
2015-03-08	Skrede	100	4	Bart fjell	Øyegneis, granitt, foliert granitt	Bilder fra Statens Vegvesen	Bildekilde viser tre skred ved siden av hverandre. Dette trolig den største av de. Hvor er 3?
2015-03-08	Skrede	101	5	Skredmateriale, ikke inndelt etter mektighet	Øyegneis, granitt, foliert granitt	Bilder fra Statens Vegvesen	
2014-10-28	Ljøsne	25	2	Bart fjell	Monzonitt, kvartsmonzonitt	Norge i Bilder, Sogn 2015, fotodato ETTER 21.09.15. Fotodato før: Sogn 2010, 29.09.10	Trenger bekreftelse på at skredhendelse er relatert til registrert skred med ID 25, Ljøsne.
2014-10-28	Raudi, Lovatnet	21	1	Bart fjell	Monzonitt, kvartsmonzonitt	ETTER: Norge i Bilder, Sogn 2015, fotodato, 21/09/15. FØR: Stryn 2012, 23/09/12	Usikkert hvor flomskredet startet.
2014-10-28	Undredal	69	3	Skredmateriale, sammenhengende dekke, stedvis med stor mektighet.	Mangerittsyenitt	Bilder fra media	Godt oversiktsbilde fra depoits
2014-03-21	Heilevang	674	45	Forvitringsmateriale, ikke inndelt etter mektighet	Diorittisk til granittisk gneis, migmatitt	ETTER: Norge i Bilder, Vestlandet 2014, 29/08/14. FØR: Norge i Bilder, Førde 2009, foto, 14/05/09.	
2014-02-23	Eitrestrondi, Arnafjorden, Vik	671	44	Bart fjell	Fyllitt, glimmerskifer	ETTER: Norge i Bilder, Midtre Sogn 2016, 16/08/16. FØR: Norge i Bilder, Sogn	Noe vanskelig å definere nøyaktig startområde for jordskredet pga overgang fra snøskred..

						2010, 29/09/10	
2013-11-15	Anestølen, Sogndal	665	43	Skredmateriale, sammenhengende dekke, stedvis med stor mektighet.	Diorittisk til granittisk gneis, migmatitt	Private fotoer fra bacheloroppgave. Norge i Bilder. Midtre Sogn 2016 16/08/16 og Sogn 2010, 29/09/10	Ganske presist polygon. Grundig polygon tegnet fra bacheloroppgave fra geofarer i Sogndal.
2013-11-15	Flostranda	613	37	Bart fjell	Monzonitt, kvartsmonzonitt	Bilde fra nyheter.	Polygon tegnet fra bilde fra siden. Trolig noe upresist.
2013-11-15	Gytri	615	38	Skredmateriale, sammenhengende dekke, stedvis med stor mektighet.	Monzonitt, kvartsmonzonitt	ETTER: Norge i Bilder, Sogn 2015, 21/09/15. NRK Sogn og Fjordane	NorgeiBilder dekker ikke hele fjellsiden. NRK bilder er mindre dekkende.
2013-11-15	Hjelle	659	41	Skredmateriale, sammenhengende dekke, stedvis med stor mektighet.	Diorittisk til granittisk gneis, migmatitt	ETTER: Norge i Bilder, Sogn 2015, 21/09/15. NRK Sogn og Fjordane. FØR: Stryn 2012, 23/09/12	Eksakt avsetningsområde, googlemaps. Source area noe usikkert.
2013-11-15	Skredestranda	662	42	Bart fjell	Øyegneis, granitt, foliert granitt	ETTER: Norge i Bilder, Sogn 2015, 21/09/15. Nyhetsartikler.	Gode bilder fra Norge i bilder og fra nyheter pga størrelsen.
2013-11-15	Yri	594	36	Morenemateriale, usammenhengende eller tynt dekke over berggrunnen.	Monzonitt, kvartsmonzonitt	ETTER: Norge i Bilder, Sogn 2015, 21/09/15. NRK Sogn og Fjordane	Veldig godt dokumentert skred. Mange bilder og gode flybilder.
2013-11-15	Yri	586	35	Bart fjell	Monzonitt, kvartsmonzonitt	ETTER: Norge i Bilder, Sogn 2015, 21/09/15. NRK Sogn og Fjordane	Gode bilder fra nrk sogn og fjordane og Norge i Bilder.
2013-05-18	Skjerdal, Aurland	650	40	Skredmateriale, sammenhengende dekke, stedvis med stor mektighet.	Gabbro, amfibolitt	Etter: Norge i Bilder, Hardangervidda 2013, 27/09/13. Før: Sogn 2010, 29/09/10. Nyhetsartikler.	Snøskred har gått ned i utløsningsområde i 1300-1400 meters høyde.
2012-07-24	Askvoll, Stongfjorden	642	39	Bart fjell	Grønnstein, amfibolitt	Etter: Norge i Bilder, Vestlandet 2014, 29/08/14. Før: Ytre	Startet som steinskred. Tok med seg materiae lenger nede og omdannet til jordskred.

						Sogn, 22/08/07. Nyhetsartikler.	
2011-12-26	Bakkeviki, Skrednes, Balestrand	475	24	Skredmateriale, sammenhengende dekke, stedvis med stor mektighet.	Diorittisk til granittisk gneis, migmatitt	Bilder fra faktaark: jordskred og flomskred (2013-01, NVE)	Stort flomskred. Starter oppe i snøen, noe uvisst akkurat hvor det starter. Få bilder tilgjengelig.
2011-12-26	Berge	548	33	Forvitringsmateriale, ikke inndelt etter mektighet	Øyegneis, granitt, foliert granitt	Etter: Norge i bilder, Sunnfjord Høyanger 2015, 14/08. Google earth, 15/08/2012.	Ferskere bilder vil gi mer presis utbredelse. Noe usikkert hvor langt utstikkeren til venstre gikk
2011-12-26	Gjærvika, Hyen	442	20	Bart fjell	Diorittisk til granittisk gneis, migmatitt	Etter: Norge i bilder, Sogn 2015, 21/09. Før, Sogn 2010, 29/09.	Omfattende skred. Vanskelig å tegne. Mangler source area og tidspunkt. Kanskje ID: 442
2011-12-26	Gudvangen	503	27	Bart fjell	Mangerittsyenitt	Etter: Norge i bilder, Hardangervidda 2013, 27/09. Før, Sogn 2010, 29/09.	Ingen bilder, media. Skredet antas å ha relateres til dagmar, begge utløpene er registrert på dagen
2011-12-26	Juklestad	447	21	Bart fjell	Diorittisk til granittisk gneis, migmatitt	Etter: Norge i bilder, Sogn 2015, 21/09. Før, Sogn 2010, 29/09.	
2011-12-26	Kandalen, Kjørvika	362	14	Bart fjell	Diorittisk til granittisk gneis, migmatitt	Naturfotograf Ronny Solheim. Norge i Bilder, Sogn 2015, 21/09.	Muligens noe upresis tregnet opp mot source area da skyggen mørkelegger detaljene.
2011-12-26	Lisjeneset	481	25	Morenemateriale, sammenhengende dekke, stedvis med stor mektighet.	Diorittisk til granittisk gneis, migmatitt	Etter: Norge i bilder, Sogn 2015, 21/09. Før, Sogn 2010, 29/09.	Liten utglidning som trolig har gått litt ut på vegen.
2011-12-26	Litt før Sætra	416	19	Bart fjell	Monzonitt, kvartsmonzonitt	Etter: Norge i Bilder, Stryn 2012, 23/09. Før, Sogn 2010, 29/09.	Noe usikkert hvor flomskredet startet fra.
2011-12-26	Marsåbakkane	365	15	Bart fjell	Monzonitt, kvartsmonzonitt	Etter: Norge i bilder, Stryn 2012, 23/09. Før, Sogn 2010, 29/09.	Bra bilde fra Norge i bilder.

2011-12-26	Prestteigelvi, fv92, utenfor Arnafjorden	999	56	Bart fjell	Diorittisk til granittisk gneis, migmatitt	Etter: Norge i bilder, Midtre Sogn 2016, 16/08. Google Earth, 28/06/2012.	Jordskred som går over til flomskred. Utløpet godt dokumentert med bilder fra media.
2011-12-26	Sandvika, Høyanger	549	34	Skredmateriale, sammenhengende dekke, stedvis med stor mektighet.	Diorittisk til granittisk gneis, migmatitt	Etter: Norge i bilder, Sunnfjord Høyanger 2015, 14/08. Google earth, 15/08/2012.	Noe usikkert om skredet initieres av materiale fraktet med elven ovenfor.
2011-12-26	Seimsdalen	498	26	Skredmateriale, sammenhengende dekke, stedvis med stor mektighet.	Mangeritt til gabbro, gneis og amfibolitt	Google Earth, 26/05/2012.	Bare ca. polygon. Trenger bedre før-og-etter bilder for mer nøyaktighet og for source area.
2011-12-26	Sæbelhaggrovi, Hemri, E16	386	17	Bart fjell	Anortositt	Etter: Norge i bilder, Hardangervidda 2013, 27/09. Før: Norge i bilder, Aurland 2008, 14/09	Skredtidspunkt trolig 26/12. Sjekk om det er relatert til skredhendelse med ID: 386 under Dagmar
2011-12-26	Sætra 1 og 2	990	47	Bart fjell	Monzonitt, kvartsmonzonitt	NRK Sogn og Fjordane. Etter: Norge i Bilder, Stryn 2012, 23/09. Før, Sogn 2010, 29/09.	Nøyaktig posisjon på utløsningsområde mangler. Antas at bekkeløpet har blitt overmetta av vann.
2011-12-26	Sætra 1 og 2	398	18	Bart fjell	Monzonitt, kvartsmonzonitt	NRK Sogn og Fjordane. Etter: Norge i Bilder, Stryn 2012, 23/09. Før, Sogn 2010, 29/09.	Nøyaktig posisjon på utløsningsområde mangler. Antas at bekkeløpet har blitt overmetta av vann.
2011-12-26	Ålhus, Sårheim	544	32	Morenemateriale, usammenhengende eller tynt dekke over berggrunnen.	Diorittisk til granittisk gneis, migmatitt	Etter: Norge i bilder, Sogn 2015, 21/09. Før, Sogn 2010, 29/09. Firda, nyhende.	Polygon tegnet på 4 år eldre bilde. Elven øverst i source area kan ha kommet senere.
2011-11-30	Kannesteinen	382	16	Morenemateriale, sammenhengende dekke, stedvis med stor mektighet.	Diorittisk til granittisk gneis, migmatitt	NRK Sogn og fjordane. Norge i bilder, Etter: Bremanger-Vågsøy-Selje 2015, 11/09. Før: Sogn 2010	Mediabilder bekrefter lokalitet, og har annen dato enn reg. Usikkert om skred 2 er på samme sted.
2011-11-	Myklemyr	458	22	Bart fjell	Diorittisk til granittisk	Norge i bilder. Etter:	Lite jordskred. Også et lite et som

27					gneis, migmatitt	Luster 2012, 27/08. Før: Sogn 2010, 29/09.	har gått rett ovenfor. Dato for dette er ukjent.
2011-11-27	Myrdal Stasjon	538	28	Bart fjell	Mangerittsyenitt	Bilder fra media. Norge i bilder, Etter: Hardangervidda 2013, 27/09. Før: Aurland 2008, 14/09.	Vanskelig å tegne nøyaktig avsetningsområde utfra bildene. Nytt tak kan indikere noe.
2011-09-05	Mel	464	23	Skredmateriale, sammenhengende dekke, stedvis med stor mektighet.	Diorittisk til granittisk gneis, migmatitt	Bilde fra media og street view	Kun bilde fra avsetning, men bilde fra street view korrelerer
2011-06-28	Tynning	539	29	Morenemateriale, usammenhengende eller tynt dekke over berggrunnen.	Mangeritt til gabbro, gneis og amfibolitt	Bilder fra media. Norge i bilder, Etter: Vestlandet 2013, 28/09. Før: Gulen 2009, 01/06.	Ingen bilder visualiserer hvor langt på jordet skredet gikk. Ellers god dokumentasjon.
2011-03-21	Ese	541	31	Skredmateriale, sammenhengende dekke, stedvis med stor mektighet.	Diorittisk til granittisk gneis, migmatitt	Bilder fra NGI rapport.	Mangler bilder oppi dalen, så ikke mulig å tegne fullstendig path eller source area.
2011-03-21	Tuftadalen	540	30	Torv og myr (Organisk materiale)	Diorittisk til granittisk gneis, migmatitt	Bilder fra media.	Skredet skal ha startet på kote 550. Men ikke synlig fra bilder. Fly-satelittbilder vil hjelpe.

APPENDIX II: Dataset 2

List of the 56 landslide events that were mapped during the research and constitute to dataset 2. The following landslide parameters are given in this table: date of event, location, landslide typology, ID from the NLDB, ID from dataset 2, height at starting point of landslide, range in elevation, slope angle at starting point of landslide, landslide area, runout distance, H/L ratio and thickness of deposit. Norwegian terms are used for landslide typology.

Date	Location	Landslide typology	Height at starting point [m a.s.l.]	Elevation range [m]	Slope Angle at starting point	Area [m^2]	Runout Distance	H / L	Thickness of deposit
2017-12-23	Mellom Fagersand og Klåbekkgrovi, rv.214	Steinskred / flomskred	415	364	56,020	3153,237	466,530	0,780	0-0,5
2017-12-23	Mellom Vines og Fagersund, rv.214	Flomskred	361	225	46,410	1954,379	326,020	0,690	1,0
2017-12-07	Bell, Viksdalen	Jordskred	260	82	25,760	5055,223	203,930	0,402	0,3-0,4
2017-11-09	Dalsøyra, Gulen	Jordskred	13	12	16,730	786,094	41,010	0,293	0,5-1
2017-11-09	Matbjøra, Gulen	Utglidning	152	3	21,430	146,387	22,900	0,131	0,5
2017-10-02	Almhol, Luster	Flomskred	404	404	40,230	6347,982	612,930	0,659	1
2017-10-02	Kviteskredneset, Luster	Flomskred	460	457	32,000	11807,604	887,360	0,515	
2017-10-02	Skjoldateigen, Luster	Flomskred	62	59	29,030	319,885	100,940	0,585	
2016-12-30	Hyestranda	Flomskred	43	30	20,700	536,699	89,460	0,335	1
2016-12-30	Ommedalsvatnet	Jordskred	566	536	46,700	16403,862	811,350	0,661	2
2016-12-08	Mellom Hammar og Strand ved Jølstravatnet	Jordskred	434	225	28,740	8928,771	616,480	0,365	0,7
2016-11-25	Viksdalen	Jordskred	700	547	27,270	53448,573	1107,740	0,494	0,2-0,3
2016-09-03	Øksland	Jordskred	272	145	42,380	4841,374	197,350	0,735	2
2016-01-29	Mastenes	Jordskred	216	213	48,540	7719,585	176,570	1,206	0,2-0,3

2015-12-05	Brukaskreda	Sørpeskred	597	596	66,530	15914,642	802,180	0,743	
2015-12-05	Helgabakken	Sørpeskred	660	511	34,620	18967,011	1021,990	0,500	
2015-07-05	Krundalen i Jostedalen	Jordskred	619	325	41,040	66745,432	738,520	0,440	0,8-1
2015-03-08	Skrede	Jordskred	575	522	40,920	65924,000	916,160	0,570	1
2015-03-08	Skrede	Jordskred	408	353	30,540	7343,243	623,070	0,567	
2014-10-28	Ljøsne	Flomskred	1099	949	47,220	24438,024	1689,900	0,562	
2014-10-28	Raudi, Lovatnet	Flomskred	799	747	40,920	20366,048	1554,380	0,481	
2014-10-28	Undredal	Flomskred	606	475	25,520	16412,137	1519,100	0,313	0,4
2014-03-21	Heilevang	Jordskred	266	261	51,690	4539,155	306,760	0,851	0,3
2014-02-23	Eitrestrondi, Arnafjorden, Vik	Snøskred / Jordskred	856	856	53,730	70485,656	917,770	0,933	2,5
2013-11-15	Anestølen, Sogndal	Jordskred	685	245	35,510	10365,249	536,550	0,457	0,5-0,7
2013-11-15	Flostranda	Flomskred	317	285	46,430	6018,149	574,290	0,496	0,2-0,5
2013-11-15	Gytri	Jordskred	701	665	48,170	65078,408	1096,660	0,606	0,5-1
2013-11-15	Hjelle	Flomskred	510	480	33,100	14940,711	1086,470	0,442	0,5-1
2013-11-15	Skredestranda	Jordskred	608	554	35,800	96752,417	833,530	0,665	1,5
2013-11-15	Yri	Jordskred	471	435	39,900	49695,694	787,050	0,553	1
2013-11-15	Yri	Flomskred	307	272	31,790	9540,680	467,710	0,582	0,5
2013-05-18	Skjerdal, Aurland	Sørpesked	1452	1450	36,140	63615,275	3694,110	0,393	0,5
2012-07-24	Askvoll, Stongfjorden	Steinskred / jordskred	515	414	53,430	15511,805	472,170	0,877	
2011-12-26	Bakkeviki, Skrednes, Balestrand	Flomskred	359	359	32,010	22894,114	836,630	0,429	0,2-0,5
2011-12-26	Berge	Sørpeskred	702	697	28,810	93311,764	1935,920	0,360	0,2-0,5
2011-12-26	Gjærvika, Hyen	Flomskred	597	597	48,330	41201,669	1660,200	0,360	
2011-12-26	Gudvangen	Flomskred	179	179	51,480	2590,548	256,680	0,697	
2011-12-26	Juklestad	Flomskred	215	7	18,540	714,306	85,850	0,082	
2011-12-26	Kandalen, Kjørvika	Jordskred	346	284	33,330	7204,135	450,220	0,631	0,5-1
2011-12-26	Lisjeneset	Utglidning	216	5	23,130	256,658	24,770	0,202	
2011-12-26	Litt før Sætra	Flomskred	476	445	48,100	7112,093	787,270	0,565	
2011-12-26	Marsåbakkane	Utglidning	63	32	47,040	1103,334	53,530	0,598	
2011-12-26	Prestteigelvi, fv92, utenfor Arnafjorden	Jordskred / flomskred	612	610	39,120	33897,540	923,060	0,661	1-2
2011-12-26	Sandvika, Høyanger	Jordskred	249	249	41,050	13239,953	481,950	0,517	0,5
2011-12-26	Seimsdalen	Flomskred	398	396	45,020	9955,060	748,800	0,529	0,3-0,5
2011-12-26	Sæbelhaggrovi, Hemri, E16	Flomskred	619	554	46,380	24889,626	1082,940	0,512	
2011-12-26	Sætra 1 og 2	Flomskred	560	530	26,100	20557,072	849,810	0,624	1-2
2011-12-26	Sætra 1 og 2	Flomskred	352	322	47,430	10307,294	580,690	0,555	1-2
2011-12-26	Ålhus, Sårheim	Jordskred / flomskred	596	388	33,100	12081,144	959,550	0,404	0,4-0,7
2011-11-30	Kannesteinen	Utglidning	26	22	32,970	536,803	67,420	0,326	
2011-11-27	Myklemyr	Jordskred	118	16	31,310	191,982	43,430	0,368	

2011-11-27	Myrdal Stasjon	Jordskred	948	81	42,020	5435,296	188,780	0,429	1-2
2011-09-05	Mel	Flomskred	168	89	18,010	4384,983	459,700	0,194	0,2
2011-06-28	Tynning	Jordskred	277	249	42,700	7014,072	381,100	0,653	0,3
2011-03-21	Ese	Sørpeskred	324	299	27,160	124228,097	1388,250	0,215	
2011-03-21	Tuftadalen	Sørpeskred	550	549	8,990	50724,197	2703,030	0,203	0,5-1

APPENDIX III: Magnitude-frequency analysis

Landslide inventory and data for magnitude-frequency analysis.

Landslide magnitude [m^2]	Landslide type	Individual debris slide frequency (f_i/years)	Cumulative debris slide frequency [F_i]	Date	Location
124228,1	Sørpeskred	0,14285714	0,14285714	2011-03-21	Ese
96752,417	Jordskred	0,14285714	0,28571429	2013-11-15	Skredestranda
93311,764	Sørpeskred	0,14285714	0,42857143	2011-12-26	Berge
70485,656	Snøskred / Jordskred	0,14285714	0,57142857	2014-02-23	Eitrestrondi, Arnafjorden, Vik
66745,432	Jordskred	0,14285714	0,71428571	2015-07-05	Krundalen i Jostedalen
65924	Jordskred	0,14285714	0,85714286	2015-03-08	Skrede
65078,408	Jordskred	0,14285714	1	2013-11-15	Gytri
63615,275	Sørpeskred	0,14285714	1,14285714	2013-05-18	Skjerdal, Aurland
53448,573	Jordskred	0,14285714	1,28571429	2016-11-25	Viksdalen
50724,197	Sørpeskred	0,14285714	1,42857143	2011-03-21	Tuftadalen
49695,694	Jordskred	0,14285714	1,57142857	2013-11-15	Yri
41201,669	Flomskred	0,14285714	1,71428571	2011-12-26	Gjærvika, Hyen
33897,54	Jordskred / flomskred	0,14285714	1,85714286	2011-12-26	Prestteigelvi, fv92, utenfor Arnafjorden
24889,626	Flomskred	0,14285714	2	2011-12-26	Sæbelhaggrovi, Hemri, E16
24438,024	Flomskred	0,14285714	2,14285714	2014-10-28	Ljøsne
22894,114	Flomskred	0,14285714	2,28571429	2011-12-26	Bakkeviki, Skrednes, Balestrand
20557,072	Flomskred	0,14285714	2,42857143	2011-12-26	Sætra 1 og 2
20366,048	Flomskred	0,14285714	2,57142857	2014-10-28	Raudi, Lovatnet
18967,011	Sørpeskred	0,14285714	2,71428571	2015-12-05	Helgabakken
16412,137	Flomskred	0,14285714	2,85714286	2014-10-28	Undredal
16403,862	Jordskred	0,14285714	3	2016-12-30	Ommedalsvatnet
15914,642	Sørpeskred	0,14285714	3,14285714	2015-12-05	Brukaskreda
15511,805	Steinskred / jordskred	0,14285714	3,28571429	2012-07-24	Askvoll, Stongfjorden
14940,711	Flomskred	0,14285714	3,42857143	2013-11-15	Hjelle
13239,953	Jordskred	0,14285714	3,57142857	2011-12-26	Sandvika, Høyanger
12081,144	Jordskred / flomskred	0,14285714	3,71428571	2011-12-26	Ålhus, Sårheim
11807,604	Flomskred	0,14285714	3,85714286	2017-10-02	Kviteskredneset,

					Luster
10365,249	Jordskred	0,14285714	4	2013-11-15	Anestølen, Sogndal
10307,294	Flomskred	0,14285714	4,14285714	2011-12-26	Sætra 1 og 2
9955,0603	Flomskred	0,14285714	4,28571429	2011-12-26	Seimsdalen
9540,6803	Flomskred	0,14285714	4,42857143	2013-11-15	Yri
8928,7706	Jordskred	0,14285714	4,57142857	2016-12-08	Mellom Hammar og Strand ved Jølstravatnet
7719,5848	Jordskred	0,14285714	4,71428571	2016-01-29	Mastenes
7343,2428	Jordskred	0,14285714	4,85714286	2015-03-08	Skrede
7204,1355	Jordskred	0,14285714	5	2011-12-26	Kandalen, Kjørvika
7112,0933	Flomskred	0,14285714	5,14285714	2011-12-26	Litt før Sætra
7014,0724	Jordskred	0,14285714	5,28571429	2011-06-28	Tynning
6347,9822	Flomskred	0,14285714	5,42857143	2017-10-02	Almhol, Luster
6018,1492	Flomskred	0,14285714	5,57142857	2013-11-15	Flostranda
5435,2961	Jordskred	0,14285714	5,71428571	2011-11-27	Myrdal Stasjon
5055,2229	Jordskred	0,14285714	5,85714286	2017-12-07	Bell, Viksdalen
4841,3742	Jordskred	0,14285714	6	2016-09-03	Øksland
4539,1547	Jordskred	0,14285714	6,14285714	2014-03-21	Heilevang
4384,9825	Flomskred	0,14285714	6,28571429	2011-09-05	Mel
3153,2373	Steinskred / flomskred	0,14285714	6,42857143	2017-12-23	Mellom Fagersand og Klåbekkgrovi, rv.214
2590,5484	Flomskred	0,14285714	6,57142857	2011-12-26	Gudvangen
1954,3786	Flomskred	0,14285714	6,71428571	2017-12-23	Mellom Vines og Fagersund, rv.214
1103,3343	Utglidning	0,14285714	6,85714286	2011-12-26	Marsåbakkane
786,0944	Jordskred	0,14285714	7	2017-11-09	Dalsøyra, Gulen
714,30554	Flomskred	0,14285714	7,14285714	2011-12-26	Juklestad
536,80309	Utglidning	0,14285714	7,28571429	2011-11-30	Kannesteinen
536,69928	Flomskred	0,14285714	7,42857143	2016-12-30	Hyestranda
319,88497	Flomskred	0,14285714	7,57142857	2017-10-02	Skjoldateigen, Luster
256,65797	Utglidning	0,14285714	7,71428571	2011-12-26	Lisjeneset
191,98237	Jordskred	0,14285714	7,85714286	2011-11-27	Myklemyr
146,3868	Utglidning	0,14285714	8	2017-11-09	Matbjøra, Gulen

APPENDIX IV: Threshold analysis

List of the data that were used for the threshold analysis. Grid-values of rekative water supply (QTTrel) and relative soil saturation (SSSrel) were extracted from Xgeo and plotted in the threshold plot.

Date	Location	Landslide typology	Landslide-ID in applied version of NLDB	Landslide-ID in dataset 2	Time of occurrence	Water supply (QTTrel) Grid-value	Soil saturation (SSSrel) Grid-value	Elevation of gauge [m a.s.l.]
2017-12-23	Mellom Fagersand og Klåbekkgrovi, rv.214	Steinskred / flomskred	998	55	11:42	0,00	51,00	690
2017-12-23	Mellom Vines og Fagersund, rv.214	Flomskred	997	54	13:27	1,00	87,00	138
2017-12-07	Bell, Viksdalen	Jordskred	996	53	16:45	2,00	88,00	177
2017-11-09	Dalsøyra, Gulen	Jordskred	995	52	06:00	NoData	NoData	NoData
2017-11-09	Matbjøra, Gulen	Utglidning	994	51	07:30	1,00	66,00	274
2017-10-02	Almhol, Luster	Flomskred	991	48	08:18	0,00	16,00	413
2017-10-02	Kviteskredneset, Luster	Flomskred	992	49	08:52	0,00	26,00	852
2017-10-02	Skjoldateigen, Luster	Flomskred	993	50	07:47	0,00	17,00	493
2016-12-30	Hyestranda	Flomskred	186	10	12:00 - usikkert	NoData	0,00	0
2016-12-30	Ommedalsvatnet	Jordskred	188	11	01:00	1,00	76,00	323
2016-12-08	Mellom Hammar og Strand ved Jølstravatnet	Jordskred	692	46	08:30	1,00	65,00	556
2016-11-25	Viksdalen	Jordskred	308	13	06:00	0,00	41,00	837
2016-09-03	Øksland	Jordskred	231	12	15:30	0,00	65,00	396
2016-01-29	Mastenes	Jordskred	117	7	01:00 - 30min usikkert	NoData	NoData	0

2015-12-05	Brukaskreda	Sørpeskred	111	6	Natt - 12t usikkert	0,00	55,00	818
2015-12-05	Helgabakken	Sørpeskred	174	9	09:00	0,00	49,00	923
2015-07-05	Krundalen i Jostedalen	Jordskred	155	8	10:00	1,00	85,00	938
2015-03-08	Skrede	Jordskred	100	4	"Natt til sundag"	4,00	92,00	407
2015-03-08	Skrede	Jordskred	101	5	"Natt til sundag"	4,00	92,00	407
2014-10-28	Ljøsne	Flomskred	25	2	Usikkert	3,00	67,00	1063
2014-10-28	Raudi, Lovatnet	Flomskred	21	1	02:40	3,00	100,00	1408
2014-10-28	Undredal	Flomskred	69	3	01:00	3,00	100,00	837
2014-03-21	Heilevang	Jordskred	674	45	01:00 - 12t usikkerhet	1,00	77,00	5
2014-02-23	Eitrestrondi, Arnafjorden, Vik	Snøskred / Jordskred	671	44	Kveld	2,00	65,00	865
2013-11-15	Anestølen, Sogndal	Jordskred	665	43	01:00 - 12t usikkerhet	3,00	86,00	545
2013-11-15	Flostranda	Flomskred	613	37	20:20	4,00	82,00	791
2013-11-15	Gytri	Jordskred	615	38	Natt til 16/11	4,00	76,00	547
2013-11-15	Hjelle	Flomskred	659	41	Natt til 16/11	4,00	85,00	278
2013-11-15	Skredestranda	Jordskred	662	42	Kveld	4,00	85,00	407
2013-11-15	Yri	Flomskred	586	35	Natt til 16/11	4,00	75,00	471
2013-11-15	Yri	Jordskred	594	36	Natt til 16/11	4,00	77,00	347
2013-05-18	Skjerdal, Aurland	Sørpeskred	650	40	08:00	0,00	43,00	1333
2012-07-24	Askvoll, Stongfjorden	Steinskred / jordskred	642	39	19:45	0,00	46,00	663
2011-12-26	Bakkeviki, Skrednes, Balestrand	Flomskred	475	24	Trolig natt	2,00	70,00	601
2011-12-26	Berge	Sørpeskred	548	33	21:45	3,00	78,00	654
2011-12-26	Gjærvika, Hyen	Flomskred	442	20	03:00	0,00	40,00	1002
2011-12-26	Gudvangen	Flomskred	503	27	Trolig natt	1,00	64,00	369
2011-12-26	Juklestad	Flomskred	447	21	20:00	2,00	88,00	207
2011-12-26	Kandalen, Kjørvika	Jordskred	362	14	03:00	2,00	95,00	123
2011-11-30	Kannesteinen	Utglidning	382	16	19:00	NoData	NoData	NoData
2011-12-26	Lisjeneset	Utglidning	481	25	03:00	1,00	76,00	207
2011-12-26	Litt før Sætra	Flomskred	416	19	Trolig natt	2,00	76,00	429
2011-12-26	Marsåbakkane	Utglidning	365	15	03:10	2,00	90,00	29
2011-12-26	Prestteigelvi, fv92, utenfor	Jordskred /	999	56	Trolig natt	2,00	85,00	201

	Arnafjorden	flomskred						
2011-12-26	Sandvika, Høyanger	Jordskred	549	34	Ettermiddag	3,00	96,00	96
2011-12-26	Seimsdalen	Flomskred	498	26	Trolig natt	0,00	63,00	478
2011-12-26	Sæbelhaggrovi, Hemri, E16	Flomskred	386	17	01:00 - Usikkert	1,00	68,00	487
2011-12-26	Sætra 1 og 2	Flomskred	398	18	03:10	0,00	50,00	791
2011-12-26	Sætra 1 og 2	Flomskred	990	47	03:10	2,00	76,00	429
2011-12-26	Ålhus, Sårheim	Jordskred / flomskred	544	32	03:10	1,00	59,00	518
2011-11-27	Myklemyr	Jordskred	458	22	Ukjent	0,00	70,00	286
2011-11-27	Myrdal Stasjon	Jordskred	538	28	15:40	0,00	55,00	987
2011-09-05	Mel	Flomskred	464	23	23:09	0,00	42,00	78
2011-06-28	Tynning	Jordskred	539	29	08:30	1,00	60,00	32
2011-03-21	Ese	Sørpeskred	541	31	23:30	5,00	88,00	306
2011-03-21	Tuftadalen	Sørpeskred	540	30	20:20	4,00	71,00	560

APPENDIX V: Poster

Poster presentation of thesis at Geofaredagen at NGU in 2017.

Frequency-magnitude analysis for landslides in Sogn og Fjordane

UNIVERSITY OF OSLO

Håvard Mongstad[1], Graziella Devoli[1,2] , Karianne Staalesen Lilleøren[1]

[1]Department of Geosciences, University of Oslo/Norway. [2] Hydrology Department, Norwegian Water Resources and Energy Directorate, Oslo/Norway

A study to improve landslide warning

The county of Sogn og Fjordane has a climate and topography which makes it vulnerable for debris avalanches, debris flows and slush flows. The recently established landslide forecasting service at NVE (www.varsom.no) is able to predict their spatial and temporal occurrence. However, a better understanding of these processes, their spatial distribution, dimensions, mechanisms and dynamics is needed to improve the performance of the service, especially at local scale.

Figure 2. A house in Gulen municipality got to feel the devastating forces a debris avalanche can have. Photo: NRK.

Figure 3. Pictures from media are an important part of gathering information about the landslide event. Photo: Jan Helge Aalbu.

Objective

The warning level for landslide informs you about expected number of landslide events and their qualitative size. But what landslide magnitude is most typical and what is the return period for these magnitudes in the county?

One big problem of the national landslide database is the lack of information on the spatial extension of the landslide area (surface area, volume, travel distance etc.). For this I will use different type of tools to map the extension of the events that occurred in the area. Another objective is to prepare F-M curves for the different rainfall-triggered events and compare them to see their typical dimensions and frequencies.

Table 1. There are four levels of landslide warning. Each of them contain a general description of the situation, together with the expected outcome. Classification criteria is used for validation later on. Source: www.varsom.no

Level	General Explanation	Classification criteria used to evaluate the performance of the landslide EW
4	• Extreme situation that occurs very rarely requires immediate attention and may cause severe damages. • Expected many landslide events, several with considerable consequences. • Extensive flooding, erosional damage and flood damage to buildings and infrastructure. • Flood: Return period of more than 50 years.	• Large and smaller landslides are expected, in many numbers and within a large geographical area. • >50 landslide events. • Several road blockings due to landslides or flooding.
3	• Severe situation that occurs rarely requires contingency preparedness and may cause severe damages. • Expected many landslide events, some with considerable consequences. • Extensive flooding, erosional damage and flood damage to certain prone areas. • Flood: Return period of more than 5 years.	• Some large and smaller landslides are expected. • 6-10 landslide events are expected in an area of about 10-15.000 km2) • Several road blockings due to landslides or flooding.
2	• Situation that requires vigilance and may cause local damages. • Expected some landslide events, certain large events may occur. • Local flooding and/or erosional damage due to rapid increase of discharge in streams/ small rivers, ice drift, ice in streams/rivers and frozen soil. • High flow/water level in comparison to normal seasonal variations. • Discharge close to orange level.	• 1-4 landslide events are expected in an area of about 10-15.000 km2 • Hazard signs: Flooding/erosion in streams
1	• Generally safe conditions	• No landslide events are expected • But: • 1-2 landslide events caused by local rain showers may occur. • 1 small debris slide if in area with no signs of elevated hazard level. • Man-made landslide events can occur in this level

So far..

Landslide events with sufficient data has been selected from the database. Polygons have been drawn for the events with good images, and LiDAR and aerial photos have been ordered for further analysis on events of interest.

Further work will involve a field trip to one or several landslide locations from the database for landslide parameter analysis. More detailed polygons will be made from the ordered pictures and a frequency-magnitude curve will be drawn. The study will also analyse the performance of the forecasting service. How accurate were the warning messages sent in the period analysed, focusing on the number of events, but also on the dimensions.

References

FJELDLAND, E. J., HAGDELAND, I., HANSSEN-BAUER, I., HISDAL, H., MAYER, S., NESJE, A., ØIE NILSEN, J. E., SANDVEN, S., SANDØ, A. B., SORTEBERG, A. & ÅDLANDSVIK, B. 2015. Klima i Norge 2100. NCCS report no 2/2015. 2.

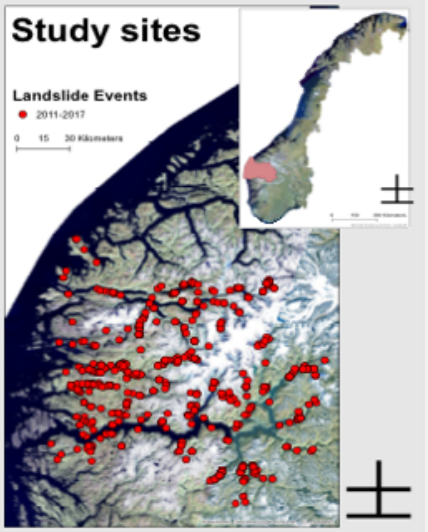

Figure 1. Figure shows all registered landslide events from 2011 to 2017 that has been examined. Time of period were chosen due to a more comprehensive registration for these years.

Figure 4. It can be hard to find the exact location of a landslide if it is poorly described in database. GoogleMaps is a helpful tool which allows you to compare images from street view to the pictures from the event to prove the correct location. Photo: Googlemaps.com

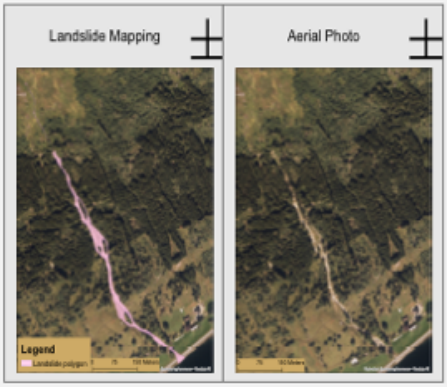

Figure 5. It is possible to map historical landslides if there are images available after the event. This one was mapped from aerial photos. Images from e.g. newspapers (figure 2 and 3) can also be helpful. This event was triggered by the winter storm «Dagmar» in 2011.

APPENDIX VI: Poster

Poster presentation of thesis at the EGU conference 2018 (European Geoscience Union General Assembly) at Vienna.